UNIVERSIDADE ESTADUAL PAULISTA
PÓS GRADUAÇÃO EM CIÊNCIA E TECNOLOGIA DE MATERIAIS
CÂMPUS DE SOROCABA

PATRÍCIA LUIZA DE FREITAS PROENÇA

MECANISMOS DE AÇÃO DE NANOPESTICIDAS: ESTRATÉGIAS DE FUNCIONALIZAÇÃO PARA ESTUDOS DE INTERAÇÃO NANOPARTÍCULA E PLANTAS

Sorocaba
2023

PATRÍCIA LUIZA DE FREITAS PROENÇA

MECANISMOS DE AÇÃO DE NANOPESTICIDAS: ESTRATÉGIAS DE FUNCIONALIZAÇÃO PARA ESTUDOS DE INTERAÇÃO NANOPARTÍCULA E PLANTAS

Tese apresentada como parte dos requisitos para obtenção do título de Doutora em Ciência e Tecnologia de Materiais do Programa de Pós-Graduação em Ciência e Tecnologia de Materiais da Universidade Estadual Paulista "Júlio de Mesquita Filho" – UNESP.

Orientador: Prof. Dr. Leonardo Fernandes Fraceto

Sorocaba
2023

P964m

PROENÇA, PATRÍCIA LUIZA DE FREITAS
MECANISMOS DE AÇÃO DE NANOPESTICIDAS: ESTRATÉGIAS DE FUNCIONALIZAÇÃO PARA ESTUDOS DE INTERAÇÃO NANOPARTÍCULA E PLANTAS / PATRÍCIA LUIZA DE FREITAS PROENÇA. -- Bauru, 2023
124 p. : il., tabs., fotos

Tese (doutorado) - Universidade Estadual Paulista (Unesp), Faculdade de Ciências, Bauru
Orientador: Leonardo Fernandes Fraceto

1. Caracterização de nanopartículas. 2. Ensaios biológicos contra ácaros e lagartas. 3. Absorção e translocação de nanopartículas. I. Título.

Sistema de geração automática de fichas catalográficas da Unesp. Biblioteca da Faculdade de Ciências, Bauru. Dados fornecidos pelo autor(a).

Essa ficha não pode ser modificada.

UNIVERSIDADE ESTADUAL PAULISTA

Câmpus de Bauru

Faculdade de Ciências

ATA DA DEFESA PÚBLICA DA TESE DE DOUTORADO DE PATRÍCIA LUIZA DE FREITAS PROENÇA, DISCENTE DO PROGRAMA DE PÓS-GRADUAÇÃO EM CIÊNCIA E TECNOLOGIA DE MATERIAIS, DA FACULDADE DE CIÊNCIAS - CÂMPUS DE BAURU.

Aos 24 dias do mês de outubro do ano de 2023, às 08:30 horas, no(a) por videoconferência, realizou-se a defesa de TESE DE DOUTORADO de PATRÍCIA LUIZA DE FREITAS PROENÇA, intitulada **MECANISMOS DE AÇÃO DE NANOPESTICIDAS: ESTRATÉGIAS DE FUNCIONALIZAÇÃO PARA ESTUDOS DE INTERAÇÃO NANOPARTÍCULA E PLANTASMECANISMOS DE AÇÃO DE NANOPESTICIDAS: ESTRATÉGIAS DE FUNCIONALIZAÇÃO PARA ESTUDOS DE INTERAÇÃO NANOPARTÍCULA E PLANTAS**. A Comissão Examinadora foi constituida pelos seguintes membros: Prof. Dr. LEONARDO FERNANDES FRACETO (Orientador(a) - Participação Virtual) do(a) Departamento de Engenharia Ambiental / Instituto de Ciência e Tecnologia - Unesp/ Câmpus de Sorocaba, Profa. Dra. MARCIA REGINA DE MOURA AOUADA (Participação Virtual) do(a) Departamento de Física e Química / Faculdade de Engenharia de Ilha Solteira - Unesp, Profª. Drª. DANIELE RIBEIRO DE ARAUJO (Participação Virtual) do(a) Centro de Ciências Naturais e Humanas / Universidade Federal do ABC, Prof. Dr. ADRIANO ARRUÊ MELO (Participação Virtual) do(a) Departamento de Defesa Fitossanitária / Universidade Federal de Santa Maria, Profª. Drª. MARYSTELA FERREIRA (Participação Virtual) do(a) Departamento de Físico-Química / Universidade Federal de São Carlos (UFSCar) - Sorocaba. Após a exposição pela doutoranda e arguição pelos membros da Comissão Examinadora que participaram do ato, de forma presencial e/ou virtual, a discente recebeu o conceito final: Aprovada. Nada mais havendo, foi lavrada a presente ata, que após lida e aprovada, foi assinada pelo(a) Presidente(a) da Comissão Examinadora.

Prof. Dr. LEONARDO FERNANDES FRACETO

Leonardo Fraceto

Assinado de forma digital por Leonardo Fraceto
Dados: 2023.10.24 14:17:46 -03'00'

EPÍGRAFE

“Siga seus caminhos misteriosos para que consigas fazer seu milagre, pois o esforço se transformará em bálsamo para seu corpo e sua alma.”

(Anônimo)

DEDICATÓRIA

A Dr. Estefânia, minha amiga e parceira de todas as horas e ao Prof. Dr. Leonardo, orientador exemplar.

AGRADECIMENTOS

A Deus por não me deixar desviar desta caminhada e me permitir mais este belo desafio;

Aos meus pais, pelo apoio sempre incondicional;

Ao meu marido, por todas as conversas e palavras de incentivo;

A minha filha Alanis pelo apoio, pela compreensão nos momentos em que me fiz ausente e pelos bilhetinhos de incentivo! As minhas filhas Alícia e Ágata por renovarem minha vontade de sonhar;

Ao Prof. Dr. Leonardo, meu orientador, primeiramente pela oportunidade de me permitir realizar um sonho antigo e por ser um exemplo a ser seguido, como Pesquisador e Professor. Agradeço por toda orientação, paciência e compreensão.

A Estefânia, minha amiga e companheira de jornada, por tudo… pelo apoio, incentivo, por dividir seu conhecimento comigo, pela ajuda na realização dos experimentos e na escrita deste documento, inúmeras vezes deixando de lado seus próprios afazeres e seu descanso para me ajudar.

Aos meus amigos Jhones e Anderson, por todo apoio, conhecimento compartilhado e companheirismo.

Aos companheiros de laboratório por sempre estarem dispostos a ajudar e compartilhar conhecimento. Pelas conversas e muitas risadas que deixam o ambiente descontraído e muito prazeroso de se estar e trabalhar;

Aos colegas Tais, Ana, Claudiane e aos Professores Renata, Halley, Daniel e Ricardo expresso minha gratidão pela parceria e contribuição. Sem esta ajuda jamais alcançaríamos tantos resultados experimentais;

A Universidade Estadual Paulista e ao Programa de Pós graduação em Ciência e Tecnologia de Materiais por proporcionarem educação de qualidade;

O presente trabalho foi realizado com apoio da Coordenação de Aperfeiçoamento de Pessoal de Nível Superior - Brasil (CAPES) - Código de Financiamento 001.Bolsisita pelo Programa de Excelência Acadêmica (processo 88887.351694/2019-00)

RESUMO

Atualmente os nanopesticidas representam uma tecnologia emergente e muito estudada devido aos seus potenciais benefícios. Os nanopesticidas em sua maioria apresentam maior eficácia, além de uma degradação mais lenta quando aplicados no ambiente. Desta forma, há uma diminuição no consumo geral destes compostos, tornando-os mais rentáveis, resultando num maior rendimento das culturas e segurança alimentar. Embora muitos benefícios sejam associados a estes sistemas, os riscos associados com os pesticidas em escala nanométrica são complexos, ainda pouco estudados e não completamente entendidos. Portanto, nossa pesquisa envolveu o desenvolvimento de um nanocarreador composto por polímeros naturais para o carreamento de curcumina e carvacrol (inseticidas botânicos) e estudos para determinar a toxicidade sobre ácaros e lagartas. Além disso, essas nanopartículas foram marcadas empregando corantes fluorescentes para possibilitar o rastreamento na planta após a aplicação. O nanocarreador desenvolvido apresentou tamanho em torno de 100 ± 12 nm e com índice de polidispersão de 0,159 ± 0,02 e potencial zeta de 30 ± 4 mV. A eficiência de encapsulação ficou em torno de 90% para ambos os ativos e mantiveram sua estabilidade pelo tempo analisado (90 dias). Estudos para determinar a toxicidade sobre ácaros e lagartas indicam uma tendencia ao efeito acaricida e repelente para o ácaro *T.urticae*. Entretando, para algumas lagartas do gênero *Spodoptera sp*. a diferença na mortalidade entre os ativos nanoencapsulados e emulsionados foi bem expressiva, 87,5 ± 7,4% contra 5,2 ± 2,1% para *S. cosmiode* e 64,2 ± 21% contra 29,6 ± 12,3% para *S. eridania*. O emprego de corantes fluorescentes possibilitou o rastreamento das nanopartículas na planta após a aplicação. Através dessa estratégia conseguimos mostrar que a nanopartícula foi absorvida pela folha, ocorrendo translocamento dentro do tecido foliar em direção ao ápice e também em direção a raiz após um período de exposição de 24h. Esses resultados são promissores para uma agricultura mais sustentável.

ABSTRACT

Currently, nanopesticides represent an emerging and much studied technology due to their potential benefits. Most nanopesticides are more effective, in addition to slower degradation when applied in the environment. In this way, there is a decrease in the overall consumption of these compounds, making them more profitable, resulting in higher crop yields and food security. Although many benefits are associated with these systems, the risks associated with nanoscale pesticides are complex, understudied and not fully understood. In this sense, our research involved the development of a nanocarrier composed of natural polymers for the transport of curcumin and carvacrol (botanical insecticides) and studies to determine the toxicity on mites and caterpillars. In addition, these nanoparticles were marked using fluorescent dyes to enable tracking in the plant after application. The develop nanocarrier presented a size of around 100 ± 12 nm and a polydispersity index of 0.159 ± 0.02 and zeta potential of 30 ± 4 mV. The encapsulation efficiency was around 90% for both active ingredients and maintained their stability for the time analyzed (90 days). Studies to determine toxicity on mites and caterpillars indicate a tendency towards an acaricidal and repellent effect on the *T.urticae* mite. However, for some caterpillars of the genus Spodoptera sp. the difference in mortality between nanoencapsulated and emulsified active ingredients was quite significant, 87.5 ± 7.4% versus 5.2 ± 2.1% for *S. cosmiode* and 64.2 ± 21% versus 29.6 ± 12.3 % for *S. eridania*. The use of fluorescent dyes made it possible to track plants after application.The use of fluorescent dyes made it possible to track plants after application to show that the nanoparticle was absorbed by the leaf, translocating within the leaf tissue towards the apex and also towards the root after an exposure period of 24 hours. These results are promising for more sustainable agriculture.

Sumário

Introdução Geral

Um dos principais desafios da agricultura do século XXI é alcançar a segurança alimentar e nutricional para a crescente população mundial diante das mudanças climáticas, juntamente com a escassez de recursos naturais, perda da biodiversidade e outros ecossistemas (SILVA; GILLER, 2020). De acordo com a Organização das Nações Unidas para a Alimentação e Agricultura (FAO), a população mundial deverá alcançar a marca de 9,7 bilhões de habitantes em 2050 (ONU, 2019), o que demandará um aumento de até 70% na produção de alimentos em comparação com o que é produzido atualmente (FA0, 2016). Os desafios da produção de alimentos não estão restritos apenas ao aumento da demanda de alimentos, mas também envolve a necessidade de redução da emissão dos gases do efeito estufa provenientes da agricultura, interromper a conversão de florestas em terras agrícolas e tornar a agricultura resiliente as mudanças climáticas que afetam a capacidade produtiva (SEARCHINGER, 2019)

Além dos problemas anteriormente citados, as pragas e agentes causadores de doenças, como por exemplo, vírus, bactérias, fungos, nematoides, ácaros, insetos e plantas daninhas estão entre os principais fatores que reduzem a produção agrícola. De acordo com a FAO, em média as pragas e doenças respondem por 20-40% das perdas de produção em todo o mundo, custando à economia global um total de US$ 290 bilhões. No Brasil, os estados de Mato Grosso e Pará são os maiores produtores de soja, milho e algodão, e alta produtividade aliado ao clima quente e úmido, tornam está região altamente suscetível a disseminação e surto de diferentes pragas e doenças (CONAB, sd). Se estas não forem corretamente tratadas e controladas, podem levar a perdas de 30-40% da produção das culturas supracitadas (CEPEA, 2019).

A agricultura moderna é altamente dependente do uso de defensivos agrícolas para o controle de pragas e doenças. Em 2020 o consumo global de agrotóxicos foi de cerca de 2,7 milhões de toneladas, o que corresponde a um aumento de aproximadamente 50% em relação a 1990 (FAO, 2022a). Dentre os agrotóxicos, os herbicidas são os mais utilizados (40%), seguidos pelos inseticidas (30%) e fungicidas (20%) (FORINI et al., 2022) Apesar dos efeitos positivos dos agrotóxicos na agricultura, em termos de controle de pragas e aumento da produtividade, essas formulações desencadearam efeitos colaterais significativos ao meio ambiente e ao ser humano

devido à sua toxicidade fora do alvo e alta persistência (QU et al., 2021). Além disso, já se sabe que, entre 10-75% dos pesticidas aplicados não atingem seus alvos, indo para o ecossistema vizinho, e da quantidade que atinge o alvo, apenas 1% exerce sua atividade biológica, dentro do corpo do inseto (HE; ZHAO; YU, 2016; MASSINON et al., 2017; ZHAO et al., 2018). Outro problema acerca do uso intensivo dos agroquímicos é a seleção de pragas que apresentam resistência aos ingredientes ativos presentes nas formulações de agroquímicos.

Apesar dos efeitos benéficos dos agrotóxicos no controle de uma ampla gama de pragas e doenças, recentemente, há uma crescente preocupação pública em relação às questões ambientais e de saúde a respeito do uso excessivo destes compostos. Essa preocupação crescente tem desafiado a academia e a indústria do setor a desenvolver novas tecnologias e métodos mais seguros e eficientes para controlar pragas e doenças (BALAH, 2020). Nesse sentido, a utilização de compostos de origem natural, como os biopesticidas, surgem como uma opção para ajudar na redução da dependência da agricultura as moléculas sintéticas. Essas moléculas naturais são, na maioria dos casos, mais seguras, mais ecológicas e menos persistentes do que as compostos sintéticos. Além disso, esses biopesticidas possuem diferentes modos de ação, o que reduz o desenvolvimento de pragas resistentes (MUÑOZ et al., 2020).

A *Curucuma longa* L. (Zingiberales: Zingiberaceae) é uma planta herbácea, a qual possui ramificações laterais alongadas e é originária da Ásia. A cúrcuma em pó é extraída dos rizomas secos desta planta e é amplamente empregada na culinária. Além disso, os produtos naturais extraídos desta planta apresentam diversas atividades de fins terapêuticos, tais como antimicrobiana, antifúngica, inseticida, anti-inflamatória, analgésica, digestiva e propriedades antioxidantes. Ademais, extratos aquosos, suco fresco e o óleo essencial extraído da *C. longa* têm demonstrado atividade pesticida contra diferentes pragas de interesse agrícola, bem como atividade repelente contra mosquitos vetores de doenças (CUI et al., 2022; DAMALAS, [s.d.]; DE SOUZA TAVARES et al., 2016; MATIADIS et al., 2021; RIAZ et al., 2015; TAVARES et al., 2013). O exato mecanismo de ação da curcumina ainda não é totalmente elucidado, mas em insetos os curcuminóides agem inibindo atividade enzimática do sistema nervoso central e através

da inibição da proliferação celular (CUI; LI; ZHU, 2016; PRASAD; MURALIDHARA, 2014; ZHANG et al., 2018)

O carvacrol é um monoterpeno fenólico que constitui diferentes óleos essenciais da família Lamiaceae, como por exemplo *Coridothymus, Origanum, Satureja, Thymbra* e *Thymus* (MUÑOZ et al., 2020). Estudos do efeito do carvacrol nos receptores de GABA em mosca doméstica e barata-americana demonstraram que este monoterpeno é um modulador positivo do receptor de GABA em insetos, o que pode causar efeitos inibitórios no sistema nervoso central (TONG; COATS, 2010) Além disso, o carvacrol é um inibidor da enzima acetilcolinesterase, através da ligação não competitiva a receptores nicotínicos de acetilcolina (TONG et al., 2013a).

Embora os compostos naturais apresentem múltiplas vantagens, sugerindo que em breve poderão diminuir e/ou substituir o uso dos pesticidas sintéticos, existem algumas limitações que precisam ser melhoradas. As limitações que dificultam a plena implementação dos compostos naturais são a escassez de produtos para atender às demandas dos agricultores, a lentidão de ação que eles geralmente apresentam, a sensibilidade a diferentes fatores ambientais, a estabilidade de curta duração e diferentes métodos e diretrizes de preparo padrão.

Para contornar os problemas mencionados, a combinação de compostos naturais com sistemas carreadores é fundamental para o desenvolvimento de formulações de biopesticidas mais eficientes. Através do encapsulamento destes compostos é possível modular a liberação dos ingredientes ativos, melhorar a estabilidade físico-química, protege-los da influência dos fatores ambientais , diminuir as perdas por volatilização, aumentar a solubilidade aquosa e melhorar a bioatividade, além de reduzir possíveis efeitos tóxicos a organismos não-alvo (ALBUQUERQUE et al., 2022; CAMPOS et al., 2018a; DE OLIVEIRA et al., 2020; MENOSSI et al., 2021).

Nanopartículas poliméricas tem sido amplamente estudadas para o carreamento de compostos naturais visando o controle de pragas e doenças de importância agrícola tanto pré como pós-colheita (OLUOCH et al., 2021; YEGUERMAN et al., 2022).Os polímeros naturais, também conhecidos como biopolímeros, são moléculas formadas naturalmente, que são sintetizadas ao longo do ciclo de vida de diversos tipos de organismos, como plantas, microrganismos e animais. Sua estrutura é composta por

unidades monoméricas repetidas, que podem ser do mesmo tipo ou uma combinação de diferentes tipos. Polímeros naturais, apresentam biocompatibilidade, alta biodegradabilidade, baixa ou nenhuma toxicidade, boa estabilidade e baixo custo. Os polímeros naturais podem ser agrupados em polissacarídeos, proteínas, polipeptídeos, polinucleotídeos, polifenóis e polihidroxialcanoatos.

As proteínas têm se destacado como sistemas carreadores, pois apresentam propriedades desejáveis como material encapsulante, tais como solubilidade adequada, viscosidade, capacidade de emulsificação e formação de filme (HONG et al., 2020; ZHONG; QIAO; YUAN, 2022). Proteínas vegetais hidrofóbicas, como por exemplo, a zeína são menos onerosas e apresentam menor toxicidade quando comparadas com proteínas de origem animal (ELZOGHBY; SAMY; ELGINDY, 2012; OLIVEIRA et al., 2018; YAN et al., 2022).

A zéina é uma proteína de armazenamento encontrada em plantas de milho, a qual apresenta em sua estrutura aproximadamente 50% de aminoácidos de caráter hidrofóbico (alanina, leucina e prolina), conferindo a esta proteína um caráter anfifílico (PATEL, 2020). Devido a sua estrutura, a zeína é solúvel em acetona, acetil acetona e etanol, mas é insolúvel em água (LI et al., 2012; MOMANY et al., 2006) . Além disso a zeína apresenta uma certa resistência a ação de algumas enzimas, fazendo com que a sua degradação ocorra de forma mais lenta, possibilitando assim o desenvolvimento de sistemas carreadores de liberação controlada responsivos a ação enzimática (LUO; WANG, 2014; MONTEIRO et al., 2021a).

As formulações baseadas em nanotecnologia têm-se mostrado promissoras para o desenvolvimento da agricultura sustentável como mostra o crescente número de estudos disponíveis na literatura, porém, a validação e comercialização de tais produtos no mercado ainda são incipientes. Para a comercialização bem-sucedida desses produtos será necessário uma melhor validação do desempenho destas formulações em condições de campo, bem como a criação de um acordo regulatório a nível mundial (CAMPOS et al., 2022c). As aplicações de tais produtos na agricultura podem afetar diversos organismos-alvo e não-alvo, demandando desta forma, uma ampla avaliação nos estudos de segurança destas formulações.

Logo, o objetivo da presente tese foi preparar e caracterizar nanopartículas de zeína para o carreamento conjunto de curcumina e carvacrol para ser usado como formulação alternativa para o controle de pragas de interesse agrícola. Além disso, foi avaliada a citotoxicidade em culturas de células *in vitro* e atividade biológica dos sistemas produzidos em ácaro rajado *Tetranychus urticae* e diferentes espécies de lagarta (*Spodoptera cosmioide, Spodoptera eridania, Spodoptera frugiperda* e *Helicoverpa armigera).* A tese está estruturada em capítulos compostos por artigos publicados e/ou submetidos para periódicos científicos internacionais. **O primeiro capítulo,** consiste em um artigo de revisão de literatura sobre as estratégias para o uso de sondas fluorescentes como ferramenta para tornar as nanopartículas poliméricas rastreáveis e estudar a captação e translocação desses sistemas em plantas, bem como seu destino ambiental. Neste capitulo são abordadas as diferentes formas de marcação dos polímeros com sondas fluorescentes e também são sumarizados os principais corantes empregados para rastreamento em plantas. Também foram apresentados os recentes avanços e principais limitações desta abordagem. **O segundo capítulo** discorre sobre o preparo e caracterização das nanopartículas de zeína co-encapsulando curcumina e carvacrol. Os possíveis efeitos citotóxicos a organismos não-alvo *in vitro* usando cultura de células, bem como a atividade biológica em diferentes pragas de interesse agrícola. **O terceiro capítulo**, é focado no desenvolvimento e caracterização de sistemas carreadores marcados com sondas fluorescentes, bem como a avaliação do movimento foliar dessas partículas. Por conseguinte, a translocação das nanopartículas da folha para o caule e raízes foi avaliado.

Referências

ALBUQUERQUE, P. M. et al. Biotechnological Applications of Nanoencapsulated Essential Oils: A Review. **Polymers**, v. 14, n. 24, p. 5495, jan. 2022.

BALAH, M. A. Weed control ability of Egyptian Natural Products against annual, perennial and parasitic weeds. **Acta Ecologica Sinica**, v. 40, n. 6, p. 492–499, 1 dez. 2020.

CAMPOS, E. V. R. et al. Carvacrol and linalool co-loaded in β-cyclodextrin-grafted chitosan nanoparticles as sustainable biopesticide aiming pest control. **Scientific Reports**, v. 8, n. 1, p. 7623, 16 maio 2018.

CAMPOS, E. V. R. et al. Nature-Based Nanocarrier System: An Eco-friendly Alternative for Improving Crop Resilience to Climate Changes. **Anthropocene Science**, v. 1, n. 3, p. 396–403, 1 set. 2022.

Cepea_EstudoPragaseDoencas_Parte 1.pdf. , [s.d.]. Disponível em: <https://www.cepea.esalq.usp.br/upload/kceditor/files/Cepea_EstudoPragaseDoencas_Parte%201.pdf>. Acesso em: 8 fev. 2023

Conab - Séries Históricas das Safras. Disponível em: <http://www.conab.gov.br/info-agro/safras/serie-historica-das-safras?start=20>. Acesso em: 9 fev. 2023.

CUI, G. et al. Synergistic effects of botanical curcumin-induced programmed cell death on the management of Spodoptera litura Fabricius with avermectin. **Ecotoxicology and Environmental Safety**, v. 229, p. 113097, 1 jan. 2022.

CUI, Q.; LI, X.; ZHU, H. Curcumin ameliorates dopaminergic neuronal oxidative damage via activation of the Akt/Nrf2 pathway. **Molecular Medicine Reports**, v. 13, n. 2, p. 1381–1388, 1 fev. 2016.

DAMALAS, C. A. Potential Uses of Turmeric ('Curcuma longa') Products as Alternative Means of Pest Management in Crop Production. **Plant Omics**, v. 4, n. 3, p. 136–141, [s.d.].

DE OLIVEIRA, J. L. et al. Hydrogels Containing Botanical Repellents Encapsulated in Zein Nanoparticles for Crop Protection. **ACS Applied Nano Materials**, v. 3, n. 1, p. 207–217, 24 jan. 2020.

DE SOUZA TAVARES, W. et al. Turmeric powder and its derivatives from Curcuma longa rhizomes: Insecticidal effects on cabbage looper and the role of synergists. **Scientific Reports**, v. 6, n. 1, p. 34093, 2 nov. 2016.

ELZOGHBY, A. O.; SAMY, W. M.; ELGINDY, N. A. Protein-based nanocarriers as promising drug and gene delivery systems. **Journal of Controlled Release**, v. 161, n. 1, p. 38–49, 10 jul. 2012.

FORINI, M. M. L. et al. Nano-enabled weed management in agriculture: From strategic design to enhanced herbicidal activity. **Plant Nano Biology**, v. 1, p. 100008, 1 jun. 2022.

HONG, S. et al. Protein-Based Nanoparticles as Drug Delivery Systems. **Pharmaceutics**, v. 12, n. 7, p. 604, jul. 2020.

LI, Y. et al. Understanding the Dissolution of α-Zein in Aqueous Ethanol and Acetic Acid Solutions. **The Journal of Physical Chemistry B**, v. 116, n. 39, p. 12057–12064, 4 out. 2012.

LUO, Y.; WANG, Q. Zein-based micro- and nano-particles for drug and nutrient delivery: A review. **Journal of Applied Polymer Science**, v. 131, n. 16, 2014.

MASSINON, M. et al. Spray droplet impaction outcomes for different plant species and spray formulations. **Crop Protection**, v. 99, p. 65–75, 1 set. 2017.

MATIADIS, D. et al. Curcumin Derivatives as Potential Mosquito Larvicidal Agents against Two Mosquito Vectors, Culex pipiens and Aedes albopictus. **International Journal of Molecular Sciences**, v. 22, n. 16, p. 8915, jan. 2021.

MENOSSI, M. et al. Essential oil-loaded bio-nanomaterials for sustainable agricultural applications. **Journal of Chemical Technology & Biotechnology**, v. 96, n. 8, p. 2109–2122, 2021.

MOMANY, F. A. et al. Structural Characterization of α-Zein. **Journal of Agricultural and Food Chemistry**, v. 54, n. 2, p. 543–547, 1 jan. 2006.

MONTEIRO, R. A. et al. Zein based-nanoparticles loaded botanical pesticides in pest control: An enzyme stimuli-responsive approach aiming sustainable agriculture. **Journal of Hazardous Materials**, v. 417, p. 126004, 5 set. 2021.

MUÑOZ, M. et al. Phytotoxic Effects of Three Natural Compounds: Pelargonic Acid, Carvacrol, and Cinnamic Aldehyde, against Problematic Weeds in Mediterranean Crops. **Agronomy**, v. 10, n. 6, p. 791, jun. 2020.

OLIVEIRA, J. L. DE et al. Zein Nanoparticles as Eco-Friendly Carrier Systems for Botanical Repellents Aiming Sustainable Agriculture. **Journal of Agricultural and Food Chemistry**, v. 66, n. 6, p. 1330–1340, 14 fev. 2018.

OLUOCH, G. et al. Nanoencapsulation of Thymol and Eugenol with Chitosan Nanoparticles and the Effect against Ralstonia solanacearum. **Advances in Microbiology**, v. 11, n. 12, p. 723–739, 10 dez. 2021.

PATEL, A. R. Functional and Engineered Colloids from Edible Materials for Emerging Applications in Designing the Food of the Future. **Advanced Functional Materials**, v. 30, n. 18, p. 1806809, 2020.

Pesticides use, pesticides trade and pesticides indicators. [s.l.] FAO, 2022.

PRASAD, S. N.; MURALIDHARA. Neuroprotective effect of geraniol and curcumin in an acrylamide model of neurotoxicity in Drosophila melanogaster: Relevance to neuropathy. **Journal of Insect Physiology**, v. 60, p. 7–16, 1 jan. 2014.

QU, R.-Y. et al. Where are the new herbicides? n. 77, p. 2620–2625, 2021.

RIAZ, M. R. et al. POTENTIAL OF TURMERIC EXTRACT AND ITS FRACTIONS TO CONTROL PEACH FRUIT FLY (DIPTERA: TEPHRITIDAE). **Ciência e Agrotecnologia**, v. 39, p. 545–552, dez. 2015.

SEARCHINGER, T. (ED.). **Creating a Sustainable Food Future: a Menu of Solutions to Feed Nearly 10 Billion People by 2050. Final Report, July 2019**. Washington D.C. (Washington - USA): World Resources Institute, 2019.

SILVA, J. V.; GILLER, K. E. Grand challenges for the 21st century: what crop models can and can't (yet) do. **The Journal of Agricultural Science**, v. 158, n. 10, p. 794–805, dez. 2020.

TAVARES, W. DE S. et al. Ar-turmerone from Curcuma longa (Zingiberaceae) rhizomes and effects on Sitophilus zeamais (Coleoptera: Curculionidae) and Spodoptera frugiperda (Lepidoptera: Noctuidae). **Industrial Crops and Products**, v. 46, p. 158–164, 1 abr. 2013.

TONG, F. et al. The phenolic monoterpenoid carvacrol inhibits the binding of nicotine to the housefly nicotinic acetylcholine receptor. **Pest Management Science**, v. 69, n. 7, p. 775–780, 2013.

TONG, F.; COATS, J. R. Effects of monoterpenoid insecticides on [3H]-TBOB binding in house fly GABA receptor and 36Cl− uptake in American cockroach ventral nerve cord. **Pesticide Biochemistry and Physiology**, v. 98, n. 3, p. 317–324, 1 nov. 2010.

YAN, X. et al. Zein-based nano-delivery systems for encapsulation and protection of hydrophobic bioactives: A review. **Frontiers in Nutrition**, v. 9, 2022.

YEGUERMAN, C. A. et al. Essential oils loaded on polymeric nanoparticles: bioefficacy against economic and medical insect pests and risk evaluation on terrestrial and aquatic non-target organisms. **Environmental Science and Pollution Research**, v. 29, n. 47, p. 71412–71426, 1 out. 2022.

ZHANG, L. L. et al. Bioinformatics analysis to identify possible mechanisms of action of curcumin against tea geometrid. **Journal of Applied Entomology**, v. 142, n. 3, p. 333–339, 2018.

ZHAO, X. et al. Development Strategies and Prospects of Nano-based Smart Pesticide Formulation. **Journal of Agricultural and Food Chemistry**, v. 66, n. 26, p. 6504–6512, 5 jul. 2018.

ZHONG, J.; QIAO, R.; YUAN, W.-E. Editorial: Protein-based nanocarriers for delivery of nutraceutical, diagnostic and therapeutic agents. **Frontiers in Pharmacology**, v. 13, 2022.

CAPÍTULO I

Fluorescent labeling as a strategy to evaluate uptake and transport of polymeric nanoparticles in plants

Artigo publicado em https://doi.org/10.1016/j.cis.2022.102695

Abstract

The use of biodegradable nanopolymers in agriculture offers an excellent alternative for the efficient delivery of agrochemicals that promote plant protection and development. However, tracking of these systems inside plants requires complex probe tagging strategies. In addition to providing a basis for better understanding such nanostructures to optimize delivery system design, these probes allow monitoring the migration of nanoparticles through plant tissues, and determine accumulation sites. Thus, these probes are powerful tools that can be used to quantify and visualize nanoparticle accumulation in plant cells and tissues. This review is an overview of the methods involved in labeling nanocarriers, mainly based on polymeric matrices, for the delivery of nanoagrochemicals and the recent advances in this field.

Keywords: chemical uptake, translocation, plants, nanoparticles, fluorescent probe

Introduction

The world population has already exceeded 7.9 billion, and is expected to reach 9.2 billion by 2050. This increase is expected to increase the worldwide food demand by approximately 59-102%. Therefore, agricultural production will need to be increased by 60-70% to properly meet the nutritional needs of the world population by 2050 (VAN DIJK et al., 2021). Although numerous initiatives have been undertaken to combat hunger and malnourishment worldwide, food insecurity remains a serious issue in many countries. Due to the adverse effects of the COVID-19 pandemic, approximately 9.9% of the world population was affected by hunger in 2020, which is higher compared to the rate in 2019 (FOA et al., 2021).

Several factors are responsible for the decrease in agricultural productivity and the consequent reduction in global food supply. Among these factors, pests alone account for approximately 45% of the total global food losses. Pre-harvest pests, such as weeds, insects, and plant pathogens, contribute to 30% of these losses, whereas post-harvest pests, such as rodents, microorganisms, and insects, are responsible for 10-20% of them (PIMENTEL, 2019). Thus, it is imperative to identify new measures for pest control. Pesticides (mainly herbicides, followed by insecticides and fungicides) have been reported as the most widely used pest control agents since 1940 (CARVALHO, 2017).

Hedlund et al. evaluated the association between pesticide use and economic development based on the gross domestic product (GDP) rates of different countries from 1990 to 2014. They found that economic development is positively-associated with the use of pesticides and fertilizers, as there was no decline in their use at high levels of economic development (HEDLUND; LONGO; YORK, 2020). They also found that the utilization of pesticides exponentially increased over the years as modern conventional agriculture became dependent on large amounts of these products, despite the harmful effects on the environment and human health.

It has been predicted that in general only 0.1-10% of pesticides reach their target pests, whereas the rest is lost to the environment through degradation, volatilization, and lixiviation, which results in intensification of the quantity of pesticide application (KAH et al., 2018). This intensive and extensive use of pesticides leads to increased pest resistance, decreased nitrogen fixation, reduced soil biodiversity, and increased bioaccumulation of pesticides, and thereby cause financial losses and pose great risks to the environment and human health (HAYLES et al., 2017; XIANG et al., 2017). In this regard, Carvalho et al. emphasized risks to human health such as cancer, obesity, and endocrine disturbances, which arise due to widespread environmental contamination of water and food resources, and the occupational risks generated by the excessive application of agrochemicals (CARVALHO, 2017).

Agriculture is among the socio-economic sectors that are most sensitive to climate change, which negatively affects crop and livestock production worldwide. To this end, numerous challenges are yet to be faced to maximize agricultural production sustainably and at a level sufficient to meet global food demand, and thereby to contribute to the

reduction of poverty and inequality. Thus, developing strategies to deal with the adverse effects of climate change is a great challenge, especially for developing countries, in order to achieve environment-friendly and healthy agricultural practices that are resilient to climate change as well (MULUNEH, 2021; PEDROSA et al., 2021).

In this context, the 2030 Agenda adopted by all United Nations members outlined 17 sustainable development goals (SDG) for developed and developing countries. These goals aim to create strategies to improve health and education, reduce inequality, stimulate economic growth, and preserve the environment (UNITED NATIONS, 2020). Within this framework, there is an emerging market for nanotechnologies at the forefront of the new agricultural era. Nanotechnologies have indeed offered numerous creative solutions for the sustainable development of agriculture as they directly act to reduce the environmental impacts of pesticides and improve the effectiveness of biopesticides.

Several studies have demonstrated the potential of nanotechnology in agriculture. Regardless of material type, high surface area per unit volume at the nanoscale provides nanomaterials with unique properties such as high solubility, reactivity, dispersibility, stability, fluidity, and better targeting of pesticides with higher efficiency and longer life (CHEN et al., 2020; SASSON et al., 2020). These properties enable the development of nanoformulations that significantly improve the delivery of agrochemicals to their respective sites of action when compared to conventional applications, and thereby support sustainable agricultural practices, increase safety, and provide financial gains (FEREGRINO-PEREZ et al., 2018).

Macro- and micro-nutrients are also absorbed better when encapsulated within nanoparticles. Thus, the issue of reduced efficiency in the use of these nutrients (macronutrients) observed in recent decades, which consequently led to decreased production, may also be overcome using nanotechnology (LIU; LAL, 2015; SU et al., 2019). In this context, nano-based formulations used in plant nutrition aim to increase the efficiency of existing fertilizers either by improving the bioavailability of elements or by decreasing the loss of mobile nutrients to the surrounding environment (LIU; LAL, 2015).

Different types of materials can be used to produce agrochemical-loaded nanoparticles. Polymers, proteins, lipids, and carbohydrates have received considerable

attention as they are less harmful to the environment compared to the other alternatives (SASSON et al., 2020). The choice of material depends on the desired characteristics, such as biodegradability, biocompatibility, properties related to nanoparticle formation, complexation, and surface functionalization capacity. This choice will also depend on whether the active compound used is hydrophobic or hydrophilic, the release rate, radiation protection, light-responsive release, pH, and temperature (MAKVANDI et al., 2021; ZIELIŃSKA et al., 2020). Finally, the choice of nanoparticle fabrication technique also depends on the substances chosen for fabrication, such as the active ingredient, polymer, and surfactant (SHAKIBA et al., 2020).

Tracking of systems based on polymeric matrices or organic compounds in different media and organisms is cumbersome, and thus requires adequate strategies for monitoring. Insertion of functionalized probes into these systems allows tracking of their location and even quantification in plants, organisms, and soil through a series of analytical and imaging techniques (SASSON et al., 2020). A detailed understanding of the path and final goal of the use of nanopesticides leads to a better understanding of their mode of action, allows an assessment of the benefits and possible risks associated with these nanostructures (KAH et al., 2018), and contributes to their regulation in agricultural practices.

The visualization of polymeric nanoparticles and its quantification in biological compartments are concerns of major importance to evaluate their fate, intracellular trafficking and cell levels on the plants and the environment. In addition, the dose quantification is essential to determine the relationship between dose and toxicological end-points. In this way, labelling polymeric nanoparticles with fluorescent probe is pivotal for their visualization and quantification on the biological compartments. Organic dyes are the most used probes in fluorescent biological imaging due its particularity, such as versatility, availability and low price (FÄRKKILÄ et al., 2021). To produce fluorescently labelled nanoparticles the dye could be encapsulated in the core during nanoparticles synthesis or the covalently attachment on the polymer backbone before nanoparticles synthesis. In this review, we provide an overview of labeling methods used to render nanoparticles traceable in biological matrices to better

understand their uptake and translocation by plants as well as their fate in the environment.

Plant-nanoparticle interactions

Nanoparticles can be administered either to the aerial parts or the roots of plants. Several methods have been used for this purpose, including seed priming, foliar spraying, irrigation, stem injection, and biolistic or hydroponic treatments (SINGH et al., 2021) (Figure 1).

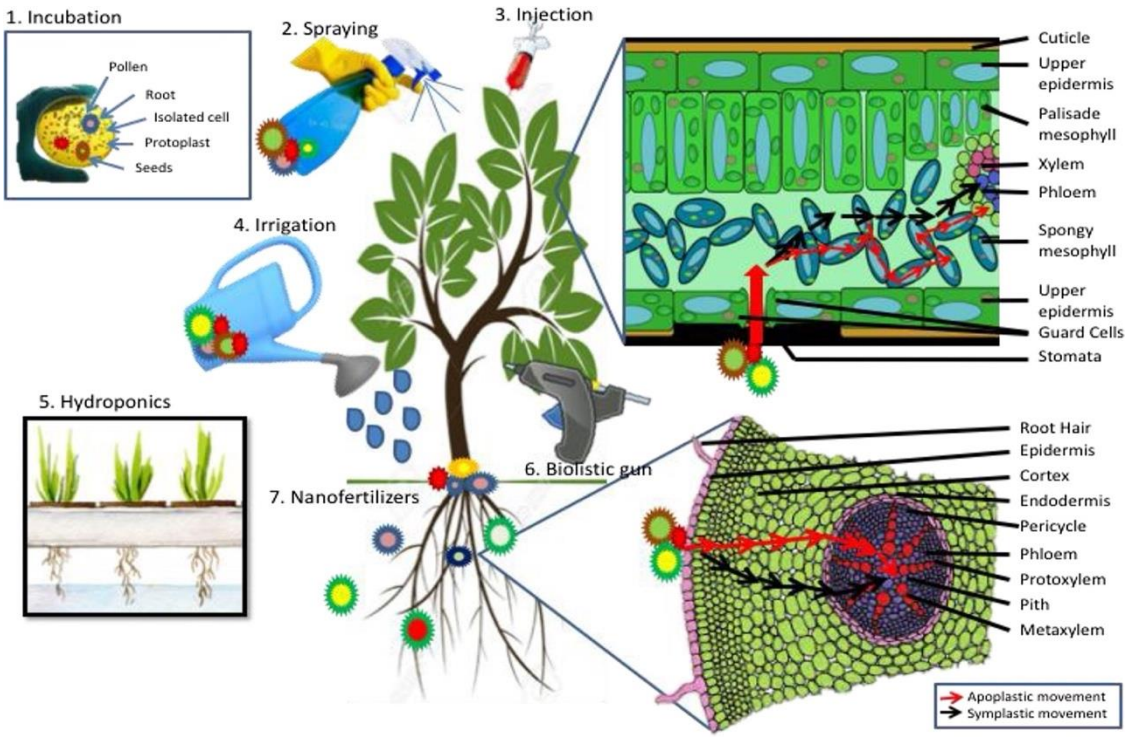

Figure 1-0-I: Different modes of application, uptake and apoplastic and symplastic translocation of nanoparticles in plants. The image is reprinted with permission from SINGH et al. (2021).

Several factors can influence the interaction of nanomaterials with plants (*i.e.,* their adsorption, internalization, translocation, and bioaccumulation). Plant-related factors include the plant species itself, location of the plant, age, transpiration rate, biotic and abiotic stress. Nanomaterial-related factors include the size, chemical composition, physicochemical properties, surface functionalization, stability, and exposure time. These interactions are responsible for beneficial (*e.g.* increase in yield

and quality of products) as well as harmful effects (*e.g.* consumption of nanomaterials by the final consumer and nanotoxicity) (KRANJC; DROBNE, 2019)

Kranjc and Drobne (2019) provided an overview of interactions between nanoparticles and plants. When foliar spray is applied, nanoparticles can be retained in the outermost layer of the cuticle (Figure 2-A), internalized through the openings of the stomata, and translocated to the roots through the phloem (KRANJC; DROBNE, 2019). The stomata are usually present in 5% of the leaf surface mainly in the lower part of the leaf, which reduces the spray application efficiency. However, the stomata also have an average size of 10 μm, which allows nanoparticle entry. The stomata regulate the exchange of water and gas with the environment by opening and closing according to CO_2 concentration, humidity, temperature, and light intensity in the environment (SU et al., 2019).

Even when nanoparticles reach the phloem either by overcoming the cuticle/epidermis or through the stomata, internal components, such as mucilage and excreted exudates can still hinder the translocation of these nanoparticles by holding and preventing them from reaching the root system. Moreover, external factors may be involved as well, such as epicuticular waxes, which increase the hydrophobicity of the leaf surface and prevent the nanoparticles from remaining on the surface for longer durations, thus reducing absorption possibility (SU et al., 2019).

Nanomaterials can be delivered to the roots, internalized together with water and nutrients, and then translocated to aerial parts (KRANJC; DROBNE, 2019). The type of plant greatly influences the penetration of nanoparticles through the root. For example, monocots are more sensitive to exposure to nanoparticles as they have a fibrous root system and larger surface area (SU et al., 2019). When nanoparticles are absorbed at the root, the reach of the xylem and phloem can be impeded by the Casparian strip, which deviates from the route for symplastic transport through the cellular plasmodesmata to the destination (KRANJC; DROBNE, 2019). The endodermis of plants, which is the innermost cell layer nearby central vasculature is composed of two types of cells: the passage cells, which are know as thin-walled cells and “impermeable” endodermal cells with thickened walls. Each endodermal cells contain a Casparian strip, which impedes the apoplastic flow of water into the root structure. On the other hand, the passage cells cells allow symplastic transport, which constitutes the pathway to

water and dissolved solutes from the root to xylem. This is likely the only passageway for nanoparticles in intact roots. Damaged roots and secondary root emergence points can be alternative crossing points for NPs (KRANJC; DROBNE, 2019). Several other factors can also interfere with root absorption, including growth medium, beneficial microorganisms such as mycorrhizal fungi, and chemical interferences such as pH, ion exchange capacity, and root exudates (SINGH et al., 2021).

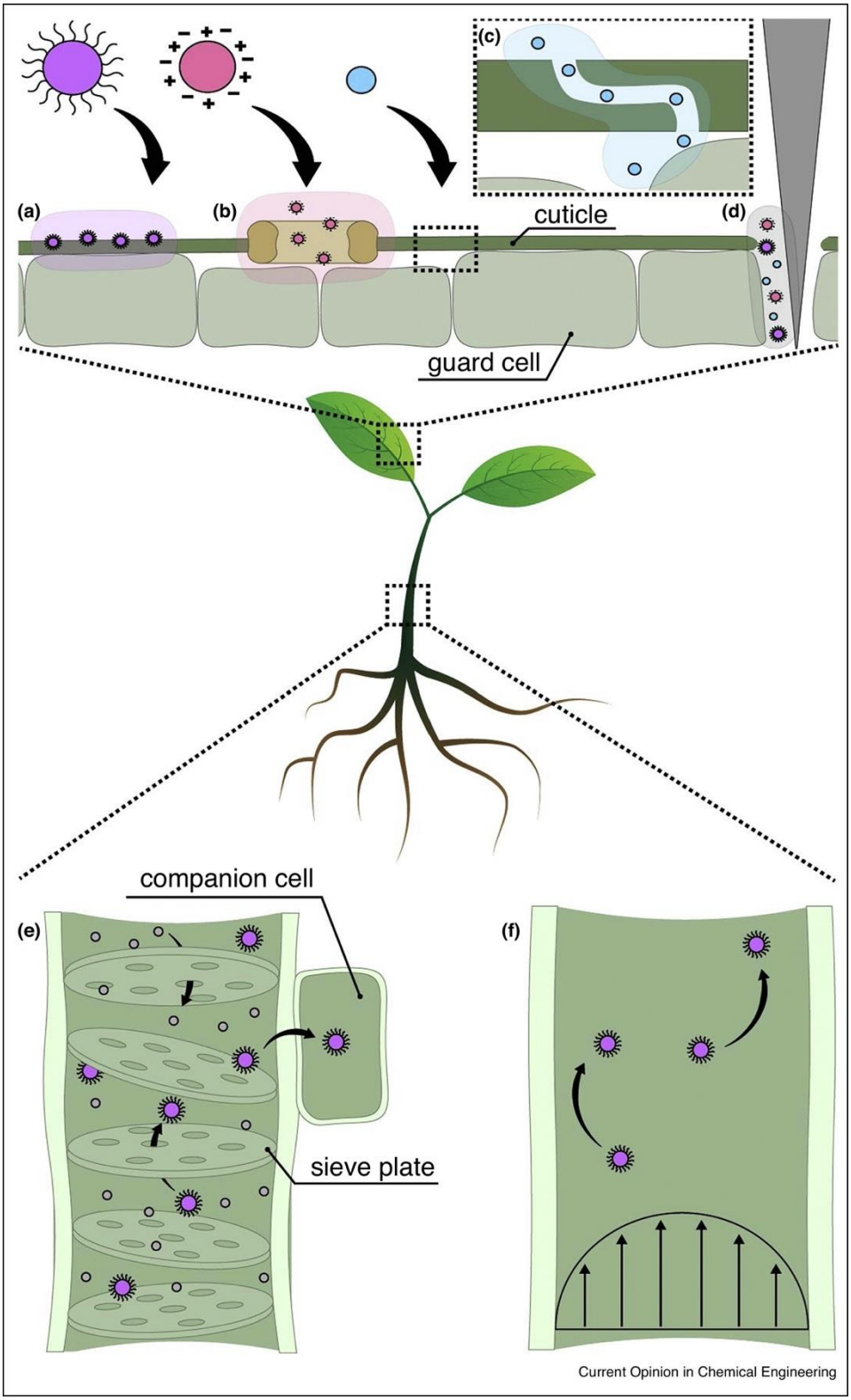

Figure 1-0-II: Different modes of application, uptake and apoplastic and symplastic translocation of nanoparticles in plants. The image is reprinted with permission from Ref.(SINGH et al., 2021)

Nano-based formulations are developed to systemically deliver both nutrients and pesticides. Thus, translocation of nanoparticles via the plant vascular route is essential to achieve the required biological effects. The phloem mostly contains sieve cells connected by sieve plates (HÖLTTÄ; MENCUCCINI; NIKINMAA, 2009) (Figure 2-E) with diameters ranging from 200 nm to 1.5 μm in most plants, forming a porous arrangement (RICO et al., 2011; SCHULZ, 2015; UZU et al., 2010; WANG; TARAFDAR; BISWAS, 2013). Unless aggregated, it is considered that most nanoparticles are able to pass the phloem. The xylem (Figure 2-F) is composed of tracheids and vessel elements, which are conductive cells that form a porous membrane with pore sizes between 43 and 340 nm (JANSEN; CHOAT; PLETSERS, 2009; NOTAGUCHI; OKAMOTO, 2015; ZHANG; KLEPSCH; JANSEN, 2017). These pores can limit nanoparticle transportation, and thereby lead to their accumulation in cells (CORREDOR et al., 2009; WANG et al., 2012). Binding of different types of nanoparticles to chelators has been demonstrated to facilitate their transport through the phloem (SUN et al., 2014; TAN; PERALTA-VIDEA; GARDEA-TORRESDEY, 2018; WANG et al., 2012; ZHAI et al., 2014). In addition, negatively-charged nanoparticles are also shown to be transported from roots to shoots via the xylem (SPIELMAN-SUN et al., 2017; ZHU et al., 2012). Similarly, metallic and polymeric nanoparticles were also shown to be efficiently translocated via the phloem (AVELLAN et al., 2019; KARNY et al., 2018; LICO; BENVENUTO; BASCHIERI, 2015; WU et al., 2021; ZHANG et al., 2020). For example, Raliya et al. applied gold nanoparticles to watermelon leaves, and found that the nanoparticles were transported from mesophyll cells to the phloem via the symplastic pathway (RALIYA et al., 2016). However, the vascular transport of NPs in plants has been reported only in few past studies. Thus, it is not possible to draw conclusions regarding the patterns of NP transport via this route. In addition, the route of NP translocation was also found to be determined mainly by the NP size, surface charge, and chemical properties (XIA et al., 2021).

In addition to the physicochemical characteristics of nanoparticles, their transport via the vascular route can be affected by the sap composition and flow rate as well. Sap composition varies according to the development stage of the plant and its location (leaf, stem, root trunk), and it may constitute varying amounts of water and nutrients, which can cause aggregation, sedimentation, and even dissolution of NPs. In addition, interaction of the NPs with organic molecules is also a poorly-studied aspect

that might affect nanoparticle transport as well via the formation of protein corona on the nanoparticle surface and the changes in the hydrodynamic size and surface modifications. The types of methods of corona protein formation on nanoparticles, their influence on nanoparticle transport in plants, and the resulting biological response have not been fully understood yet (SU et al., 2019; XIA et al., 2021).

Strategies to evaluate uptake, translocation and environmental fate of nanoparticles

The increasing global population, food insecurity, and aggravated effects of climate change have enhanced the interest in nanotechnological applications to increase agricultural productivity. However, nano-based formulations in the agrobusiness sector should also be used responsibly after performing a precise assessment of the interaction between nanoparticles and plants. To this end, a good understanding of the uptake mechanisms, routes of translocation and accumulation, and possible toxicities of the nanoparticles is essential. Evaluation of the aspects of nano-based formulations on non-target organisms and their fate in the environment to predict their effects on the ecosystem is also crucial.

Although several studies on the interaction of different nanoparticles with plants have been conducted recently, issues related to how likely the nanoparticles are taken up by the plant leaves and/or roots and systemically transported, and which characteristics control nanoparticle uptake and accumulation remain unclear. Most studies published in the literature are related to the uptake and translocation of metallic nanoparticles, as these materials have intrinsic properties that enable easy tracking by microscopy and X-ray scattering techniques. In contrast, tracking of polymeric nanoparticles in the environment has rarely been reported, as these materials lack intrinsic characteristics that allow traceability (SHAKIBA et al., 2020). Therefore, alternative strategies are used to detect these polymers.

Association with inorganic nanoparticles, such as gold and silver, iron oxide nanoparticles, quantum dots, carbon-based nanomaterials, and dye-doped silica nanoparticles is a strategy used detect polymers in an organic matrix (WOLFBEIS, 2015). These materials have been employed for bioimaging using electron microscopy, magnetic resonance imaging (MRI), computed tomography and fluorescent based

images. However, there are still few protocols in the literature to synthesize this nanocomposite system (inorganic nanoparticles in colloidal systems). Furthermore, disturbances in the physicochemical properties of polymeric nanoparticles, generating colloidal instability as well as low encapsulation efficiency, are recurrent in these kind of preparations (ALKILANY; ABULATEEFEH; MURPHY, 2018). Also, there are many reports in the literature that synthesized nanocomposite system using miniemulsion polymerization (CASSANO et al., 2021; HARUN et al., 2013; TU; YANG; GAO, 2008; WANG et al., 2020; YAO et al., 2019), however, this strategy in most cases use harsh organic solvent, monomers and surfactants and it is a complex and an expensive process (LOVELL; SCHORK, 2020).

In this review, however, we focus only on the utilization of fluorescent probes as a strategy for bioimaging applications. Fluorescent polymeric nanoparticles can be obtained mainly by two methods: physical loading into the nanoparticle core and covalent attachment to the polymer backbone (Figure 3A) (BEIJA; CHARREYRE; MARTINHO, 2011; BOU; KLYMCHENKO; COLLOT, 2021; BREUL; HAGER; SCHUBERT, 2013; PAPADIMITRIOU; SALINAS; RESMINI, 2016). Physical dye entrapment is an easy and efficient method to obtain fluorescent nanoparticles without causing changes in physicochemical properties of the polymer. However, this method requires the existence of strong hydrophobic interaction between the polymer and fluorescent probe to avoid dye leakage, which may result in misleading bioimaging conclusions as well as potential toxic effects. The dye leakage could decreases its brightness as well as generate a background signal, which difficult the accurate determination of nanoparticles sites (BOU; KLYMCHENKO; COLLOT, 2021; ONG et al., 2021). In addition, since the fluorescent probe is enclosed in a very small volume in the nanoparticle core, aggregation-caused quenching (ACQ) may occur as well. To this end, co-encapsulation of the fluorescent probe and bulky hydrophobic counterions was shown to be an efficient alternative to avoid probe leakage as well as the ACQ effect (ONG et al., 2021).

Covalent attachment of probes to the polymer structure is another approach that has been extensively studied for fluorescent labeling of polymeric nanoparticles (BREUL; HAGER; SCHUBERT, 2013). Here, covalent attachment can be performed by direct or post-polymerization labeling (Figure 3B). In direct labeling, incorporation of the fluorescent dye occurs during the polymerization step. However, a limitation of this

method is the need to synthesize a fluorescent probe that remains intact under highly destabilizing conditions such as high temperatures and the presence of Lewis acids or radicals which are required for the polymerization reaction. Direct labeling can be performed using a fluorescent probe that initiates the polymerization reaction (Figure 3B), or by adding a monomer that is fluorescent labeled during the polymerization reaction (Figure 3B.ii) (BOU; KLYMCHENKO; COLLOT, 2021; PAPADIMITRIOU; SALINAS; RESMINI, 2016). In post-polymerization labeling, the fluorescent probe is inserted into the pre-existing functional groups along the polymer backbone (Figure 3B.iii) or at the terminal position of the polymer using initiators (Figure 3B.iv). Post-polymerization labeling maintains the stability of the fluorescent probe since milder conditions are used compared to direct labeling. It is important to keep in mind that the fluorescent probe can impact the polymer chain arrangement. Similarly, the polymer can also alter the spectroscopic characteristics of the fluorescent probe (BEIJA; CHARREYRE; MARTINHO, 2011; BOU; KLYMCHENKO; COLLOT, 2021; PAPADIMITRIOU; SALINAS; RESMINI, 2016).

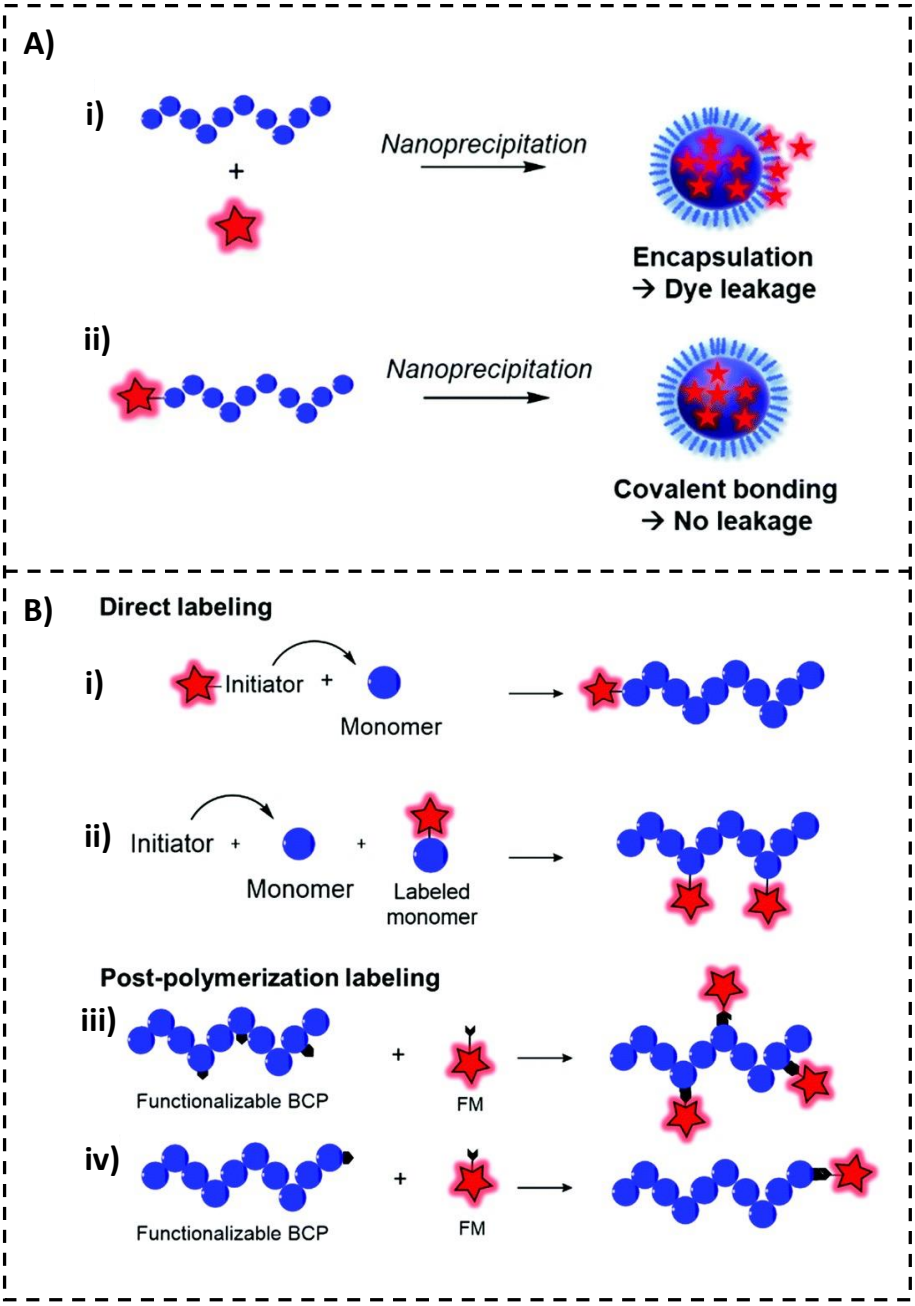

Figure 1-0-III: A) Difference between fluorescent labeling performed by (i) encapsulation of a fluorescent marker (FM) that is prone to dye leakage and (ii) covalent labeling avoiding the leakage. B) General strategies to incorporate a FM into a block copolymer backbone. Direct labeling by means of a fluorescent initiator (i) or a labeled monomer (ii). Post-polymerization labeling using reactive functional groups at the polymer backbone (iii) or the terminal end (iv). The FM is denoted with a red star. Reproduced

from Ref (BOU; KLYMCHENKO; COLLOT, 2021) with permission from the Royal Society of Chemistry.

To date, several types of fluorescent dyes have been synthesized, and are commercially available for fluorescence imaging applications. However, the choice of the fluorescent probe is still a crucial step in the development of fluorescent labelled polymeric nanoparticles for biological applications and to obtain images that provide the desired information efficiently. The following criteria are considered when choosing a fluorescent probe: i) the probe should show strong hydrophobic interaction with the polymer (physical entrapment), or have functional groups that allow covalent attachment to the polymer backbone; ii) the physicochemical properties such as charge, size, polarity and solubility should be compatible with the polymer; iii) the probe must be small with a high molar absorption coefficient (ϵ), quantum yield (ϕ), a substantial Stokes change, and reasonably photostable with low background interference; and iv) the toxicity of the probe should be taken into consideration even though only small amounts of probe are necessary for labeling (BEIJA; CHARREYRE; MARTINHO, 2011; BOU; KLYMCHENKO; COLLOT, 2021; ROBIN; O'REILLY, 2015). Figure 4 summarizes the interaction of different organic fluorescent probes with both polymeric and lipid-based nanoparticles. The choice of the organic dye as well as the most appropriate probe will vary with the type of material used and the intend application. Table 1 shows the most commonly used probes for fluorescent labeling of polymers as well as examples of studies that used these probes to label polymer-based nanoparticles.

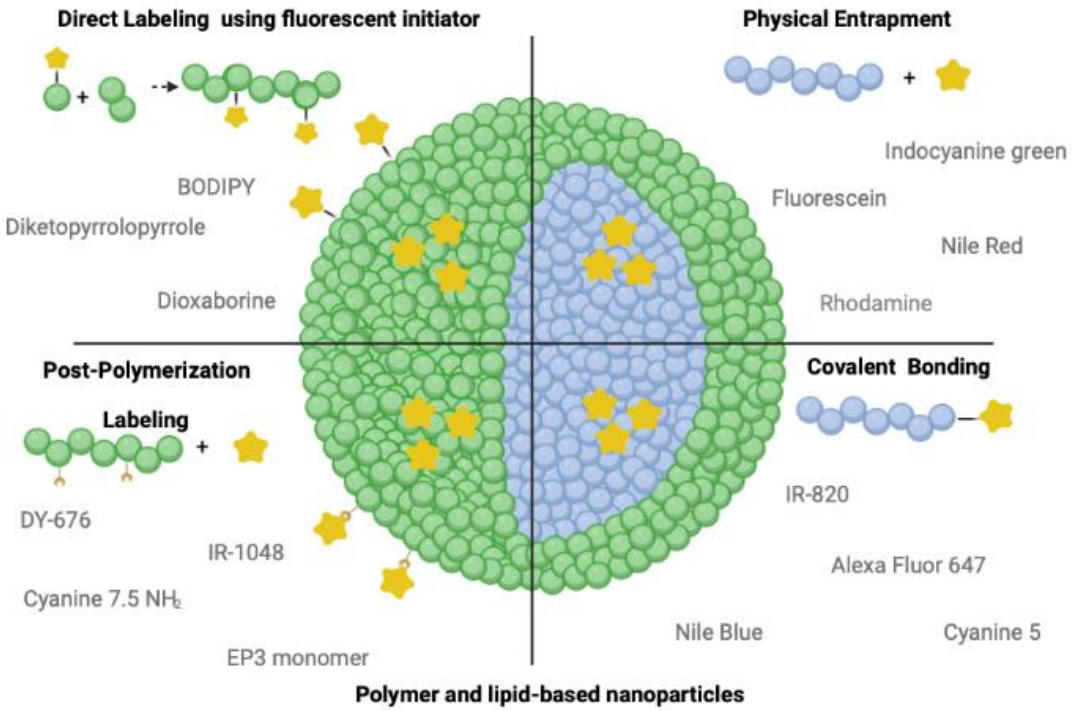

Figure 1-0-IV: Overview of the different strategies used to combine organic fluorescent dye and polymer and lipid-based nanoparticles discussed in this review. For each labeling methodology, the most used organic dyes are represented according to the table 1. The dye localization is represented by the yellow star. Some examples or organic dyes used for NPs labeling using the different techniques are exemplified. It is worth to mention that some dyes could be combined with NPs using more than one labeling approach.

Table 1-1: Main fluorescent probes used to label polymers and their main photophysical features. The references used in this table is to exemplify the method used for fluorescent labelled, but some examples are not used to agricultural applications.

Family	Fluorescent Probe	Main characteristics	Chemical structure	Label Method	References
Carbocyanines - Shows positive charge delocalized through a conjugated	Indocyanine green	**Extinction coefficient (ε):** 230,000 cm^{-1} M^{-1} **Quantum Yield (Φ)**: 0.04 **λexc/λem (nm):** 790/850 **Log P:** -0.29 at pH 7.4 **Solubility:** 1 mg/mL**	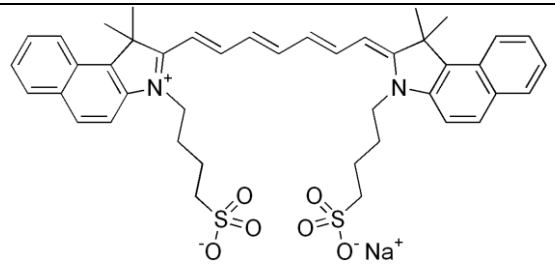	Physical entrapment	(CHEN et al., 2016; ZHU et al., 2019)
	Alexa Fluor 647	**Extinction coefficient (ε):** 270,000 cm^{-1} M^{-1} **Quantum Yield (Φ)**: 0.33 **λexc/λem (nm):** 650/665	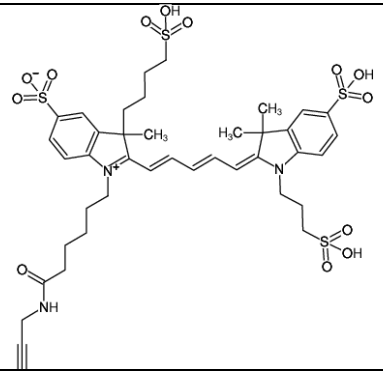	Covalent bonding and Physical entrapment	(BAGALKOT et al., 2015; MIAO et al., 2020)

polymethine chain - High extinction coefficients and high quantum yields in non-polar environment and organic solvents	IR-820	**Extinction coefficient (ε): ≥** 270,000 cm^{-1} M^{-1} **Quantum Yield (Φ)**: 0,12 **λexc/λem (nm):** 740/780*	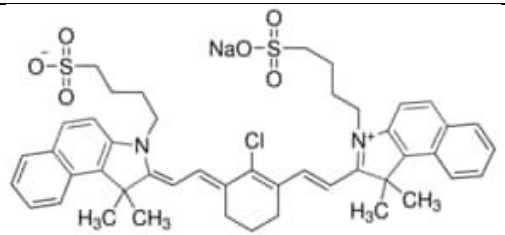	Covalent bonding and Physical entrapment	(MENDOZA et al., 2018)
	Cyanine 7.5 NH_2	**Extinction coefficient (ε):** 240,000 cm^{-1} M^{-1} **Quantum Yield (Φ)**: 0.30 **λexc/λem (nm):** 740/800	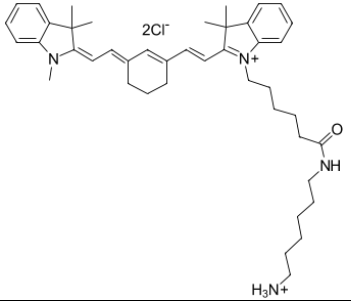	Post-labelling in polymer backbone	(MIKI et al., 2011)
	Cyanine 7-azide	**Extinction coefficient (ε):** 250,000 cm^{-1} M^{-1} **Quantum Yield (Φ)**: 0.30 **λexc/λem (nm):** 740/800	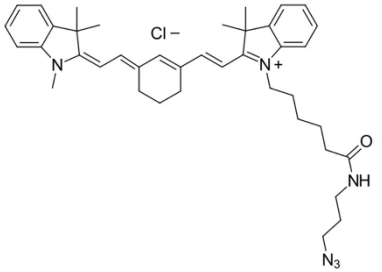	Physical entrapment	(SOBSKA et al., 2021)

	Cyanine 5	**Extinction coefficient (ε):** 250,000 cm^{-1} M^{-1} **Quantum Yield (Φ)**: 0.28 **λexc/λem (nm):** 640/680 **Solubility:** < 2 μM	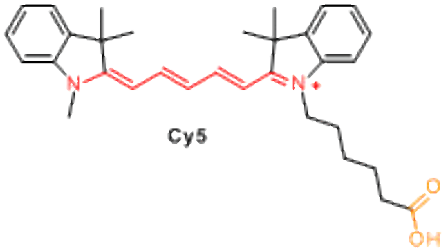	Covalent bonding and Physical entrapment	(O'CONNELL; NOONEY; MCDONAGH, 2017; TEXIER et al., 2009)
	Cyanine 5.5	**Extinction coefficient (ε):** 209,000 cm^{-1} M^{-1} **Quantum Yield (Φ)**: 0.20 **λexc/λem (nm):** 680/720 **Solubility:** 1 mg/L	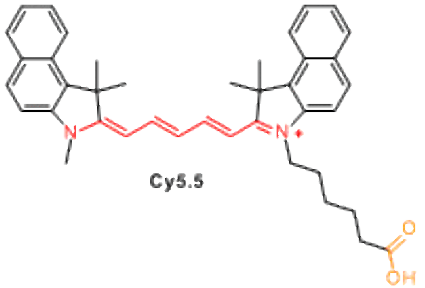	Physical entrapment	(SOBSKA et al., 2021)
	DY-547	**Extinction coefficient (ε):** 150,000 cm^{-1} M^{-1}** **Quantum Yield (Φ)**: 0.18 **λexc/λem (nm):** 550/570	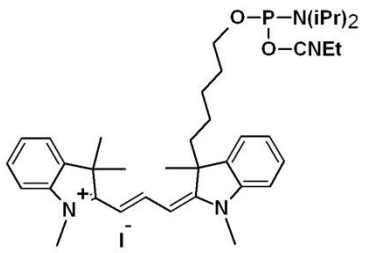	Post-labelling in polymer backbone	(VOLLRATH et al., 2012)
Benzopyrylium	DY-700	**Extinction coefficient (ε):** 140,000 cm^{-1} M^{-1}**		Covalent bonding (post-labelling)	(REUL et al., 2012)

- Shows positive charge delocalized between a nitrogen and oxygen - High brightness and long absorption and emission wavelengths - Functionalizable		**Quantum Yield (Φ)**: 0.25 **λexc/λem (nm):** 707/730**	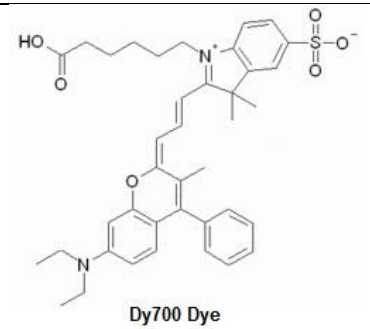 Dy700 Dye		
	DY-676	**Extinction coefficient (ε):** 180,000 cm^{-1} M^{-1}** **Quantum Yield (Φ)**: 0.04 **λexc/λem (nm):** 625/676**	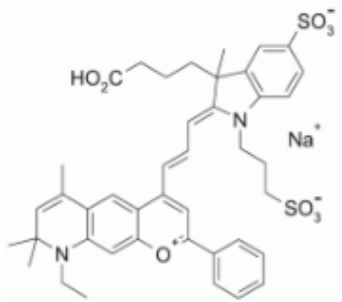	Post-labelling in polymer backbone	(WEISS et al., 2018)
Push-pull - Shows an eléctron donor portion linked to and electron withdrawing group	Nile Blue	**Extinction coefficient (ε):** 76,800 cm^{-1} M^{-1}** **Quantum Yield (Φ)**: 0.27 **λexc/λem (nm):** 600/670-700 **Log P:** 2.7 **Solubility:** 50 mg/mL**	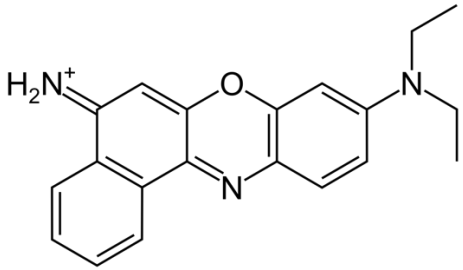	Covalent bonding	

- Emissions are solvent dependent - Functionalizable and chemically stable	Nile Red	**Extinction coefficient (ε):** 38,000 cm^{-1} M^{-1} **Quantum Yield (Φ)**: 0,38 **λexc/λem (nm):** 590/620** **Log P:** 3.8 **Solubility:** 1 mg/mL**	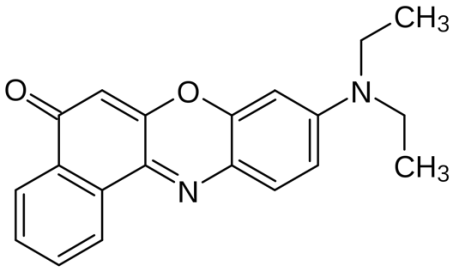	Physical entrapment and covalent bonding	(LI; LI; TONG, 2016; MA et al., 2013)
	Coumarin	**Extinction coefficient (ε):** 46,800 cm^{-1} M^{-1} **Quantum Yield (Φ)**: 0.68 **λexc/λem (nm):** 390/410 **Log P:** 1.39 **Solubility:** 0.0017 mg/mL	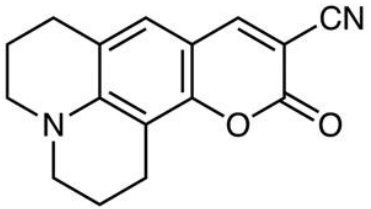	Physical entrapment	(ZHUKOVA et al., 2021)
	Rhodamine and its derivatives	**Extinction coefficient (ε):** 106,000 cm^{-1} M^{-1}** **Quantum Yield (Φ)**: 0.59 **λexc/λem (nm):** 525-550/560-590 **Log P:** 1.95	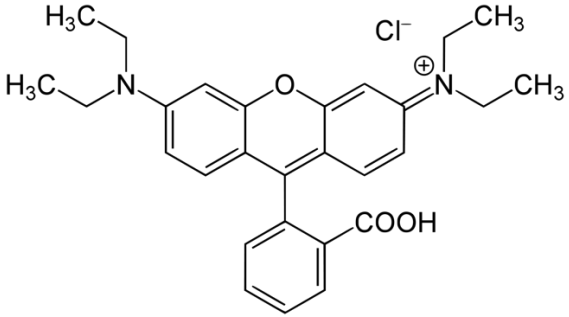	Physical entrapment and Covalent bonding	(CRAPARO et al., 2021; XUE et al., 2020)

Xanthene - Shows high Chemical stability - High emission coefficients and quantum yield and resistant to harsh conditions - Functionalizable, allows synthesis of several derivatives		**Solubility:** 1 mg/mL**			
	Fluorescein and its derivatives	**Extinction coefficient (ε):** 92,300 cm^{-1} M^{-1}** **Quantum Yield (Φ)**: 0.79 **λexc/λem (nm):** 450-510/500-550 **Log P:** 3.35 **Solubility:** 1 mg/mL	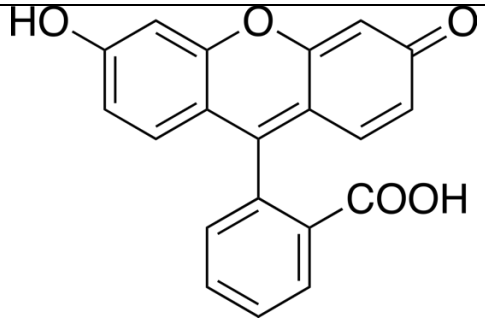	Physical entrapment and Covalent bonding	(ROSIUK et al., 2019; WOO et al., 2020)
	BODIPY and its derivatives	**Extinction coefficient (ε):** 80,000 cm^{-1} M^{-1}** **Quantum Yield (Φ)**: 0.90 **λexc/λem (nm):** 520-530/540-550 **Log P:** -0.3-4.5 **Solubility:** 0.5 mg/mL**	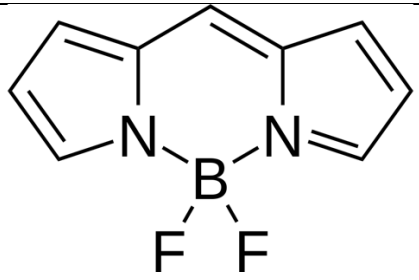	Direct labeling	(GRAZON et al., 2011; SI et al., 2020)
	Dioxaborine based fluorophores	**Extinction coefficient (ε):** 120,000 cm^{-1} M^{-1} **Quantum Yield (Φ)**: 0.93 **λexc/λem (nm):** 380-420/530-620	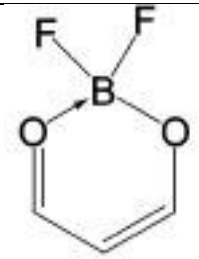	Direct labeling	(KERSEY et al., 2010; SAMONINA-KOSICKA et al., 2015)

	Epoxy monomer EP3	**λexc/λem (nm):** 365/510	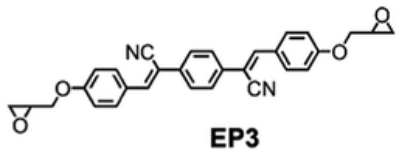 **EP3**	Ring-opening polymerization	(XIE et al., 2017)
	Diketopyrrolopyrrole	**Extinction coefficient (ε):** 76,000 cm^{-1} M^{-} **Quantum Yield (Φ)**: 0.4-0.9 **λexc/λem (nm):** 480/550	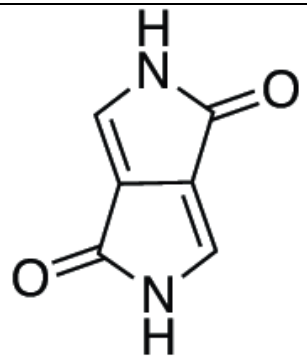	Direct labeling	(WANG et al., 2015; ZHANG et al., 2014)
NIR-II - Higher spatial resolution and higher contrast due to minimal auto-fluorescence and tissue scaterring	IR-1048	**Extinction coefficient (ε):** 236,000 cm^{-1} M^{-} **Quantum Yield (Φ)**: 0.001 **λexc/λem (nm):** 732/1048*	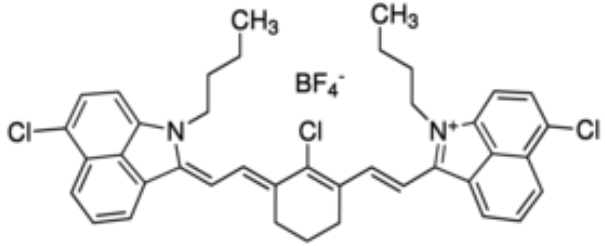	Covalent bonding (Post-labeling) and Physical entrapment	(HUANG et al., 2018; VALCOURT; DANG; DAY, 2019)

*measured in methanol; ** measured in ethanol, *** measured in DMSO

Polymeric nanoparticles show great potential for diagnosis and application of novel therapies. However, they can be metabolized via cellular processes, and thus may no longer be traceable in biological environments, which hinders the study of the interaction of nanoparticles in terms of their uptake, translocation, and fate with biological systems. To this end, nanoparticles with intrinsic fluorescence are more easily tracked than those with extrinsic fluorescence as they do not disrupt the structural integrity of the nanosystem. Therefore, it is interesting to use more than one probe, one that does not degrade along with the nanoparticle, and another one that shows fluorescence variation with nanoparticle degradation (MEDER et al., 2016). Interestingly, fluorescein isocyanate and rhodamine isocyanate fluorescent probes do not degrade in the presence of 1M KOH unlike most nanoparticles, and can therefore be extracted from plant tissue. Fluorescein isocyanate also does not undergo particle degradation (MEDER et al., 2016).

Both fluorescein isothiocyanate and rhodamine have been widely used as fluorescent probes for nanoparticulate systems through polymer functionalization or physical entrapment within nanoparticles. Fluorescence emission increases due to the large amount of fluorescent probes. However, encapsulation also improves the residence time by increasing the stability of the probe and reducing photodegradability (ROBIN; O'REILLY, 2015). In most cases, fluorescent probes do not lead to changes in the structural integrity of the nanoparticles (MEDER et al., 2016).

Rhodamine is a probe that is soluble in water or organic solvents, and can be used at low concentrations as it has an excellent quantum yield (DREXHAGE, 1973; ZHENG et al., 2013). Fluorescein isothiocyanate has a high molar extinction coefficient and quantum yield, and its aqueous solutions can take different forms, making the electronic spectrum of these solutions' pH dependent. Fluorescein isothiocyanate is poorly soluble in water, yet soluble in ethanol (QUAH; PARISH, 2010; WANG et al., 2005).

Fluorescent techniques to detect nanoparticles in plant tissues

The tracking of polymer nanoparticles is achieved using microscopic techniques based on fluorescence. The techniques described below have been used to demonstrate uptake and translocation of polymeric nanoparticles in plants. These techniques are

most commonly used in animal or plant cell biology, and especially in biomedicine studies.

Fluorescence occurs when atoms absorb photons at a determined wavelength. The absorbed wavelength excites the electron, causing it to jump from the fundamental energy level to a higher energy level, and then decays back to its fundamental energy state, first losing vibrational energy and after emitting a photon with a wavelength longer than the one that generated the excitation (TUOVINEN; LI; DICK, 2004).

A common practice in fluorescence microscopy is the application of a high-energy light source that is focused on the sample. The emitted fluorescence is then collected to produce the image. The light only reaches the sample after passing through light-separating optical filters, and allows only a certain range of wavelengths to reach the sample and promote excitation. The optical path of light, transmission, or incidence (epi-illumination) has both advantages and disadvantages. Excitation light can interfere with capturing of fluorescence if the components of the transmission microscope (objective and condenser) are not well-aligned, which is not the case for epifluorescence (objective lens is the condenser). Transmitted-light fluorescence microscopes cannot be used for contrast imaging (TUOVINEN; LI; DICK, 2004).

In epifluorescence, all of the emitted light is captured, i.e., both the excitation-generating light and the generated photons, and subsequently separated into wavelengths by dichroic mirrors and optical filters, causing only the emitted fluorescence to reach the detector. Although the fluorescent image is captured fast, the generated image does not reach maximum distinctness since images are produced with low photon emissions. Moreover, since the entire sample field and not just a focal point is illuminated, a high noise signal is generated. However, the high speed of image capture significantly reduces the photocytotoxic effect that live samples may be subjected to (DEVREE et al., 2021; ROSE et al., 2020). PLGA nanoparticles loaded with coumarin 6 and vines were previously demonstrated to penetrate cells and tissues as well as their subcellular location using the epifluorescence technique. However, the location of an isolated nanoparticle could not be determined, as demonstrated by transmission electron microscopy (TEM) (VALLETTA et al., 2014).

Images with superior distinctness can be achieved by confocal laser scanning microscopy (CLSM) with longer capture times allowing more photons to be captured, as

(laser) illumination is performed at a focal point. The laser has coherent light that passes through a pinhole filter and is directed at a focal point in the sample. The emitted fluorescence is then collected and passed through another pinhole filter that excludes out-of-focus emitted fluorescence (DEVREE et al., 2021). This is performed for each focal point within the scan area. The working principle is the same as that of the epifluorescence microscope, yet has advantages over it: more accurate images are produced due to better resolution, detection sensitivity, and elimination of out-of-focus light (TUOVINEN; LI; DICK, 2004). CLSM can also produce 3D images by joining several 2D images captured along the z axis. Thus, CLSM scans the sample in the three orthogonal axes (SHIN et al., 2019).

The basic function of a fluorescence stereomicroscope is the same as that of a regular microscope; however, in this case, visualization takes place on a macro scale. Using a fluorescence stereomicroscope, Sasson et al. (SASSON et al., 2020) produced images of plants with scales ranging from 100 to 2000 um, and identified fluorescent nanoparticles in the root protoxylem. Cohen et al. also used this technique to evaluate the delivery of fluorescent probe-labeled zinc by modified carboxymethylcellulose-based nanoparticles to pepper leaf petioles (COHEN et al., 2021). An advantage of using this technique is that it is possible to analyze the entire plant or leaves and roots without being removed from the plant and without the need for additional cuts and treatments, in relation to other types of microscopies. In this way, it is possible to analyze the specimen over the time. For example, Shimada et al. used a fluorescent stereomicroscope to select transgenic seeds from non-transgenic ones, which were successfully cultivated after selection (SHIMADA; SHIMADA; HARA-NISHIMURA, 2010).

The absorption and distribution of NPs in plants can also be analyzed using non-image-based methods. Devices equipped with fluorescence detectors, such as fluorescence spectrometry and high-performance liquid chromatography (HPLC-FLD), were used for this purpose. HPLC-FLD was used to evaluate the translocation of fluorescein isocyanate-labeled zein nanoparticles. In this type of measurement, plant parts (root, stem, and leaves) undergo a digestion process where fluorescein is released, and this can then be quantified. In this methodology, the absorption and translocation of NPs can be indirectly inferred by measuring the fluorescence in these parts (RISTROPH et al., 2017).

The techniques mentioned above may be used to complement each other. For example, Prasad et al. (PRASAD et al., 2018) used a spectrometer to assess absorption and accumulation by quantifying fluorescence in roots and leaves, CLSM stick to visualize translocation along the root epidermis, and TEM to verify the interaction of nanoparticles with plant cells.

Evaluation of uptake, translocation and fate of nanoparticles in plants

The uptake and translocation of zein nanoparticles labeled with fluorescein isothiocyanate have been studied in hydroponic soybean (RISTROPH et al., 2017) and sugar cane (PRASAD; BHATTACHARYYA; NGUYEN, 2017) cultures. The used nanoparticles had a mean diameter, polydispersity index, and positive zeta potential of 135 $\pm$ 3 nm, 0.202 $\pm$ 0.034, and 81 $\pm$ 4 mV, respectively. The soybean plants were exposed to two different concentrations of zein nanoparticles, namely low (0.88 mg NP/mL) and high doses (1.75 mg NP/mL). After 10 days, the amount of nanoparticles associated with the roots, which included both internalized nanoparticles and those on the root surface, was found to be concentration-and time-dependent. A total of 0.37 mg NP/mg dry weight roots and 0.58 mg NP/mg dry weight roots were found on plants treated with low and high doses, respectively. In leaves, the fluorescence detected was much lower than in roots, and increased until days 4 and 6 for high and low doses, respectively, and decreased thereafter (not statistically different). Thus, a small quantity of nanoparticles or any fluorescent compound of zein (contaminants) was likely taken up by the roots, and translocated to the shoots. Therefore, the authors were unable to estimate whether the fluorescence displayed on the leaves was due to the translocation of whole nanoparticles or the presence of these unidentified fluorescent particles (RISTROPH et al., 2017). In a similar study, zein nanoparticles with the same physicochemical characteristics were hydroponically studied in sugar cane. Confocal images of the sugarcane roots showed fluorescent signals of nanoparticles along the epidermal layer. In addition, nanoparticles were translocated to the cortex and endodermis at the highest concentration used (1.75 mg/L). The number of nanoparticles translocated to the leaves of sugarcane was found to depend on the dosage used. Plants treated with low (0.88 mg NP /mL) and high (1.75 mg NP/mL) doses of nanoparticles

were found to contain 4.8 μg NP/mg dry weight and 12.9 μg NP/mg dry weight, respectively (PRASAD; BHATTACHARYYA; NGUYEN, 2017).

In another study conducted with vine seedlings cultivated *in vitro*, Valletta et al. demonstrated that PLGA nanoparticles loaded with coumarin 6 were taken up by the roots, reached the vascular cylinder, and were then transported to the shoot. Monitoring of absorption upon foliar application showed that the nanoparticles were internalized in non-granular trichomes, sequentially penetrating the ventral walls of the stomata. A total of 15 to 30 min of incubation could be observed inside guard cells. PLGA nanoparticles were found to be abundant in palisade parenchyma cells, and nanoparticles reached all mesophilic cells within 12 h of incubation. The internalization of nanoparticles in plant cells was monitored by TEM, which showed that only PLGA nanoparticles with diameters smaller than 50 nm could penetrate cells, while nanoparticles that did not cross the cell wall barrier, possibly due to their size, were bound to it (VALLETTA et al., 2014). Palocci et al. demonstrated that PLGA NPs are selected based on their size for uptake into grapevine cells mainly by the cell wall. This limits the absorption of PLGA NPs with diameters above 50 nm, which strongly adhere onto the outside of the cell wall via electrostatic interactions (PALOCCI et al., 2017).

Analyses of the uptake and transport of polymeric nanoparticles in plants are important to assess the benefits of applying these formulations (VALLETTA et al., 2014). In addition, the evaluation of uptake and transport behavior in plant tissues enables optimum design of nanostructured systems to meet specific demands in terms of absorption and transport mechanisms associated with plants. Table 2 provides an overview of different types of labeling techniques that have been used to understand the mechanism of uptake and translocation of nanoparticles in plants, and their environmental fate.

Table 1-2: Example studies that employed strategies to track nanoparticles in agricultural applications.

Polymer	Labeling agent	Method of localization	Plant/ Organism	Main results	References
Poly lactic-co-glycolic acid (PLGA)	Cumarin-6 $\lambda_{exc/em}$ 457/501 Physical entrapment	epifluorescence and Transmission microscopy	Cells and tissues of *Vitis vinifera* and fungal cells of pathogens *Botrytis cinerea, Aspergillus niger* and *Aspergillus carbonarius*	PLGA NPs were found to cross the cell wall and membrane of *Vitis vinifera* and pathogenic fungi. NPs ≤ 50 nm were found to enter cells, where the larger ones were found to attach to the cell wall. Leaf uptake was found to take place through stomatal openings and also via roots. NPs were also transported through vascular tissues to the aerial part.	(VALLETTA et al., 2014)
Poly(lactide-co-glycolide)-b-poly (ethylene glycol) methyl ether (mPEG-PLGA)	Cyanine 5 (Cy5) $\lambda_{exc/em}$ 640/680 Physical entrapment	Fluorescence microscopy	*Oryza sativa*	Metalachlor-loaded mPEG-PLGA NPs were found to show a small hydrophilic portion on their surface enabling permeation by rice roots along with water uptake, increasing metolachlor absorption. Micrographs of the cross-section of rice roots indicated that internalization into the plant must occur via the apoplastic route.	(TONG et al., 2017)

Proteinoid polymers	Cyanine 3 (Cy3) $\lambda_{exc/em}$ 548/561 Covalent attachment	Fluoresce stereoscopic microscopy	*Solanum lycopersicum* and *Lactuca sativa*	The penetration of Cy3-conjugated NPs was found to occur through tomato roots, probably passing through the regions of the proto-xylem, where there was considerable detection of labeled NPs, and through the Casparian strip. The detection of Cy3-conjugated NPs in tomato leaves demonstrated that NPs were transported from roots to leaves. In foliar application on lettuce plants, fluorescent signals were observed in untreated leaves, mainly in the vascular region of the leaves, indicating that the mobility of NPs occurs through the xylem route.	(SASSON et al., 2020)
Zein	Fluorescein Isothiocyanate (FITC) $\lambda_{exc/em}$ 490/525 Covalent attachment	Fluorescence Spectroscopy	Soybean plants	The study reported an intense association of positively charged zein nanoparticles to soybean roots, as a function of time and NPs concentration. Weak fluorescence was also identified in the leaf extracts, indicating that small amount of NP uptake by the roots and	(RISTROPH et al., 2017)

				translocation to the aerial parts of the plant.	
Zein	Fluorescein Isothiocyanate (FITC) $\lambda_{exc/em}$ 490/525 Covalent attachment	Fluorescence spectroscopy, fluorescence microscopy and transmission electron microscopy.	Sugarcane plants	The uptake of NPs was time and concentration dependent, with a significantly greater amount of fluorescence in the roots (cortex and endodermis) than in the leaves. However, the detection of increasing fluorescence in the leaves indicated internalization and translocation of zein NPs.	(PRASAD; BHATTACHARYYA; NGUYEN, 2017)
Methyl ester-conjugated polysuccinimide (PGA)	Fluorescein Isothiocyanate (FITC) $\lambda_{exc/em}$ 490/525 Covalent attachment	confocal laser scanning microscopy	Castor bean plants	After 2 h of treatment, strong green FITC fluorescence was observed in the epidermal and mesophilic cells of the castor bean cotyledon, indicating that PGA nanocarriers were rapidly taken up by plant cells. Xylem and phloem fluorescence was detected, and evidence suggested that phloem loading occurred symplastically.	(WU et al., 2021)
Lignin	Fluorol Yellow 088 (FY088) $\lambda_{exc/em}$ 450/515	Fluorescence stereoscopic, Fluorescence microscopy	*Eragrostis tef*	After 24 hours of treatment, NPS were able to penetrate Teff roots and reach the xylem vessels, and through this	(FALSINI et al., 2020)

	Physical entrapment			route, together with water pressure, the NPs were rapidly translocated to the plants leaves.	
Lignin	Fluorol Yellow 088 (FY088) $\lambda_{exc/em}$ 450/515 Physical entrapment	Fluorescence microscopy	*Solanum lycopersicum*	After 24 h, tomato seeds treated with NPs showed a strong yellow color in the seed coat and hairs, indicating that NPs were able to penetrate the innermost layer of seed coat. In addition, after germination of root it was possible observe NPs in the cortex layers beneath the rizodhermis.	(FALSINI et al., 2019)
Polymer dots	Polymer dots $\lambda_{exc/em}$ 508/590	*In vivo* fluorescence (IVIS) and Photoacoustic imaging	*Hydrocotyle vulgaris L.*	The results showed that the uptake and translocation are dependent to polymer dots ligands. COOH-dots were transported by stomatal routes, and were mainly localized in the vascular bundles; whereas NH_2-dots were transported via both stomatal and cuticular routes, and distributed though the endodermis and pith.	(LI et al., 2020)

Previous studies on polymeric nanoparticles in plants also highlighted that the efficiency of the analysis of nanoparticles by fluorescence microscopy is dependent on the internalization capacity and fluorescence emission intensity of the probe used. The complexity of required manipulation can restrict the application of this technique, such as the need to carry out tests in the dark, and a distortion related to the natural photoperiod of plants, which can influence the processes of absorption and mobility in tissues.

Nevertheless, the findings of studies discussed here demonstrate that the use of fluorescent probes for polymeric nanoparticles is a powerful tool to localize these materials in plant tissues. Combined with analytical and imaging techniques, it is possible to evaluate not only the uptake of nanoparticles by plants, but also their mobility and the tissues and cells where there is an accumulation of polymeric nanoparticles. Understanding the dynamics of nanoparticle transport within plants is highly relevant for the design of nanostructured systems that can deliver active ingredients according to the specific needs of each application.

Previous studies have attempted to explain the mechanisms involved in the capture, translocation, and accumulation of nanoparticles in plant tissues and cells. Conjugation with probes has enabled researchers to clarify these mechanisms, and also helped elucidate other specific mechanisms and mode of action of nanoparticles in plants (FINCHEIRA et al., 2020). Although they are potentially less toxic due to easier degradation compared to metallic nanosystems, there are nevertheless concerns regarding the toxicity of polymeric nanoparticles to the environment, human health, and other organisms. Thus, rigorous assessment of toxicity effects of polymeric nanoparticles on plants is necessary to establish safe doses that avoid adverse effects on plants and throughout the food chain (FINCHEIRA et al., 2020).

Previous studies also indicate that the penetration of nanoparticles in plant cells is limited by the cell wall, and the exclusion limit may increase up to 50 nm for polymeric nanoparticles (FINCHEIRA et al., 2020). Although the plant cell wall is usually reported to have exclusion pores in the range of 5 to 20 nm (FINCHEIRA et al., 2020), biocompatibility of polymeric nanoparticles may still confer good potential for internalization as they are able to interact with the cell wall to enable the pores to adopt specific conformations that allow the passage of the nanoparticles (SASSON et al., 2020)

There is still a considerable gap in the literature regarding the tracking of NPs of organic origin in plants. Several studies reported screening and evaluation of the uptake and mobility of these systems in plants. Despite its limitations, the fluorescence tracking technique is one of the best methods for tracking non-metallic nanoparticles (PRASAD et al., 2018). Tracking of nanoparticles through fluorescent probes thus may contribute to revolutionize agrochemical delivery systems by providing information regarding models of interaction of polymeric nanoparticles with plants.

In this review, we have showed that the utilization of fluorescently labelled nanoparticles either through physical entrapment or covalent attachment is very promising for the visualization and quantification of polymeric nanoparticles in different plant tissues. However, most of these studies used different types of nanoparticles and experimental results based on specific dyes. Future research on fluorescently labelled nanoparticles should be focus on a systematic pool of data, in order to evaluate the effect of essential parameters, such as nanoparticle synthesis route and the physicochemical properties of the dye, over the physicochemical properties of nanoparticles, since changes in these parameters can alter drastically its biological activity as well as the label performance. In addition, better understanding on the chemical stability of the fluorescently labelled nanoparticles must be deeper studied for each application.

Conclusions and perspectives

The interest in development of nanoformulations to improve agricultural productivity is growing, and mainly focused on circumventing limiting factors and/or optimizing manufacturing processes for plant development and protection. Nanomaterials based on biodegradable organic matrices, especially polymeric nanoparticles, are considered safe alternatives for the encapsulation of active agrochemicals.

Although nanotechnology has the promise to revolutionize the management of plant diseases and pest as well as enhance the efficiency of numerous natural and synthetic pesticides, their application into the agricultural sector must be done in a sustainable and careful way. Therefore, green nanotechnology, which uses the

principles of green chemistry, emerged from the need to develop formulations that are efficient and less harmful to the ecosystem. In this way, an intense research strategy should be done to develop agricultural formulation using nature-based polymers, such as lignin, zein, alginate, pectin, and cellulose, which have particular characteristics, such as biocompatibility, biodegradability, low toxicity, and affordability. In addition, the association of nanotechnology with natural molecules, known as biopesticides, bio stimulants and pheromones can decrease environmental contamination and adverse effects on non-target organism.

The development of nanocarriers requires design of intelligent systems capable of delivering active ingredients to plant tissues and/or target organisms efficiently. In addition to a good understanding of the impact, modes of interaction with plants, and mobility in plant tissues, tracking of these systems inside plants is also necessary.

Unlike metallic nanoparticles, polymeric nanoparticles require complex tracking strategies. Metallic and fluorescent probes are used to label these nanostructures. Labeling can be performed through functionalization of these probes to the components of the polymeric matrices or through nanoencapsulation. The intrinsic properties of these probes allow their evaluation using spectroscopic, microscopic, and X-ray scattering techniques. Transmission electron microscopy and fluorescence electron microscopy are the most commonly used techniques for visualization of nanoparticles in plant tissues.

There is still much to be explored until absorption processes and mode of action of polymeric nanoparticles in plant protection are fully elucidated. In addition to the strategies described in this review, radiochemical markers should also be used to develop new agricultural formulations. Although the use of radiolabeled compounds in agricultural research is surrounded by safety restrictions, this strategy will nevertheless provide great precision in the quantification and localization of nanoparticles and active ingredients, even at very low concentrations.

Currently we do not believe that there is a single method to tracking nanoparticles that could be considered as a golden standard, which is applied for all types of polymeric nanoparticles and fluorescent labels. However, we believe that the dual-label approach with fluorescent dyes with different band gaps, or the combination of fluorescent dyes and dual-functional nanoparticles, where there is the combination

of magnetic and fluorescent label should be further explored and well-studied for the traceability of polymeric nanoparticles in plant tissues and environment.

In conclusion, the use of labeling strategies in polymeric nanoparticles with probes, whether metallic, fluorescent, or radiochemical, should be further explored, taking in consideration the complex interferences of different labels or their combination on the nanoparticles' physicochemical properties, supporting a more sustainable development associated with the production of more efficient nanoformulations with possible economic and environmental gains.

Acknowledgement

The authors are grateful to the São Paulo Research Foundation (FAPESP, grants #2017/21004-5, #2018/23608-8), Conselho Nacional de Desenvolvimento Científico e Tecnológico (CNPq – 405623/2018-6, 301466/2018-1, 308439/2021-0), and Coordenação de Aperfeiçoamento de Pessoal de Nível Superior – Capes (88887.620205/2021-00, 88887.351694/2019-00).

Conflit of interesting

The authors declare that the research was conducted in the absence of any commercial or financial relationships that could be construed as a potential conflict of interest.

Author Contributions

PLFP, LBC and EVRC wrote the original draft, EVRC and LFF revised and edited critically the manuscript. All authors read and approved the final manuscript.

References

ALKILANY, A. M.; ABULATEEFEH, S. R.; MURPHY, C. J. Facile Functionalization of Gold Nanoparticles with PLGA Polymer Brushes and Efficient Encapsulation into PLGA Nanoparticles: Toward Spatially Precise Bioimaging of Polymeric Nanoparticles. **Particle & Particle Systems Characterization**, p. 1800414, 14 dez. 2018.

AVELLAN, A.; YUN, J.; ZHANG, Y.; SPIELMAN-SUN, E.; UNRINE, J. M.; THIEME, J.; LI, J.; LOMBI, E.; BLAND, G.; LOWRY, G. V. Nanoparticle Size and Coating Chemistry Control Foliar Uptake Pathways, Translocation, and Leaf-to-Rhizosphere Transport in Wheat. **ACS Nano**, v. 13, n. 5, p. 5291–5305, 28 maio 2019.

BAGALKOT, V.; BADGELEY, M. A.; KAMPFRATH, T.; DEIULIIS, J. A.; RAJAGOPALAN, S.; MAISEYEU, A. Hybrid Nanoparticles Improve Targeting to Inflammatory

Macrophages through Phagocytic Signals. **Journal of Controlled Release**, v. 217, p. 243–255, 10 nov. 2015.

BEIJA, M.; CHARREYRE, M.-T.; MARTINHO, J. M. G. Dye-Labelled Polymer Chains at Specific Sites: Synthesis by Living/Controlled Polymerization. **Progress in Polymer Science**, v. 36, n. 4, p. 568–602, abr. 2011.

BOU, S.; KLYMCHENKO, A. S.; COLLOT, M. Fluorescent Labeling of Biocompatible Block Copolymers: Synthetic Strategies and Applications in Bioimaging. **Materials Advances**, v. 2, n. 10, p. 3213–3233, 2021.

BREUL, A. M.; HAGER, M. D.; SCHUBERT, U. S. Fluorescent Monomers as Building Blocks for Dye Labeled Polymers: Synthesis and Application in Energy Conversion, Biolabeling and Sensors. **Chemical Society Reviews**, v. 42, n. 12, p. 5366, 2013.

CARVALHO, F. P. Pesticides, Environment, and Food Safety. **Food and Energy Security**, v. 6, n. 2, p. 48–60, maio 2017.

CASSANO, D.; LA SPINA, R.; PONTI, J.; BIANCHI, I.; GILLILAND, D. Inorganic Species-Doped Polypropylene Nanoparticles for Multifunctional Detection. **ACS Applied Nano Materials**, v. 4, n. 2, p. 1551–1557, 26 fev. 2021.

CHEN, L.; ZHOU, H.; HAO, L.; LI, Z.; XU, H.; CHEN, H.; ZHOU, X. Dialdehyde Carboxymethyl Cellulose-Zein Conjugate as Water-Based Nanocarrier for Improving the Efficacy of Pesticides. **Industrial Crops and Products**, v. 150, p. 112358, ago. 2020.

CHEN, Q.; XU, L.; LIANG, C.; WANG, C.; PENG, R.; LIU, Z. Photothermal Therapy with Immune-Adjuvant Nanoparticles Together with Checkpoint Blockade for Effective Cancer Immunotherapy. **Nature Communications**, v. 7, n. 1, p. 13193, 21 out. 2016.

COHEN, Y.; YASUOR, H.; TWOROWSKI, D.; FALLIK, E.; POVERENOV, E. Stimuli-Free Transcuticular Delivery of Zn Microelement Using Biopolymeric Nanovehicles: Experimental, Theoretical, and *In Planta* Studies. **ACS Nano**, v. 15, n. 12, p. 19446–19456, 28 dez. 2021.

CORREDOR, E.; TESTILLANO, P. S.; CORONADO, M.-J.; GONZÁLEZ-MELENDI, P.; FERNÁNDEZ-PACHECO, R.; MARQUINA, C.; IBARRA, M. R.; DE LA FUENTE, J. M.; RUBIALES, D.; PÉREZ-DE-LUQUE, A.; RISUEÑO, M.-C. Nanoparticle Penetration and Transport in Living Pumpkin Plants: In Situsubcellular Identification. **BMC Plant Biology**, v. 9, n. 1, p. 45, dez. 2009.

CRAPARO, E. F.; MUSUMECI, T.; BONACCORSO, A.; PELLITTERI, R.; ROMEO, A.; NALETOVA, I.; CUCCI, L. M.; CAVALLARO, G.; SATRIANO, C. mPEG-PLGA Nanoparticles Labelled with Loaded or Conjugated Rhodamine-B for Potential Nose-to-Brain Delivery. **Pharmaceutics**, v. 13, n. 9, p. 1508, set. 2021.

DEVREE, B. T.; STEINER, L. M.; GŁAZOWSKA, S.; RUHNOW, F.; HERBURGER, K.; PERSSON, S.; MRAVEC, J. Current and Future Advances in Fluorescence-Based Visualization

of Plant Cell Wall Components and Cell Wall Biosynthetic Machineries. **Biotechnology for Biofuels**, v. 14, n. 1, p. 78, dez. 2021.

DREXHAGE, K. H. Structure and Properties of Laser Dyes. *Em*: SCHÄFER, F. P. **Dye Lasers**. Topics in Applied Physics. Berlin, Heidelberg: Springer Berlin Heidelberg, 1973. p. 144–193.

FALSINI, S.; CLEMENTE, I.; PAPINI, A.; TANI, C.; SCHIFF, S.; SALVATICI, M. C.; PETRUCCELLI, R.; BENELLI, C.; GIORDANO, C.; GONNELLI, C.; RISTORI, S. When Sustainable Nanochemistry Meets Agriculture: Lignin Nanocapsules for Bioactive Compound Delivery to Plantlets. **ACS Sustainable Chemistry & Engineering**, v. 7, n. 24, p. 19935–19942, 16 dez. 2019.

FALSINI, S.; TANI, C.; SCHIFF, S.; GONNELLI, C.; CLEMENTE, I.; RISTORI, S.; PAPINI, A. A new method for the direct tracking of in vivo lignin nanocapsules in Eragrostis tef (Poaceae) tissues. **European Journal of Histochemistry**, v. 64, n. 2, 26 mar. 2020. Disponível em: <https://www.ejh.it/index.php/ejh/article/view/3112>. Acesso em: 17 dez. 2021.

FÄRKKILÄ, S. M. A.; KIERS, E. T.; JAANISO, R.; MÄEORG, U.; LEBLANC, R. M.; TRESEDER, K. K.; KANG, Z.; TEDERSOO, L. Fluorescent Nanoparticles as Tools in Ecology and Physiology. **Biological Reviews**, v. 96, n. 5, p. 2392–2424, out. 2021.

FEREGRINO-PEREZ, A. A.; MAGAÑA-LÓPEZ, E.; GUZMÁN, C.; ESQUIVEL, K. A General Overview of the Benefits and Possible Negative Effects of the Nanotechnology in Horticulture. **Scientia Horticulturae**, v. 238, p. 126–137, ago. 2018.

FINCHEIRA, P.; TORTELLA, G.; DURAN, N.; SEABRA, A. B.; RUBILAR, O. Current Applications of Nanotechnology to Develop Plant Growth Inducer Agents as an Innovation Strategy. **Critical Reviews in Biotechnology**, v. 40, n. 1, p. 15–30, 2 jan. 2020.

FOA; IFAD; UNICEF; WFP; WHO. **The State of Food Security and Nutrition in the World 2021**. [s.l.] FAO, IFAD, UNICEF, WFP and WHO, 2021.

GRAZON, C.; RIEGER, J.; MÉALLET-RENAULT, R.; CLAVIER, G.; CHARLEUX, B. One-Pot Synthesis of Pegylated Fluorescent Nanoparticles by RAFT Miniemulsion Polymerization Using a Phase Inversion Process. **Macromolecular Rapid Communications**, v. 32, n. 9–10, p. 699–705, 18 maio 2011.

HARUN, N. A.; BENNING, M. J.; HORROCKS, B. R.; FULTON, D. A. Gold Nanoparticle-Enhanced Luminescence of Silicon Quantum Dots Co-Encapsulated in Polymer Nanoparticles. **Nanoscale**, v. 5, n. 9, p. 3817–3827, 19 abr. 2013.

HAYLES, J.; JOHNSON, L.; WORTHLEY, C.; LOSIC, D. Nanopesticides: a review of current research and perspectives. *Em*: **New Pesticides and Soil Sensors**. [s.l.] Elsevier, 2017. p. 193–225.

HEDLUND, J.; LONGO, S. B.; YORK, R. Agriculture, Pesticide Use, and Economic Development: A Global Examination (1990–2014). **Rural Sociology**, v. 85, n. 2, p. 519–544, jun. 2020.

HÖLTTÄ, T.; MENCUCCINI, M.; NIKINMAA, E. Linking Phloem Function to Structure: Analysis with a Coupled Xylem–Phloem Transport Model. **Journal of Theoretical Biology**, v. 259, n. 2, p. 325–337, jul. 2009.

HUANG, K.; GAO, M.; FAN, L.; LAI, Y.; FAN, H.; HUA, Z. IR820 Covalently Linked with Self-Assembled Polypeptide for Photothermal Therapy Applications in Cancer. **Biomaterials Science**, v. 6, n. 11, p. 2925–2931, 24 out. 2018.

JANSEN, S.; CHOAT, B.; PLETSERS, A. Morphological Variation of Intervessel Pit Membranes and Implications to Xylem Function in Angiosperms. **American Journal of Botany**, v. 96, n. 2, p. 409–419, fev. 2009.

KAH, M.; KOOKANA, R. S.; GOGOS, A.; BUCHELI, T. D. A Critical Evaluation of Nanopesticides and Nanofertilizers against Their Conventional Analogues. **Nature Nanotechnology**, v. 13, n. 8, p. 677–684, ago. 2018.

KARNY, A.; ZINGER, A.; KAJAL, A.; SHAINSKY-ROITMAN, J.; SCHROEDER, A. Therapeutic Nanoparticles Penetrate Leaves and Deliver Nutrients to Agricultural Crops. **Scientific Reports**, v. 8, n. 1, p. 7589, dez. 2018.

KERSEY, F. R.; ZHANG, G.; PALMER, G. M.; DEWHIRST, M. W.; FRASER, C. L. Stereocomplexed Poly(lactic acid)−Poly(ethylene glycol) Nanoparticles with Dual-Emissive Boron Dyes for Tumor Accumulation. **ACS Nano**, v. 4, n. 9, p. 4989–4996, 28 set. 2010.

KRANJC, E.; DROBNE, D. Nanomaterials in Plants: A Review of Hazard and Applications in the Agri-Food Sector. **Nanomaterials**, v. 9, n. 8, p. 1094, 30 jul. 2019.

LI, J.; LI, Y.; TANG, S.; ZHANG, Y.; ZHANG, J.; LI, Y.; XIONG, L. Toxicity, Uptake and Transport Mechanisms of Dual-Modal Polymer Dots in Penny Grass (Hydrocotyle Vulgaris L.). **Environmental Pollution**, v. 265, p. 114877, out. 2020.

LI, Q.; LI, C.; TONG, W. Nile Red Loaded PLGA Nanoparticles Surface Modified with Gd-DTPA for Potential Dual-Modal Imaging. **Journal of Nanoscience and Nanotechnology**, v. 16, n. 6, p. 5569–5576, jun. 2016.

LICO, C.; BENVENUTO, E.; BASCHIERI, S. The Two-Faced Potato Virus X: From Plant Pathogen to Smart Nanoparticle. **Frontiers in Plant Science**, v. 6, 17 nov. 2015. Disponível em: <http://journal.frontiersin.org/Article/10.3389/fpls.2015.01009/abstract>. Acesso em: 15 dez. 2021.

LIU, R.; LAL, R. Potentials of Engineered Nanoparticles as Fertilizers for Increasing Agronomic Productions. **Science of The Total Environment**, v. 514, p. 131–139, maio 2015.

LOVELL, P. A.; SCHORK, F. J. Fundamentals of Emulsion Polymerization. **Biomacromolecules**, v. 21, n. 11, p. 4396–4441, 9 nov. 2020.

MA, T.; LV, Y.; LIU, H.; LV, Y.; TIAN, Z. Development of Nile Red-Functionalized Magnetic Silica Nanoparticles for Cobalt Ion Sensing and Entrapping. **Journal of Nanoparticle Research**, v. 15, n. 9, p. 1933, 24 ago. 2013.

MADSEN, J.; CANTON, I.; WARREN, N. J.; THEMISTOU, E.; BLANAZS, A.; USTBAS, B.; TIAN, X.; PEARSON, R.; BATTAGLIA, G.; LEWIS, A. L.; ARMES, S. P. Nile Blue-Based Nanosized pH Sensors for Simultaneous Far-Red and Near-Infrared Live Bioimaging. **Journal of the American Chemical Society**, v. 135, n. 39, p. 14863–14870, 2 out. 2013.

MAKVANDI, P.; IFTEKHAR, S.; PIZZETTI, F.; ZAREPOUR, A.; ZARE, E. N.; ASHRAFIZADEH, M.; AGARWAL, T.; PADIL, V. V. T.; MOHAMMADINEJAD, R.; SILLANPAA, M.; MAITI, T. K.; PERALE, G.; ZARRABI, A.; ROSSI, F. Functionalization of Polymers and Nanomaterials for Water Treatment, Food Packaging, Textile and Biomedical Applications: A Review. **Environmental Chemistry Letters**, v. 19, n. 1, p. 583–611, fev. 2021.

MEDER, F.; THOMAS, S. S.; FITZPATRICK, L. W.; ALAHMARI, A.; WANG, S.; BEIRNE, J. G.; VAZ, G.; REDMOND, G.; DAWSON, K. A. Labeling the Structural Integrity of Nanoparticles for Advanced In Situ Tracking in Bionanotechnology. **ACS Nano**, v. 10, n. 4, p. 4660–4671, 26 abr. 2016.

MENDOZA, G.; SOLORZANO, I. O. de; PINTRE, I.; GARCIA-SALINAS, S.; SEBASTIAN, V.; ANDREU, V.; GIMENO, M.; ARRUEBO, M. Near Infrared Dye-Labelled Polymeric Micro- and Nanomaterials: In Vivo Imaging and Evaluation of Their Local Persistence. **Nanoscale**, v. 10, n. 6, p. 2970–2982, 8 fev. 2018.

MIAO, T.; LITTLE, A. C.; ARONSHTAM, A.; MARQUIS, T.; FENN, S. L.; HRISTOVA, M.; KREMENTSOV, D. N.; VAN DER VLIET, A.; SPEES, J. L.; OLDINSKI, R. A. Internalized FGF-2-Loaded Nanoparticles Increase Nuclear ERK1/2 Content and Result in Lung Cancer Cell Death. **Nanomaterials**, v. 10, n. 4, p. 612, abr. 2020.

MIKI, K.; KIMURA, A.; ORIDE, K.; KURAMOCHI, Y.; MATSUOKA, H.; HARADA, H.; HIRAOKA, M.; OHE, K. High-Contrast Fluorescence Imaging of Tumors In Vivo Using Nanoparticles of Amphiphilic Brush-Like Copolymers Produced by ROMP. **Angewandte Chemie International Edition**, v. 50, n. 29, p. 6567–6570, 2011.

MULUNEH, M. G. Impact of Climate Change on Biodiversity and Food Security: A Global Perspective—a Review Article. **Agriculture & Food Security**, v. 10, n. 1, p. 36, dez. 2021.

NOTAGUCHI, M.; OKAMOTO, S. Dynamics of long-distance signaling via plant vascular tissues. **Frontiers in Plant Science**, v. 6, 18 mar. 2015. Disponível em: <http://www.frontiersin.org/Plant_Physiology/10.3389/fpls.2015.00161/abstract>. Acesso em: 15 dez. 2021.

O'CONNELL, C. L.; NOONEY, R.; MCDONAGH, C. Cyanine5-Doped Silica Nanoparticles as Ultra-Bright Immunospecific Labels for Model Circulating Tumour Cells in Flow Cytometry and Microscopy. **Biosensors and Bioelectronics**, v. 91, p. 190–198, 15 maio 2017.

ONG, S. Y.; ZHANG, C.; DONG, X.; YAO, S. Q. Recent Advances in Polymeric Nanoparticles for Enhanced Fluorescence and Photoacoustic Imaging. **Angewandte Chemie International Edition**, v. 60, n. 33, p. 17797–17809, 9 ago. 2021.

PALOCCI, C.; VALLETTA, A.; CHRONOPOULOU, L.; DONATI, L.; BRAMOSANTI, M.; BRASILI, E.; BALDAN, B.; PASQUA, G. Endocytic Pathways Involved in PLGA Nanoparticle Uptake by Grapevine Cells and Role of Cell Wall and Membrane in Size Selection. **Plant Cell Reports**, v. 36, n. 12, p. 1917–1928, dez. 2017.

PAPADIMITRIOU, S. A.; SALINAS, Y.; RESMINI, M. Smart Polymeric Nanoparticles as Emerging Tools for Imaging-The Parallel Evolution of Materials. **Chemistry - A European Journal**, v. 22, n. 11, p. 3612–3620, 7 mar. 2016.

PEDROSA, L. M.; HOSHIDE, A. K.; ABREU, D. C. de; MOLOSSI, L.; COUTO, E. G. Financial Transition and Costs of Sustainable Agricultural Intensification Practices on a Beef Cattle and Crop Farm in Brazil's Amazon. **Renewable Agriculture and Food Systems**, v. 36, n. 1, p. 26–37, fev. 2021.

PIMENTEL, D. **World Food, Pest Losses, and the Environment**. 1. ed. [s.l.] CRC Press, 2019.

PRASAD, A.; ASTETE, C. E.; BODOKI, A. E.; WINDHAM, M.; BODOKI, E.; SABLIOV, C. M. Zein Nanoparticles Uptake and Translocation in Hydroponically Grown Sugar Cane Plants. **Journal of Agricultural and Food Chemistry**, v. 66, n. 26, p. 6544–6551, 5 jul. 2018.

PRASAD, R.; BHATTACHARYYA, A.; NGUYEN, Q. D. Nanotechnology in Sustainable Agriculture: Recent Developments, Challenges, and Perspectives. **Frontiers in Microbiology**, v. 8, p. 1014, 20 jun. 2017.

QUAH, B. J. C.; PARISH, C. R. The Use of Carboxyfluorescein Diacetate Succinimidyl Ester (CFSE) to Monitor Lymphocyte Proliferation. **Journal of Visualized Experiments**, n. 44, p. 2259, 12 out. 2010.

RALIYA, R.; FRANKE, C.; CHAVALMANE, S.; NAIR, R.; REED, N.; BISWAS, P. Quantitative Understanding of Nanoparticle Uptake in Watermelon Plants. **Frontiers in Plant Science**, v. 7, 26 ago. 2016. Disponível em: <http://journal.frontiersin.org/Article/10.3389/fpls.2016.01288/abstract>. Acesso em: 15 dez. 2021.

REUL, R.; TSAPIS, N.; HILLAIREAU, H.; SANCEY, L.; MURA, S.; RECHER, M.; NICOLAS, J.; COLL, J.-L.; FATTAL, E. Near Infrared Labeling of PLGA for in Vivo Imaging of Nanoparticles. **Polymer Chemistry**, v. 3, n. 3, p. 694–702, 7 fev. 2012.

RICO, C. M.; MAJUMDAR, S.; DUARTE-GARDEA, M.; PERALTA-VIDEA, J. R.; GARDEA-TORRESDEY, J. L. Interaction of Nanoparticles with Edible Plants and Their Possible Implications in the Food Chain. **Journal of Agricultural and Food Chemistry**, v. 59, n. 8, p. 3485–3498, 27 abr. 2011.

RISTROPH, K. D.; ASTETE, C. E.; BODOKI, E.; SABLIOV, C. M. Zein Nanoparticles Uptake by Hydroponically Grown Soybean Plants. **Environmental Science & Technology**, v. 51, n. 24, p. 14065–14071, 19 dez. 2017.

ROBIN, M. P.; O'REILLY, R. K. Strategies for Preparing Fluorescently Labelled Polymer Nanoparticles. **Polymer International**, v. 64, n. 2, p. 174–182, fev. 2015.

ROSE, K. A.; MOLAEI, M.; BOYLE, M. J.; LEE, D.; CROCKER, J. C.; COMPOSTO, R. J. Particle Tracking of Nanoparticles in Soft Matter. **Journal of Applied Physics**, v. 127, n. 19, p. 191101, 21 maio 2020.

ROSIUK, V.; RUNSER, A.; KLYMCHENKO, A.; REISCH, A. Controlling Size and Fluorescence of Dye-Loaded Polymer Nanoparticles through Polymer Design. **Langmuir**, v. 35, n. 21, p. 7009–7017, 28 maio 2019.

SAMONINA-KOSICKA, J.; WEITZEL, D. H.; HOFMANN, C. L.; HENDARGO, H.; HANNA, G.; DEWHIRST, M. W.; PALMER, G. M.; FRASER, C. L. Luminescent Difluoroboron β-Diketonate PEG-PLA Oxygen Nanosensors for Tumor Imaging. **Macromolecular rapid communications**, v. 36, n. 7, p. 694–699, abr. 2015.

SASSON, E.; PINHASI, R. V. O.; MARGEL, S.; KLIPCAN, L. Engineering and Use of Proteinoid Polymers and Nanocapsules Containing Agrochemicals. **Scientific Reports**, v. 10, n. 1, p. 9171, dez. 2020.

SCHULZ, A. Diffusion or Bulk Flow: How Plasmodesmata Facilitate Pre-Phloem Transport of Assimilates. **Journal of Plant Research**, v. 128, n. 1, p. 49–61, jan. 2015.

SHAKIBA, S.; ASTETE, C. E.; PAUDEL, S.; SABLIOV, C. M.; RODRIGUES, D. F.; LOUIE, S. M. Emerging Investigator Series: Polymeric Nanocarriers for Agricultural Applications: Synthesis, Characterization, and Environmental and Biological Interactions. **Environmental Science: Nano**, v. 7, n. 1, p. 37–67, 2020.

SHIMADA, T. L.; SHIMADA, T.; HARA-NISHIMURA, I. A Rapid and Non-Destructive Screenable Marker, FAST, for Identifying Transformed Seeds of Arabidopsis Thaliana. **The Plant Journal**, v. 61, n. 3, p. 519–528, 2010.

SHIN, K.; SONG, Y.; GOH, Y.; LEE, K. Two-Dimensional and Three-Dimensional Single Particle Tracking of Upconverting Nanoparticles in Living Cells. **International Journal of Molecular Sciences**, v. 20, n. 6, p. 1424, 21 mar. 2019.

SI, Y.; GRAZON, C.; CLAVIER, G.; RIEGER, J.; TIAN, Y.; AUDIBERT, J.-F.; SCLAVI, B.; MÉALLET-RENAULT, R. Fluorescent Copolymers for Bacterial Bioimaging and Viability Detection. **ACS sensors**, v. 5, n. 9, p. 2843–2851, 25 set. 2020.

SINGH, A.; TIWARI, S.; PANDEY, J.; LATA, C.; SINGH, I. K. Role of Nanoparticles in Crop Improvement and Abiotic Stress Management. **Journal of Biotechnology**, v. 337, p. 57–70, ago. 2021.

SOBSKA, J.; ANDREIUK, B.; APARIN, I. O.; REISCH, A.; KREZEL, W.; KLYMCHENKO, A. S. Counterion-Insulated near-Infrared Dyes in Biodegradable Polymer Nanoparticles for in Vivo Imaging. **Nanoscale Advances**, v. 4, n. 1, p. 39–48, 21 dez. 2021.

SPIELMAN-SUN, E.; LOMBI, E.; DONNER, E.; HOWARD, D.; UNRINE, J. M.; LOWRY, G. V. Impact of Surface Charge on Cerium Oxide Nanoparticle Uptake and Translocation by Wheat (*Triticum Aestivum*). **Environmental Science & Technology**, v. 51, n. 13, p. 7361–7368, 5 jul. 2017.

SU, Y.; ASHWORTH, V.; KIM, C.; ADELEYE, A. S.; ROLSHAUSEN, P.; ROPER, C.; WHITE, J.; JASSBY, D. Delivery, Uptake, Fate, and Transport of Engineered Nanoparticles in Plants: A Critical Review and Data Analysis. **Environmental Science: Nano**, v. 6, n. 8, p. 2311–2331, 2019.

SUN, D.; HUSSAIN, H. I.; YI, Z.; SIEGELE, R.; CRESSWELL, T.; KONG, L.; CAHILL, D. M. Uptake and Cellular Distribution, in Four Plant Species, of Fluorescently Labeled Mesoporous Silica Nanoparticles. **Plant Cell Reports**, v. 33, n. 8, p. 1389–1402, ago. 2014.

TAN, W.; PERALTA-VIDEA, J. R.; GARDEA-TORRESDEY, J. L. Interaction of Titanium Dioxide Nanoparticles with Soil Components and Plants: Current Knowledge and Future Research Needs – a Critical Review. **Environmental Science: Nano**, v. 5, n. 2, p. 257–278, 2018.

TEXIER, I.; GOUTAYER, M.; DA SILVA, A.; GUYON, L.; DJAKER, N.; JOSSERAND, V.; NEUMANN, E.; BIBETTE, J.; VINET, F. Cyanine-Loaded Lipid Nanoparticles for Improved in Vivo Fluorescence Imaging. **Journal of Biomedical Optics**, v. 14, n. 5, p. 054005, out. 2009.

TONG, Y.; WU, Y.; ZHAO, C.; XU, Y.; LU, J.; XIANG, S.; ZONG, F.; WU, X. Polymeric Nanoparticles as a Metolachlor Carrier: Water-Based Formulation for Hydrophobic Pesticides and Absorption by Plants. **Journal of Agricultural and Food Chemistry**, v. 65, n. 34, p. 7371–7378, 30 ago. 2017.

TU, C.; YANG, Y.; GAO, M. Preparations of Bifunctional Polymeric Beads Simultaneously Incorporated with Fluorescent Quantum Dots and Magnetic Nanocrystals. **Nanotechnology**, v. 19, n. 10, p. 105601, 13 fev. 2008.

TUOVINEN, O. H.; LI, Y.; DICK, W. A. Fluorescence microscopy for visualization of soil microorganisms?a review. **Biology and Fertility of Soils**, v. 39, n. 5, p. 301–311, 1 abr. 2004.

UNITED NATIONS. **Sustainable deveopment Goals**maio 2020. . Acesso em: 19 nov. 2021.

UZU, G.; SOBANSKA, S.; SARRET, G.; MUÑOZ, M.; DUMAT, C. Foliar Lead Uptake by Lettuce Exposed to Atmospheric Fallouts. **Environmental Science & Technology**, v. 44, n. 3, p. 1036–1042, 1 fev. 2010.

VALCOURT, D. M.; DANG, M. N.; DAY, E. S. IR820-loaded PLGA nanoparticles for photothermal therapy of triple-negative breast cancer. **Journal of biomedical materials research. Part A**, v. 107, n. 8, p. 1702–1712, ago. 2019.

VALLETTA, A.; CHRONOPOULOU, L.; PALOCCI, C.; BALDAN, B.; DONATI, L.; PASQUA, G. Poly(Lactic-Co-Glycolic) Acid Nanoparticles Uptake by Vitis Vinifera and Grapevine-Pathogenic Fungi. **Journal of Nanoparticle Research**, v. 16, n. 12, p. 2744, dez. 2014.

VAN DIJK, M.; MORLEY, T.; RAU, M. L.; SAGHAI, Y. A Meta-Analysis of Projected Global Food Demand and Population at Risk of Hunger for the Period 2010–2050. **Nature Food**, v. 2, n. 7, p. 494–501, jul. 2021.

VOLLRATH, A.; SCHALLON, A.; PIETSCH, C.; SCHUBERT, S.; NOMOTO, T.; MATSUMOTO, Y.; KATAOKA, K.; SCHUBERT, U. S. A Toolbox of Differently Sized and Labeled PMMA Nanoparticles for Cellular Uptake Investigations. **Soft Matter**, v. 9, n. 1, p. 99–108, 30 nov. 2012.

WANG, H.; WANG, L.; MENG, S.; LIN, H.; CORRELL, M.; TONG, Z. Nanocomposite of Graphene Oxide Encapsulated in Polymethylmethacrylate (PMMA): Pre-Modification, Synthesis, and Latex Stability. **Journal of Composites Science**, v. 4, n. 3, p. 118, 17 ago. 2020.

WANG, K.; LUO, Y.; HUANG, S.; YANG, H.; LIU, B.; WANG, M. Highly Fluorescent Polycaprolactones Decorated with Di(Thiophene-2-Yl)-Diketopyrrolopyrrole: A Covalent Strategy of Tuning Fluorescence Properties in Solid States. **Journal of Polymer Science Part A: Polymer Chemistry**, v. 53, n. 8, p. 1032–1042, 2015.

WANG, W.-N.; TARAFDAR, J. C.; BISWAS, P. Nanoparticle Synthesis and Delivery by an Aerosol Route for Watermelon Plant Foliar Uptake. **Journal of Nanoparticle Research**, v. 15, n. 1, p. 1417, jan. 2013.

WANG, X.-Q.; DUAN, X.-M.; LIU, L.-H.; FANG, Y.-Q.; TAN, Y. Carboxyfluorescein Diacetate Succinimidyl Ester Fluorescent Dye for Cell Labeling. **Acta Biochimica et Biophysica Sinica**, v. 37, n. 6, p. 379–385, 1 jun. 2005.

WANG, Z.; XIE, X.; ZHAO, J.; LIU, X.; FENG, W.; WHITE, J. C.; XING, B. Xylem- and Phloem-Based Transport of CuO Nanoparticles in Maize (*Zea Mays* L.). **Environmental Science & Technology**, v. 46, n. 8, p. 4434–4441, 17 abr. 2012.

WEISS, V. M.; LUCAS, H.; MUELLER, T.; CHYTIL, P.; ETRYCH, T.; NAOLOU, T.; KRESSLER, J.; MÄDER, K. Intended and Unintended Targeting of Polymeric Nanocarriers: The Case of Modified Poly(Glycerol Adipate) Nanoparticles. **Macromolecular Bioscience**, v. 18, n. 1, p. 1700240, 2018.

WOLFBEIS, O. S. An Overview of Nanoparticles Commonly Used in Fluorescent Bioimaging. **Chemical Society Reviews**, v. 44, n. 14, p. 4743–4768, 2015.

WOO, J.; PARK, H.; NA, Y.; KIM, S.; CHOI, W. I.; LEE, J. H.; SEO, H.; SUNG, D. Novel Fluorescein Polymer-Based Nanoparticles: Facile and Controllable One-Pot Synthesis, Assembly, and Immobilization of Biomolecules for Application in a Highly Sensitive Biosensor. **RSC Advances**, v. 10, n. 5, p. 2998–3004, 14 jan. 2020.

WU, H.; HU, P.; XU, Y.; XIAO, C.; CHEN, Z.; LIU, X.; JIA, J.; XU, H. Phloem Delivery of Fludioxonil by Plant Amino Acid Transporter-Mediated Polysuccinimide Nanocarriers for Controlling Fusarium Wilt in Banana. **Journal of Agricultural and Food Chemistry**, v. 69, n. 9, p. 2668–2678, 10 mar. 2021.

XIA, X.; SHI, B.; WANG, L.; LIU, Y.; ZOU, Y.; ZHOU, Y.; CHEN, Y.; ZHENG, M.; ZHU, Y.; DUAN, J.; GUO, S.; JANG, H. W.; MIAO, Y.; FAN, K.; BAI, F.; TAO, W.; ZHAO, Y.; YAN, Q.; CHENG, G.; LIU, H.; JIAO, Y.; LIU, S.; HUANG, Y.; LING, D.; KANG, W.; XUE, X.; CUI, D.; HUANG, Y.; CUI, Z.; SUN, X.; QIAN, Z.; GU, Z.; HAN, G.; YANG, Z.; LEONG, D. T.; WU, A.; LIU, G.; QU, X.; SHEN, Y.; WANG, Q.; LOWRY, G. V.; WANG, E.; LIANG, X.; GARDEA-TORRESDEY, J.; CHEN, G.; PARAK, W. J.; WEISS, P. S.; ZHANG, L.; STENZEL, M. M.; FAN, C.; BUSH, A. I.; ZHANG, G.; GROF, C. P. L.; WANG, X.; GALBRAITH, D. W.; TANG, B. Z.; OFFLER, C. E.; PATRICK, J. W.; SONG, C. From Mouse to Mouse-ear Cress: Nanomaterials as Vehicles in Plant Biotechnology. **Exploration**, v. 1, n. 1, p. 9–20, ago. 2021.

XIANG, Y.; ZHANG, G.; CHI, Y.; CAI, D.; WU, Z. Fabrication of a Controllable Nanopesticide System with Magnetic Collectability. **Chemical Engineering Journal**, v. 328, p. 320–330, nov. 2017.

XIE, G.; MA, C.; ZHANG, X.; LIU, H.; YANG, L.; LI, Y.; WANG, K.; WEI, Y. Chitosan-Based Cross-Linked Fluorescent Polymer Containing Aggregation-Induced Emission Fluorogen for Cell Imaging. **Dyes and Pigments**, v. 143, p. 276–283, 1 ago. 2017.

XUE, Y.; LEE, J.; KIM, H.-J.; CHO, H.-J.; ZHOU, X.; LIU, Y.; TEBON, P.; HOFFMAN, T.; QU, M.; LING, H.; JIANG, X.; LI, Z.; ZHANG, S.; SUN, W.; AHADIAN, S.; DOKMECI, Mehmet. R.; LEE, K.; KHADEMHOSSEINI, A. Rhodamine Conjugated Gelatin Methacryloyl Nanoparticles for Stable Cell Imaging. **ACS Applied Bio Materials**, v. 3, n. 10, p. 6908–6918, 19 out. 2020.

YAO, J.; GAO, F.; LIANG, X.; LI, Y.; MI, Y.; QI, Q.; YAO, J.; CAO, Z. Efficient Preparation of Carboxyl-Functionalized Magnetic Polymer/Fe3O4 Nanocomposite Particles in One-Pot Miniemulsion Systems. **Colloids and Surfaces A: Physicochemical and Engineering Aspects**, v. 570, p. 449–461, jun. 2019.

ZHAI, G.; WALTERS, K. S.; PEATE, D. W.; ALVAREZ, P. J. J.; SCHNOOR, J. L. Transport of Gold Nanoparticles through Plasmodesmata and Precipitation of Gold Ions in Woody Poplar. **Environmental Science & Technology Letters**, v. 1, n. 2, p. 146–151, 11 fev. 2014.

ZHANG, Y.; CHEN, Y.; LI, X.; ZHANG, J.; CHEN, J.; XU, B.; FU, X.; TIAN, W. Folic Acid-Functionalized AIE Pdots Based on Amphiphilic PCL-b-PEG for Targeted Cell Imaging. **Polymer Chemistry**, v. 5, n. 12, p. 3824–3830, 20 maio 2014.

ZHANG, Y.; KLEPSCH, M.; JANSEN, S. Bordered Pits in Xylem of Vesselless Angiosperms and Their Possible Misinterpretation as Perforation Plates: Bordered Pits in Xylem of Vesselless Angiosperms. **Plant, Cell & Environment**, v. 40, n. 10, p. 2133–2146, out. 2017.

ZHANG, Y.; YAN, J.; AVELLAN, A.; GAO, X.; MATYJASZEWSKI, K.; TILTON, R. D.; LOWRY, G. V. Temperature- and pH-Responsive Star Polymers as Nanocarriers with Potential for *in Vivo* Agrochemical Delivery. **ACS Nano**, v. 14, n. 9, p. 10954–10965, 22 set. 2020.

ZHENG, H.; ZHAN, X.-Q.; BIAN, Q.-N.; ZHANG, X.-J. Advances in Modifying Fluorescein and Rhodamine Fluorophores as Fluorescent Chemosensors. **Chem. Commun.**, v. 49, n. 5, p. 429–447, 2013.

ZHU, L.; LI, P.; GAO, D.; LIU, J.; LIU, Y.; SUN, C.; XU, M.; CHEN, X.; SHENG, Z.; WANG, R.; YUAN, Z.; CAI, L.; MA, Y.; ZHAO, Q. pH-Sensitive Loaded Retinal/Indocyanine Green Micelles as an “All-in-One” Theranostic Agent for Multi-Modal Imaging in Vivo Guided Cellular Senescence-Photothermal Synergistic Therapy. **Chemical Communications**, v. 55, n. 44, p. 6209–6212, 28 maio 2019.

ZHU, Z.-J.; WANG, H.; YAN, B.; ZHENG, H.; JIANG, Y.; MIRANDA, O. R.; ROTELLO, V. M.; XING, B.; VACHET, R. W. Effect of Surface Charge on the Uptake and Distribution of Gold Nanoparticles in Four Plant Species. **Environmental Science & Technology**, v. 46, n. 22, p. 12391–12398, 20 nov. 2012.

ZHUKOVA, V.; OSIPOVA, N.; SEMYONKIN, A.; MALINOVSKAYA, J.; MELNIKOV, P.; VALIKHOV, M.; POROZOV, Y.; SOLOVEV, Y.; KULIAEV, P.; ZHANG, E.; SABEL, B. A.; CHEKHONIN, V.; ABAKUMOV, M.; MAJOUGA, A.; KREUTER, J.; HENRICH-NOACK, P.; GELPERINA, S.; MAKSIMENKO, O. Fluorescently Labeled PLGA Nanoparticles for Visualization In Vitro and In Vivo: The Importance of Dye Properties. **Pharmaceutics**, v. 13, n. 8, p. 1145, ago. 2021.

ZIELIŃSKA, A.; CARREIRÓ, F.; OLIVEIRA, A. M.; NEVES, A.; PIRES, B.; VENKATESH, D. N.; DURAZZO, A.; LUCARINI, M.; EDER, P.; SILVA, A. M.; SANTINI, A.; SOUTO, E. B. Polymeric Nanoparticles: Production, Characterization, Toxicology and Ecotoxicology. **Molecules**, v. 25, n. 16, p. 3731, 15 ago. 2020.

CAPÍTULO II

Association of Curcumin and Carvacrol Co-Loaded Zein Nanoparticles: Comprehensive Preparation and Assessment of Biological Activities

Abstract

To meet the increasing global food demand, improved farming methods are required to mitigate losses. Up to 40% of the 70 billion USD agricultural losses worldwide is attributed to pests. Conventional pesticides, though common, pose environmental and sustainability concerns. Environmentally friendly alternatives, like plant-derived Curcumin and carvacrol, offer promise but degrade in environmental conditions. Nanotechnology extends the efficacy of these compounds in pest control while reducing environmental impact. We developed Zein-based nanocarriers encapsulating curcumin and carvacrol with nanoparticles averaging 110 ± 12 nm, a polydispersion index of 0.159 ± 0.02, and a zeta potential of +30 ± 4 mV. Cytotoxicity tests on 3T3 and HaCat cells revealed 3T3 viability around 60%, contrasting with HaCat cells' 20% viability in active ingredient formulations. No phytotoxicity was observed on soybean plants as well as the evaluating biological activity against mites and caterpillars. *Tetranychus urticae* mortality rates were 82.4 ± 12.4% (active ingredients – a.i. - emulsified) and 77.1 ± 11.5% (a.i. nanoencapsulated). Nanoencapsulated actives demonstrated higher repellency rates (61.1 ± 8.8%) compared to emulsified a.i. (51.1 ± 5.4%). For *Spodoptera cosmioide* and *Spodoptera eridania*, nanoencapsulated a.i. showed significantly higher mortality rates (87.5 ± 7.4% and 64.2 ± 21%, respectively) compared to emulsified a.i. (5.2 ± 2.1% and 29.6 ± 12.3%). These results highlight nanoencapsulation's potential in enhancing compound bioactivity against specific pests and contribute to the sustainable agriculture development.

Key words: zein nanoparticle, curcumin, carvacrol, sustained release, acaricidal effect, insecticides activity.

Introduction

It is already known that the current global food supply will not be enough to guarantee the food security of the world population in 2050, estimated at 9.2 billion inhabitants, requiring an increase in food production around 70% (PAWLAK; KOŁODZIEJCZAK, 2020). In this way, 21st century agriculture has an important challenge to overcome, combating the current causes of reduced productivity and increasing food supply to adequately meet the nutritional needs of the population in 2050.

Plant diseases, such as pathogens and insect pests are major challenges to global food security both directly by reducing the productivity (quantity) and indirectly by loss of quality in both nutrient content and market quality (HAMPF et al., 2021). According to the Food and Agriculture Organization (FAO) around 40% of worldwide crop production is lost to pests. Annually, the plant's diseases cost around $220 billion while insect pests cost at least $ 70 billion to the global economy (FAO, 2021).

The family Noctuidae comprises the biggest number of insects, which are considered pest of agricultural relevance (SOSA-GÓMEZ et al., 2016). *Helicoverpa armigera* is a polyphagous pest that attacks around 200 plant species, including commodities and horticultural plants (CORDEIRO et al., 2020). In Brazil, this pest affects mainly bean, cotton, maize, soybean, bean, sorghum, wheat, tomato, sunflower, fruit, vegetables as well as some weeds (STACKE et al., 2018). The *Spodoptera* complex (*Spodoptera albula, Spodoptera cosmioides, Spodoptera eridania* and *Spodoptera frugiperda*) cause damage to many important crops, such as cotton, corn and soybean, especially in Brazil. All those species are polyphagous, according to Parra *et al.*, (2022), *S. albula, S. cosmioides, S. eridania* and *S. frugiperda* have around 55, 202, 126 and 60 host plants respectively. Only *S. frugiperda* is estimated to cause losses around U$$13 billion in Saharan Africa, including sugarcane, sorghum, rice and maize annually (OVERTON et al., 2021).

Phytophagous mites cause great damage and consequently economic losses in agriculture. Among the 1300 species of the Tetranychidae family, the spider mite, *Tetranychus urticae* is considered one of the most important due to some characteristics; it is extremely polyphagous, feeding on more than 1,100 documented

species (150 of agronomic importance), has a short life cycle (less than 10 days under ideal conditions, which can be shortened due to adaptation to climate change, such as heat and drought), high production of offspring (around 100 eggs, which depending on the situation, , occurs parthenogenesis) and a remarkable ability to develop resistance to pesticides (SANTAMARIA et al., 2020). For this reason, *T. urticae* is one of the most used mites in studies with acaricides.

Currently, synthetic chemicals continue to be the first line of defense against pests, both in agricultural and urban areas, promoting increased food production and the reduction of vector-borne diseases, however, this chemical application is not the best method when considering public health and the environment. The percentage of pesticides lost during an application in agriculture ranges from 2 to 25%, and can spread for kilometers, reaching non-targeted areas and about 80 to 90% of the pesticide that remained on the application site could be lost to volatilization in just a few days, leading to the detection of these in water, soil, air, snow and fog iat different times of the year (AKTAR; SENGUPTA; CHOWDHURY, 2009). Annually, around the world, there are about 385 million cases of accidental poisoning with 11 thousand deaths due to pesticides (BOEDEKER et al., 2020).

Due to this risk and other economic, environmental and public health reasons, there is a need for safer and more sustainable agriculture, with minimal use of pesticides (NICOLOPOULOU-STAMATI et al., 2016). In this scenario, many efforts have been made to develop methods, practices and technologies capable of improving the safety and sustainability of agriculture.

Currently, one option is the utilization of nature-based compounds, which can provide pest control, while decreasing environmental damage and side effects on non-target organisms. Curcuma longa, known as turmeric, is a herbaceous and perennial plant belonging to the Zingiberaceae family. It is a plant of great commercial importance mainly due to the properties of compounds extracted from its rhizome, curcumin (2.8 to 8%) and essential oils (2.5 to 5%). Curcumin (CUR) has been extensively used for therapeutic purposes due to its anticancer, anti-inflammatory, antioxidant, analgesic and antiseptic activities. In addition, this compound is effective in controlling plant pathogens and insect pests (IBÁÑEZ; BLÁZQUEZ, 2020; PANDEY et al., 2021; PERRONE et al., 2015). Carvacrol (2-methyl-5-(1-methylethyl) phenol) (CVC) is a phenolic

monoterpene found in several plant species. This compound is recognized to have antimicrobial properties as well as high toxicity to different invertebrates, including insects, mites and nematodes of agricultural importance. In insects, CVC binds to nicotinic acetylcholine receptors, which results in noncompetitive inhibition of acetylcholinesterase (TONG et al., 2013b).

Although nature-based compounds have been shown to be effective in pest control, their widespread use is limited due to their fast degradation under environmental conditions, low aqueous solubility and sensitivity to light and high temperatures. One way to increase the stability and efficacy of these compounds is their encapsulation into nano-based carriers (DE OLIVEIRA et al., 2014). Several matrices either natural or synthetic can be used to produce these nano-based carriers. Recently, attention has been paid to natural matrices, due to their low cost and high availability, which can facilitate large-scale production. Zein, a naturally occurring protein derived from corn, has gained prominence as an encapsulation material for delivering inputs in agriculture. Its biodegradable and biocompatible properties make it an environmentally friendly choice for encapsulating nutrients, pesticides, or other essential compounds. Zein-based encapsulation protects these inputs from degradation, prolonging their release and effectiveness in soil or on plants (PASCOLI et al., 2020). In this work we have deloped zein nanoparticles to co-delivery CUR and CVC using the antisolvent precipitation method. All formulations were characterized by mean diameter, polydispersity index, zeta potential, morphology and encapsulation efficiency. In addition, the release profile of a.i was studied using dialysis bag assay. The toxicity against non-target organism was evaluated using cell lines (MTT assay) and soybean seedlings (phytotoxic assay) exposed to different concentrations of a.i emulsified and a.i nanoencapsulated.

Materials and Methods

Materials

Curcumin (CUR), carvacrol (CVC), Zein, Pluronic-F68 (PLU) were purchased from Sigma-Aldrich and were used without further purification. Ethanol (ETOH), Acetonitrile

(ACN) was obtained from J.T. Baker. Other reagents (analytical grade or not) were obtained from local suppliers.

Preparation of zein nanoparticles loaded or not with curcumin and carvacrol

The nanoparticles were prepared by precipitation with anti-solvent methodology described by HU& McClements, 2014), with some modifications. A 2% (w/v) solution of zein was prepared with an 85% (v/v) ethyl alcohol solution, which was kept under stirring (overnight). After this time of stirring, the zein solution was heated to 75°C in a water bath for 15 min and, as soon as it reached room temperature, it was centrifuged for 25 minutes at 869 x g and the supernatant was filtered through a 0.45 µm Millipore® membrane to removing large aggregates. The active ingredients were weighed (75 mg of CVC, 2 mg CUR) and 10 mL of zein solution was added to them and kept under stirring for approximately 20 minutes. The zein solution with the actives was poured into 30 mL of Pluronic F-68® solution (pH4.0) under magnetic stirring, remaining under stirring for at least 20 minutes. The formulation was evaporated at 40°C to evaporate the ethanol solvent added together with the zein solution (10 mL), resulting in a final solution of 30 mL. In this study, zein nanoparticles without actives (ZNP_CTL) and containing curcumin and carvacrol (NPZ_CUR+CVC) were prepared. The final concentration of curcumin and carvacrol in each formulation is 0.066 mg/mL and 2.5 mg/mL, respectively.

Physical-chemical characterization of the formulations

The size and zeta potential of nanoparticles was evaluated using dynamic light scattering while the microelectrophoresis was used to evaluate the zeta potential. The samples were diluted 100-fold, equilibrated at 25°C for 120 s and analyzed using ZetaSizer ZS 90 (Malvern®). Furthermore, the nanoparticles size and concentration (nanoparticles/mL) were evaluated by nanoparticles tracking analysis (NTA). The samples were diluted 10.000-fold and analyzed using NanoSight LM 10 cell and a sCMOS camera controlled by NanoSight v. 3.1. Data were expressed as media of three determinations. The pH evaluation was performed using a potentiometer (Tecnal®), calibrated with buffer solutions at pH 4.0 and 7.0. Three measurements were performed

for each particle. Temperature control was used. The encapsulation efficiency of CUR and CVC in zein nanoparticles were analyzed using ultrafiltration/centrifugation technique, using ultracentrifugation devices with 10 kDa of MWCO (Amicon, Millipore). After the filtration, the compound's concentration was quantified using high-performance liquid chromatography. The percentage of CUR and CVC encapsulated was calculated by the difference between total amount added and concentration in the ultrafiltrate. The morphology of the nanoparticles was evaluated by atomic force microscopy (AFM) using Easy Scan Basic (Nanosurf®). The nanoparticles were diluted 10000-fold and a drop was placed onto silicon substrate and dried followed by analysis in a contact mode using TapAl-G cantilever to scan the samples (CAMPOS et al., 2022a).

In vitro release assays and mathematical modeling

In vitro release profiles of encapsulated CUR and CVC as well as non-encapsulated compounds were evaluated using a dialysis bag under sink conditions. This model is composed of a dialysis bag containing the sample (1 mL) with a molecular exclusion pore size of 1 kDa and an acceptor compartment (50 mL) filled with a phosphate buffer with 0.05% of tween 80. At predetermined times, aliquots (1 mL) were withdrawing from the acceptor compartment and the concentration of compounds was determined by HPLC. In order to maintain the same volume of medium throughout the experiment, the volume withdrawn was replaced with a fresh phosphate buffer with 0.05% of tween 80 (ZHANG et al., 2021). Zero order, first order, Higuchi and Korsmeyer-Peppas mathematical models were applied to elucidate the BZC release mechanism from all formulations (MIRCIOIU et al., 2019).

Cytotoxicity Assay

The potential harmful effects of nanoparticles, whether they contained CUR and CVC or not, as well as the non-encapsulated compounds, were assessed through the utilization of the tetrazolium dye reduction (MTT) method on keratinocyte cell lines (HaCat) and fibroblasts (3T3). These cell lines were consistently cultured using DMEM culture medium, supplemented with 10% fetal bovine serum, 100 IU/mL of penicillin, and 100 µL of streptomycin sulfate. The pH was maintained at 7.4, and the cells were kept at a temperature of 37°C under a humid atmosphere with 5% CO_2. For the

experimental procedure, cells were initially seeded into 96-well culture plates at a concentration of $1x10^4$ viable cells per well. Following this, a 24-hour incubation period was allowed. Subsequently, the cells were exposed to either CUR and CVC-encapsulated in zein nanoparticles or non-encapsulated compounds, with concentrations ranging from 0 to 100 µM, for a duration of 24 hours. Control nanoparticles were assessed using the same dilution that was applied to the CUR and CVC-loaded nanoparticles. After the treatment period, the formulations were removed from the cultures and the cells were washed with PBS buffer, 100 µL of MTT solution (3-(4,5-dimethylthiazolyl-2)-2, 5-diphenyltetrazolium bromide) was added to each well at a concentration of 0.5 mg/mL and incubated for 4 hours at 37°C - 5% CO_2. Then the MTT solution was removed and, for cell fixation, 100 µL of DMSO was added per well. Cell viability analysis was performed using the ELISA microplate reading equipment at 540 nm (CAMPOS et al., 2022a)

Phytotoxic assays

Soybean (*Glycine max*) was selected as the model plant due to its significant role in the global economy as a vital cultivar. Renowned for its substantial nutritional worth, it serves both human and animal dietary needs. For the exploration of relative chlorophyll content and quantum efficiency assays, the plants were cultivated in a greenhouse situated at the Biological Sciences Center of the State University of Londrina, PR, Brazil. Seeds from the *G. max* species, specifically the BRS 232 cultivar, were sown in 1 L plastic pots characterized by dimensions of 14 cm in upper diameter, 9.5 cm in lower diameter, and a height of 10.5 cm. These pots contained a mixture of 780 g of Oxisol and sand in a 50:50 ratio. The seeds underwent no prior treatment before planting. Throughout the duration of the experiment, the plants were maintained under natural conditions of light and temperature within the greenhouse. The entire aerial part of each plant was sprayed with 1 mL of the different formulations studied. The assessment of the relative chlorophyll content was carried out utilizing a portable SPAD chlorophyll meter (atLEAF® CHL PLUS). Measurements were continuously acquired from the apex to the base of the leaf blade, avoinding the central vein.

The photochemical efficiency of Photosystem II (PSII) was quantified on the upper surface of the fully matured xx trefoil, employing an OS1p portable fluorometer manufactured by Opti Science. The parameter under evaluation was the Fv/Fm ratio, determined at time intervals of 2, 4, 8, 24,48 and 72 hours subsequent to the application of the treatment. This analysis was conducted in quadruplicate. To establish the maximum PSII activity (Fv/Fm ratio), the leaves underwent a pre-adaptation period in darkness for 15 minutes. Following the initial fluorescence measurement (F0), the maximal fluorescence (Fm) was deduced subsequent to a saturation irradiance pulse (8,250 µmols m^{-2} s^{-1}) lasting 0.8 seconds. The variable fluorescence (Fv) was computed as the difference between Fm and F0 (CARVALHO et al., 2023).

Bioactivity assays

Repellent and acaricidal activity

The repellency and acaricidal activity of the nanoformulations was evaluated using *Tetranychus urticae* Kock (Acari: Tetranychidae) as a model. The experiments were carried out in a climate-controlled chamber (25 ± 1 °C, relative humidity (RH) of 60 ± 10% and light/dark photoperiod of 12 h/12 h) at the Laboratory of Acarology (AcaroLab) at the Faculty of Agricultural and Veterinary Sciences (UNESP/FCAV). The *T. urticae* mites evaluated in the experiment came from rearing kept in the laboratory on jack bean plants (*Canavalia ensiformes L*.), grown in 2 L capacity pots, containing soil, sand and bovine manure (1: 1:1, v:v:v) as substrate (Sato et al., 2005). Circular arenas (2.5 cm in diameter) taken from pesticide-free jack bean leaves were used. The arenas were placed in Petri dishes (9 x 2 cm) containing moistened foam (1.0 cm) and a layer of hydrophilic cotton (1.0 cm), to preserve the turgidity of the arenas (adapted from Knight et al., nineteen ninety). Then, fifteen adult females of the spider mite were transferred to each arena with the aid of a hair brush and a stereoscopic microscope (Zeiss® Stemi DV4, Jena-Germany). The treatments were applied on the arenas with the mites with the aid of a Potter's tower microsprayer (Burkard Manufacturing, Rickmansworth, England), calibrated at a pressure of 68.95 kPa (10 lb/in^2), applying 2 mL of syrup per Petri dish, which corresponded to an average deposition of 1.56 mg/cm^2. The concentrations of curcumin and carvacrol tested were 0.03 mg/mL and 1.250 mg/mL, respectively.

Evaluations were performed at 1, 3, 5 and 7 days after the applications. The mite repellency percentage (% repellency) was calculated considering the total number of mites and the number adhered to the entomological glue barrier. The acaricidal effect percentage was calculated considering the total number of mites and the number of dead mites (CAMPOS et al., 2018b).

Insecticidal activity

The insecticidal activity of the nanoformulations was also evaluated using different types of insects loopers of agricultural importance. The species used were, *Spodoptera frugiperda, Spodoptera cosmioides, Spodoptera eridania and Helicoverpa armigera.* The insecticidal bioactivity bioassays were performed at the Microbial Control of Pest Arthropods Laboratory (UNESP/FCAV, Jaboticabal campus). The formulations (800 µL) of control nanoparticles, nanoparticles loading CUR and CVC as well as the emulsified CUR and CVC were applied on the surface of artificial diet disks (4.8 cm^3) placed on acrylic plates (3.5 cm diameter) at concentration of 0.03 mg/mL for the curcumin and 1.250 mg/mL for the carvacrol. A control disk was treated with the same volume of sterilized distilled water. After complete moisture evaporation, ten second instar larvae were placed on the plates containing the treated diets, using ten replicates. The plates were incubated in a biological oxygen demand (BOD) incubator at 25 ± 1 °C and 70 ± 10% RH, with a photoperiod of 12 hours. The larval mortality was recorded on the seventh day, while the sublethal effects of the treatments were evaluated by weighing the larvae 5 days after the end of mortality evaluation (CAMPOS et al., 2018b).

Results and discussion

Physicochemical characterization and colloidal stability

Development of nano-based formulations that are able to keep the active ingredient stable under environmental conditions, increase the uptake and delivery to the target, promote a sustainable and/or controlled release and reduce the side effects to the environment and non-target organism, is one of the hotspots in the development of sustainable agriculture. Here, we have synthesized zein nanoparticles loaded with a

mixture of CUR and CVC aiming pest control. The physicochemical characterization of control nanoparticles (NP_CTL) and nanoparticles loading mixture of CUR and CVC were evaluated. The physicochemical properties such as mean diameter (nm), polydispersity index (PDI), zeta potential (mV) and pH of the formulations are summarized in Table 1.

Table 1: Physicochemical characterization of zein nanoparticles containing CUR and CVC. The parameter analyzed were size by dynamic light scattering (DLS) and nanoparticles tracking analysis (NTA), polydispersity index (PDI), zeta potential (mV), nanoparticle concentration ([NPs]), encapsulation efficiency (EE) and pH. The values represent the means of three determinations.

Sample	Size (nm)		PDI	ZP (mV)	[NPs] (10^{13} particles/mL)	EE (%)	pH
	DLS	NTA					
NP_CTL	111 ± 5	202 ± 11	0.153 ± 0.03	34 ± 12	1.08 ± 0.02	-	4.28 ± 0.08
NP_CUR+CVC	100 ± 12	169 ± 1	0.159 ± 0.02	30 ± 4	3.52 ± 0.05	89.8 ± 0.01 94.6 ± 0.70	4.48 ± 0.03

As indicated in Table 1, the initial average diameter of NP_CTL and NP_CUR+CVC stood at 111 ± 5 nm and 100 ± 12 nm, respectively. Alterations in the mean size, as determined by dynamic light scattering (DLS), were noted for both nanoparticle types over the storage duration. However, it is noteworthy to highlight that no statistically significant differences emerged between the initial dimensions and those observed after a 90-day period for both investigated formulations (data not presented). It is noted that there are no subpopulations with sizes smaller or larger than the average of the distributions, showing that the formulations, with and without active ingredients, have a monomodal size distribution (FIgure 1 A), characterized by a polydispersity index of 0.153 ± 0.03 and 0.159 ± 0.02 for NP_CTL and NP_CUR+CVC, respectively. In addition, it is worth noting that all values were below 0.2 as well as below the values normally reported for polymer-based nanoparticles produced with natural matrices, such as the zein itself used here (DE OLIVEIRA et al., 2019).

The mean diameter was also assessed through nanoparticle tracking analysis (NTA) for both nanoformulations. In this regard, the size distribution was determined to be 202 ± 11 nm for NP_CTL and 169 ± 1 nm for NP_CUR+CVC, presenting larger values than those obtained via dynamic light scattering (DLS). It is notable that while both

techniques rely on the diffusion coefficient of nanoparticles to measure size, they differ in their methodologies. DLS measures modifications in scattered light to infer the nanoparticles' diffusion coefficient, whereas NTA estimates the diffusion coefficients of individual particles based on video analysis. Moreover, NTA was employed to quantify the nanoparticles' concentration, yielding values of 1.08 ± 0.02 x 10^{13} particles/mL for NP_CTL and 3.52 ± 0.05 x 10^{13} particles/mL for NP_CUR+CVC. These results are in agreement with the Germano-Costa et al. (2022) who have synthesized zein nanoparticles co-loading icaridin and geraniol. The control NPs showed mean diameter 112 ± 3 nm while NPs loading both active ingredients showed a mean diameter 245 ± 4 nm (GERMANO-COSTA et al., 2022)

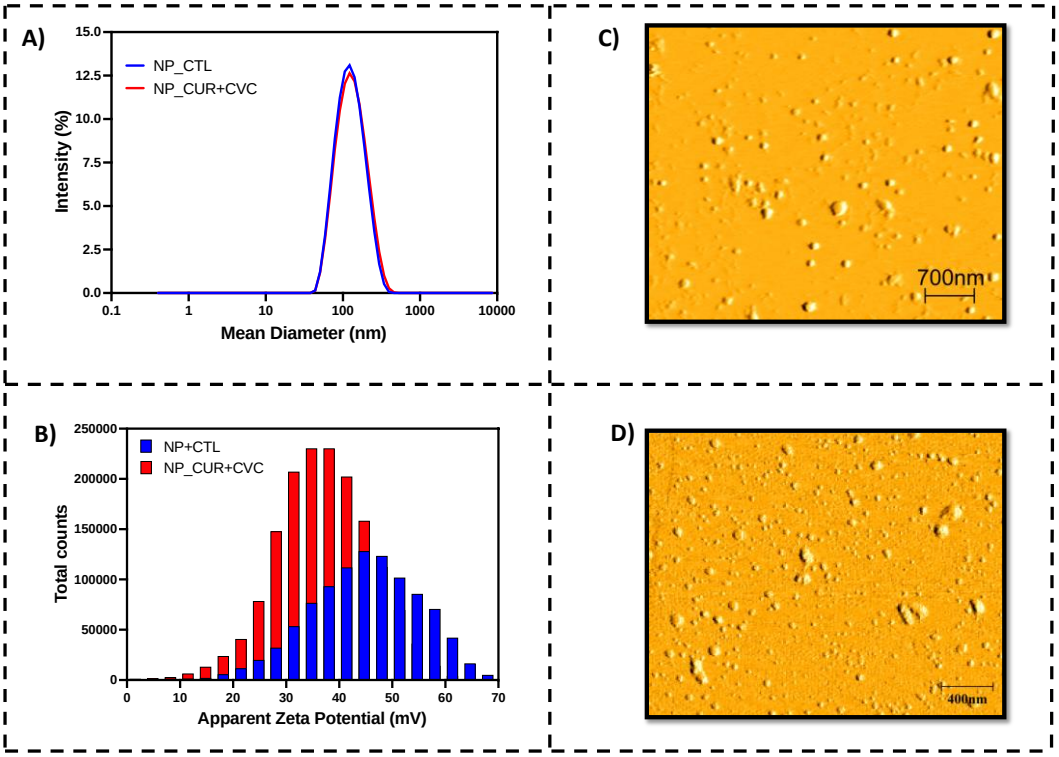

Figure 1: Physicochemical characterization of zein nanoparticles A) Size distribution of control nanoparticles (NP_CTL – blue line) and loaded zein NPs (NP_CUR+CVC – red line); B) Zeta Potential of control nanoparticles (NP_CTL – blue bar) and loaded zein NPs (NP_CUR+CVC – red bar; C) atomic force microscopy of control nanoparticles (NP_CTL) and D) atomic force microscopy of loaded zein NPs (NP_CUR+CVC).

For both nanoformulations produced here, the zeta potential was positive with initial values above 30 mV, which is considered the critical value for stable colloidal suspension (Figure 1B). Furthermore, it is noteworthy that pluronic F-68 was used as a

surfactant in the formulations produced here. This non-ionic surfactant increases steric repulsion, ensuring greater stability to the nanoformulation by reducing coalescence between particles, reducing one of the main disadvantages of zein nanoparticles, which is, according to DAVIDOV-PARDO et al., 2015), the tendency to form aggregates in aqueous solutions due to high surface hydrophobicity.

For Mora-Huertas et al. (2010) the zeta potential of the nanoparticles will depend on the pH of the medium and the chemical nature of the polymer and the stabilizing agent. The pH probably influences the intensity of the zeta potential while the polymer and the stabilizing agent influence the positivity or negativity of the charges. In the case of non-ionic stabilizing agents, the charge of the polymer or its terminal portions determine positivity or negativity. The active ingredient seems to show no influence on the zeta potential due to its entrapment in the core. The last parameter evaluated was pH (Table 1), which showed an initial value of 4.28 ± 0.08 for NP_CTL and 4.48 ± 0.03 for NP_CUR+CVC and remained stable after a 90-day period for both investigated formulations (data not presented).

Patel *et al.* (2010) also produced zein nanoparticles loaded with CUR by the anti-solvent precipitation technique and obtained positive values of zeta potential ranging from 6 to 35 mV depending on the ratio of zein:curcumin used. When the ratio of 50:1 was used, the nanoparticles had a size of around 132 nm, a polydispersity index of 0.16 and a zeta potential of 30.8 mV. The zein particle without CUR showed size of 147 nm, polydispersity index 0.18 and showed a positive zeta potential of 34.3 mV. It was observed that in proportions below 5:1 (zein:CUR) the produced particles become unstable due to the increase of hydrophobic curcumin inside and outside the polymeric matrix, as they increase the hydrophobic character of the nanoparticle due to Van der Waals interactions, even though the polyphenols have a strong affinity for proteins, especially those rich in prolines, such as zein. The nanoparticles produced here exhibit a ratio of 100:1 (zein:CUR) and are in agreement with those results. Curcumin-loaded zein nanoparticles were also produced by Zou *et al.* (2016) using a ratio of 20:1 (zein:CUR). The nanoparticles were close in size to those produced in this study, 120 ± 12 nm, but with a higher polydispersion (0.252 ± 0.005) and also obtained a positive zeta potential around 19.9 ± 0.8 mV. The authors attribute the relatively high value of the

zeta potential of his particles to pH, which was around 4.0, below the isoelectric point of zein (pH ≈ 6.5).

Shinde *et al.* (2020) produced zein and lecithin nanoparticles loaded with carvacrol and observed a direct relationship between decreasing nanoparticle size (312 ± 23 nm to 221 ± 15 nm) with increasing carvacrol concentration (0.75 to 1.25 mg). CVC encapsulation prevented the formation of chain-like aggregates and the charged nanoparticles exhibited smoother and more uniform surfaces than the control nanoparticles. The addition of carvacrol reduced the zeta potential of the nanoparticles from –22.43 ± 1.23 mV to −8.15 ± 0.91 mV, indicating that the active ingredient can indeed interfere with the zeta potential, contrary to what was observed by MORA-HUERTAS et al. (2010).

In addition, AFM was used to investigate the size distribution and morphology of CUR-loaded nanoparticles (NP_CUR+CVC) (Figure 1 C-D). The morphological characterization showed that nanoparticles have a spherical-like shape and smooth surface. The mean diameter obtained by AFM was 42 ± 27 nm, which was smaller than those obtained by DLS. This difference is due to the particularity of each technique. In the DLS, the average hydrodynamic diameter of the nanoparticles is measured, as they are in aqueous suspension, whereas in the AFM technique, the diameter measurement is made with the dry particle. These results are in agreement to those obtained by Luis *et al.*, (2020) which reported spherical zein nanoparticles loading eugenol and garlic oil, using AFM analysis.

In vitro **release kinetics**

In vitro drug release was studied for CUR and CVC-loaded zein nanoparticles and CUR and CVC non-encapsulated using dialysis bags under sink conditions at room temperature. The compounds release profiles from different formulations in function of time are shown in Figure 2. Due to the poor aqueous solubility of CUR (0,6 mg/L) and CVC (0.33 g/L), the non-encapsulated compounds (control group) were diluted in Pluronic F68 (2%), which was at the same concentration used for nanoparticles preparation. As can be observed in the Figure 2A, there is no difference in the release of CUR between the non-encapsulated CUR and CUR-loaded in zein NPS. After 24 hours, there is a release of approximately 26 ± 2 % of the amount encapsulated in the zein NPs.

The rationale for this phenomenon lies in the formation of micellar structures during the emulsification process with Pluronic. These micellar structures can be regarded as a delivery system for CUR (a poorly water-soluble compound). In recent times, there has been a significant surge in research on micellar structures, such as nanoemulsions, as a means to effectively transport hydrophobic substances to plants (FENG et al., 2018; PATIR, 2022). Zhang et al, (2021) evaluated the release of CUR-loaded zein nanoparticles coated with polydopamine using phosphate buffer with 0.5% of tween 80 as acceptor medium at 37ºC and pH 7.4 and 5. Different from observed here, the non-encapsulated CUR showed a burst release, reach 100% of release after 8 hours. However, after encapsulation the release was around 45% and 80% at pH 7.4 and 5, respectively. The higher release obtained by the authors could be attributed to the higher temperature tested as well as the coating, which could facilitate the CUR release. On the other hand, when we evaluate the release of CVC (Figure 2B), we can see that there was a more sustained release of CVC after incorporation of the compound in zein NPs, mainly between 1 and 3 hours of experiment. After that, there is a decrease in the release rate between the non-encapsulated compound and CVC-loaded to zein NPs. After 24h, the release rate of CVC was 55 ± 2% and 60 ± 3 % for non-encapsulated CVC (EM_CVC) and NP_CVC, respectively.

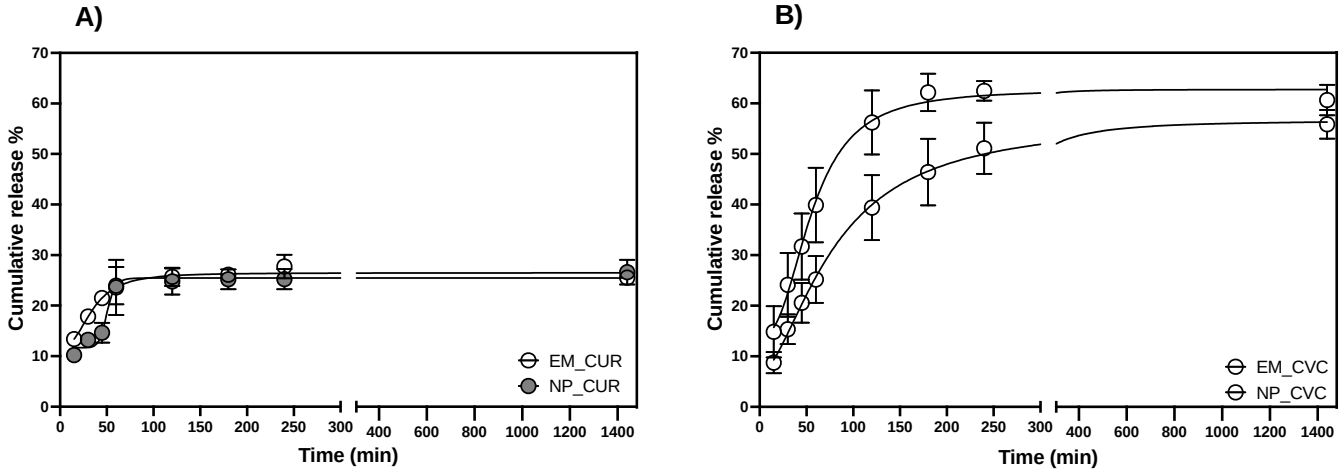

Figure 2: Kinetics of release of CUR and CVC from the zein nanoparticles. The release assay was performed using dialysis bag at (25 °C), in phosphate buffer with 0.05% of tween 80. The analyses were performed in triplicate and quantified by HPLC.

To evaluate the mechanism of CUR and CVC delivery from the nanoparticles a different mathematical modeling was applied, such as zero order, first order, Higuchi and Korsmeyer-Peppas. Linear regression was used to calculate the values of the release constants (k) and the correlation coefficient (r). The results are summarized in Table supplementary S1. As shown in the Table S1, tf both CUR and CVC from both non-encapsulated solution and encapsulated in zein NPs, the best fit to the release profile was obtained using Korsmeyer-Peppas model, with a correlation coefficient above 0.8 for all formulation studied. Regarding the release exponent (n), both non-encapsulated CUR and CUR-loaded zein nanoparticles showed a value >1, which suggest that the release mechanism correspond to the drug transport mechanism linked to stress-induced alterations and state transitions within hydrophilic glassy polymers that exhibit swelling in aqueous or biological environments. This concept encompasses not only polymer disentanglement but also erosion processes. The release of non-encapsulated CVC and CVC-loaded zein NPs showed a *n* value of 0.96 and 0.53, respectively, which suggest that the release mechanism correspond to anomalous diffusion mechanism (non-fickian transport) that depends on both diffusion and relaxation (erosion) of the polymer matrix. Similar results were founded by Oliveira et al (2019) co-delivery of geraniol and cinnamaldehyde loaded in zein nanoparticles and the release of both compounds best fit to Korsmeyer-Peppas model and the release mechanism is also anomalous diffusion (DE OLIVEIRA et al., 2019).

Cytotoxicity assay

In vitro cell viability assay was performed to evaluate the cytotoxic effect of the nanoencapsulated and emulsified active ingredients, as well as the control nanoparticles (Figure 5). The cytotoxic assay was evaluated using fibroblast cell line (3T3 - Figure 3 A) and keratinocytes cell line (HaCaT - Figure 3 B) over 24 hours. For the Pluronic F68, for both cell lines (3T3 and HaCaT) the cellular viability was around 80% in all concentrations tested and no significant differences were observed between them. On the other hand, the addition of active ingredients in the emulsion significantly increased ($p < 0.0001$) the toxicity for both cell lines when compared to the control emulsion. In addition, the HaCaT cell lines were more sensitive to EM_CUR+CVC when compared to 3T3 cell lines,

at the highest concentration tested (350 uM CVC and 0.127 uM CUR), the cell viability for 3T3 was 62 ± 2% and for HaCaT was 14 ± 2%. Both nanoparticles formulation (NP_CTL and NP_CUR+CVC) showed a similar toxicity trend to 3T3 cell line, with no significant difference between treatments, except for the concentrations of 50 and 100 uM CVC and 0.036 and 0.054 uM CUR. However, for the HaCaT cell line, NP_CUR+CVC showed significantly higher toxicity ($p < 0.05$) in all concentrations tested when compared to NP_CTL, except at the lowest concentration tested. Furthermore, for HaCaT cell lines, there is no significant difference between the emulsified and nanoencapsulated active ingredients. This result showed a different pattern of nanoformulation toxicity between the cell lines, for 3T3 it seems that the toxicity is mainly driven by the nanoparticles' physicochemical properties while for HaCaT is due to the presence of active ingredients.

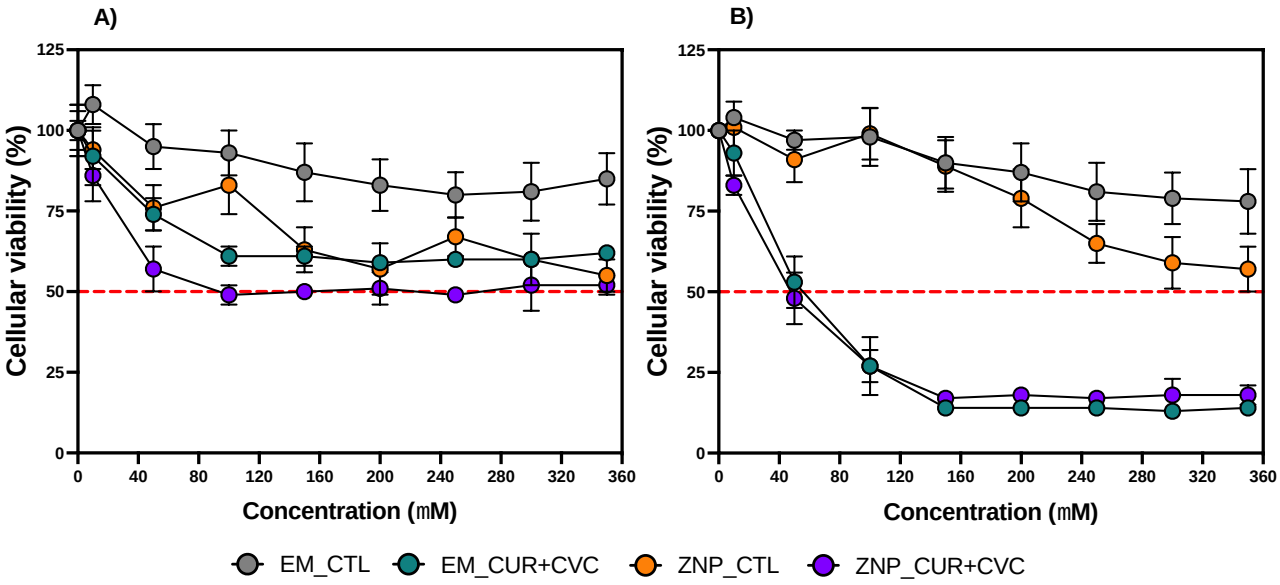

Figure 3: Cytotoxic assay of the formulations in different cell line. A) Fibroblasts (3T3) and **B)** keratinocytes (HaCat). Cells were treated with control emulsion (EM_CTL), active ingredients emulsioned (EM_CUR+CVC), control nanoparticles (NP_CTL) and nanoencapsulated active ingredients (NP_CUR+CVC) for a period of 24 hours at 37º C. Cell viability was assessed by the MTT assay, with the control group being considered 100% of cell viability. Values represent the mean ± SD of three determinations (n = 9).

It is already known that the surface charge of nanoparticles influences the interaction with the extracellular membrane of the cells. Due to the abundance of

glycosaminoglycans that have negatively charged groups, extracellular membranes show negative charge, which favors the electrostatic interaction with positively-charged nanoparticles (AUGUSTINE et al., 2020). Here, zein nanoparticles were more toxic to the cells when compared to previous works from our group (DE OLIVEIRA et al., 2018, 2019), however, is worth to mention, that the nanoparticles from the previous works, were negatively charged, which may explain the lower toxicity due to weak electrostatic interaction between nanoparticles and extracellular membrane.

The interference in the metabolic activity as well as generation of reactive oxygen species (ROS) in cells treated with positive charged polymer-based nanoparticles has been demonstrated (PATEL et al., 2010; SINGH et al., 2021). PLATEL *et al.* (2016) evaluated the cytotoxic effect of the surface charge of poly (lactic- co-glycolic acid) (PLGA) nanoparticles in three different cell lines: L5178Y mouse lymphoma cells, TK6 human B-lymphoblastoid cells, and 16HBE14o human bronchial epithelial cells. The authors showed that the positive PLGA nanoparticles were cytotoxic as well as increased ROS production for all cell lines tested, whereas negatively and neutral charged PLGA nanoparticles did not significantly affect the cells.

Phytotoxic assay

Chlorophylls serve as the pigments that take on the crucial role of capturing light energy during photosynthesis, facilitating its transformation into ATP and NADPH. As a result, a direct connection exists between a plant's photosynthetic efficacy and its capacity to thrive and acclimate to diverse environmental conditions (SHI et al., 2023). The assessment of these pigments holds significant importance in the examination of vegetative behavior and how plants react to potential harm, such as phytotoxic effects, following the application of nanoparticulate systems (PEHAREC ŠTEFANIĆ et al., 2021). These systems have the potential to influence a plant's photosynthetic capacity and overall productivity, making their study and understanding critical. In this work, we have evaluated the phytotoxic effects of the zein nanoparticles loading CUR and CVC by determining the leaf chlorophyll content (SPAD). The chlorophyll levels within soybean plants undergo fluctuations during their growth stages (SHI et al., 2023). Specifically, the SPAD values for soybean seedlings rise as the seedlings mature. Within 8 days of cultivation, corresponding to the emergence of single-leaf leaves, the SPAD values

remain below 30. However, after 16 days of cultivation, when the plants have developed two fully expanded trefoils, the SPAD indexes surpass the threshold of 30 (GUO et al., 2023). Based on Figure 4, it is evident that none of the tested substances, including the non-encapsulated compound (EM_CUR+CVC), the control nanoparticle (NP_CTL), and the nanoparticle carrying both CUR and CVC nanoencapsulated, induced significant alterations in chlorophyll content when compared to the control group at any of the observed time points. Throughout the entire 72-hour analysis period, the SPAD values remained consistently around 30 for all treatments, aligning with the established norms for soybean plant development at this stage. Consequently, it can be concluded that these treatments exhibited no phytotoxic effects on soybean plants and did not disrupt their growth and development.

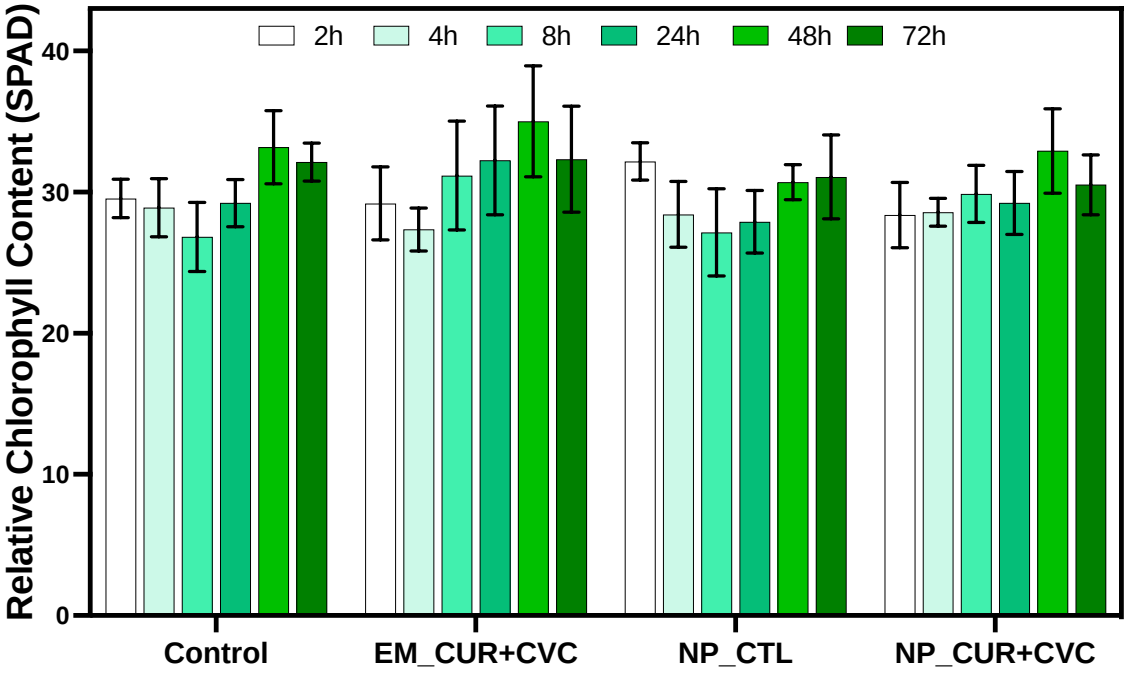

Figure 4: Phytotoxic assay of the formulations in soybean seedlings: Relative chlorophyll content (SPAD) in soybean plants treated with non-encapsulated CUR and CVC (EM_CUR+CVC), control nanoparticle (NP_CTL) and CUR+CVC-loaded in zein nanoparticles (NP_CUR+CVC) as a function of time. Data are represented as the mean + SD of three determinations. The data SPAD were transformed to arc sin raiz de x/100 for all analyses statistics. The statistic test realized were Two-way Anova with Tukey 's Multiple Comparisons test T.

Chlorophyll fluorescence serves as a valuable tool for assessing a plant's photosynthetic activity. Essentially, the photons absorbed by chlorophyll play a crucial role in photochemical reactions within photosystem II. The quantum efficiency of this process can be determined by calculating the ratio of variable fluorescence measurements to maximum fluorescence, denoted as Fv/Fm (AZEVEDO NETO et al., 2011), and it signifies the pinnacle of photosynthetic efficiency.

Fv/Fm values, when plants are thriving under optimal conditions without stress, exhibit variability across species, genotypes (AZEVEDO NETO et al., 2011), and various growth stages. Stressful conditions lead to a decline in these values, indicating a reduction in the efficiency of photosynthesis, often resulting from disturbances or damage to the plant's photosynthetic machinery (AZEVEDO NETO et al., 2011).

Even within the same species, such as sunflower plants, normal Fv/Fm values can vary among different genotypes, ranging from 0.726 to 0.803 (AZEVEDO NETO et al., 2011). Normal values for soybean seedlings typically fall around 0.82 (GUO et al., 2023), a range consistent with the findings in our study.

In our investigation, the average Fv/Fm (Figure 5) values for control groups at various time intervals (2, 4, 8, 24, 48, and 72 hours) after treatment ranged from 0.810 ± 0.016 to 0.820 ± 0.006. For the group treated with emulsified actives (EM_CUR+CVC), Fv/Fm values ranged from 0.805 ± 0.010 to 0.812 ± 0.020. In the case of the group treated with control nanoparticles (NP_CTL), the Fv/Fm values spanned from 0.775 ± 0.068 to 0.809 ± 0.017. Meanwhile, for the group treated with nanoencapsulated actives, Fv/Fm values ranged from 0.807 ± 0.007 to 0.824 ± 0.005. Importantly, no statistically significant differences were observed in Fv/Fm values across time intervals or among treatments.

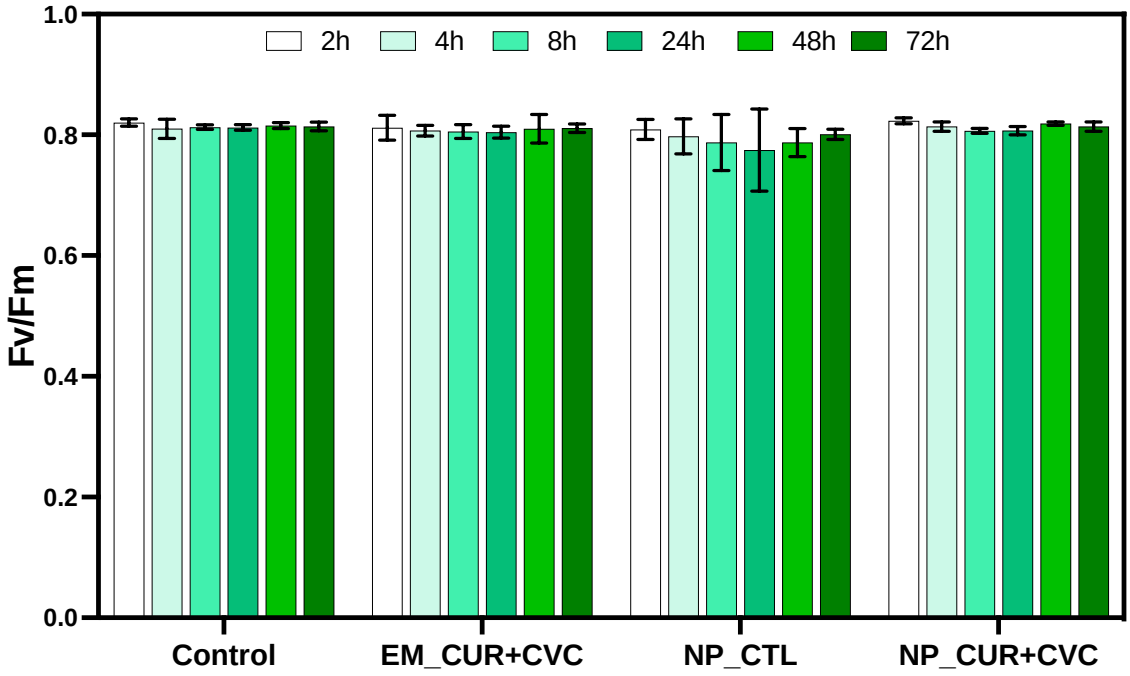

Figure 5: **Phytotoxic assay of the formulations in soybean seedlings**: Maximum quantum yield of photosystem II (Fv/Fm) in soybean plants treated with non-encapsulated CUR and CVC (EM_CUR+CVC), control nanoparticle (NP_CTL) and CUR+CVC-loaded in zein nanoparticles (NP_CUR+CVC) as a function of time. Data are represented as the mean + SD of three determinations. The statistic test realized were Two-way Anova with Tukey 's Multiple Comparisons test T.

The Fv/Fm values for the group treated with NP_CTL exhibit a slight, gradual decline in mean values up to the 24-hour mark following application. Notably, this decline, while present, does not reach statistical significance when compared across different time points within the same treatment group or when compared to the control group. It is worth mentioning that despite this observed variation in values, a subsequent recovery becomes apparent at later time intervals, suggesting that if any form of damage occurred, the plant had the ability to self-regulate and restore normalcy.

In a related context, soybean plants cultivated hydroponically with a boron-deficient solution experienced a decrease in Fv/Fm values after 72 hours (0.76), followed by a return to normalized values (0.82) after 8 days (GUO et al., 2023). These findings imply that fluctuations in Fv/Fm values over time may not necessarily be detrimental and could be part of the plant's natural adaptive mechanisms.

In light of the results, it can be inferred that zein-based carriers do not compromise plant development. This conclusion is supported by the data presented in this study and corroborated by data from previous research involving Zea mays (CARVALHO et al., 2023).

Biological activity

Mites (*Tetranychus urticae)*

The effect of the formulations was evaluated considering the acaricidal effect (mortality) and the repellent effect on mites treated with EM_CUR+CVC, NP_CTL and NP_CUR+CVC. The concentration of CUR and CVC was 0.03 mg/mL and 1.250 mg/mL, respectively, and for the control nanoparticles, the same dilutions were used. The acaricidal activity (Figure 6 A) showed a similar trend for all treatments tested, there is an increase in the mortality in function of the time (up to 7 days). After 7 days, the highest acaricidal activity was observed for EM_CUR+CVC (82.4 ± 12.4%), followed by NP_CUR+CVC (77.1 ± 11.5%), NP_CTL (63.9 ± 14.8%). There is no significant difference in the acaricidal activity between the emulsified and nanoencapsulated active ingredients. In addition, as observed for the cytotoxic assays for 3T3 cell, there is no difference in the acaricidal activity between the NPs_CTL and NP_CUR+CVC at any of the times studied. Similar results were previously achieved in our research group, initially there is no significant difference between the zein nanoparticle without active and with active, however it is observed through the residual effect test that the mortality rates of the control nanoparticle decrease while the rates of the active nanoparticles increase (PASCOLI et al., 2020). Ahmadi *et al.* (2018) shows that the mortality rate for nanoencapsulated actives has a less pronounced drop compared to free actives in a residual effect test conducted for 24 days. This is probably due to the protection and sustained release of the actives provided by nanoencapsulation.

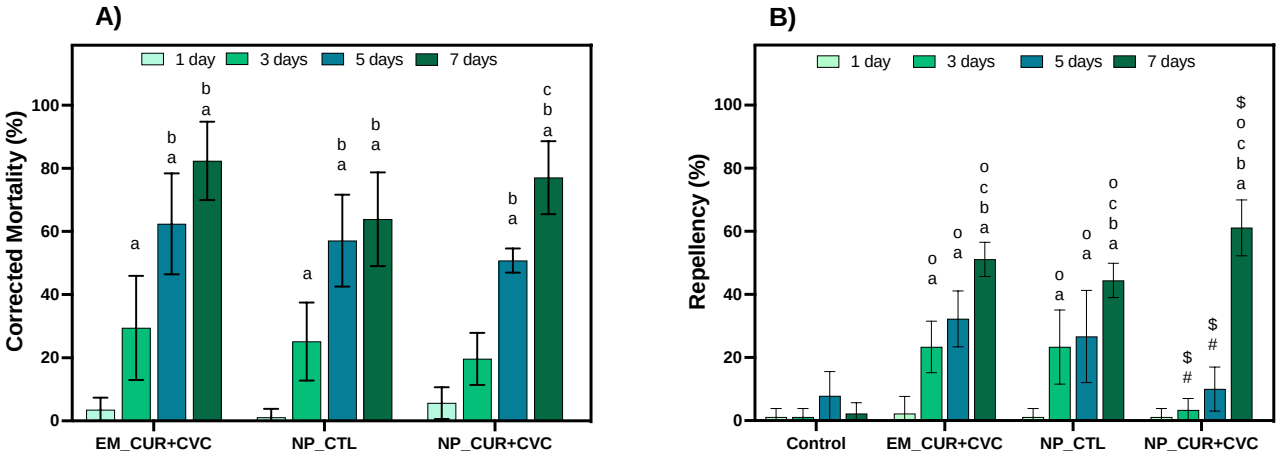

Figure 6: Evaluation of acaricidal and repellet activity of the nanoforulations against *Tetranychus urticae.* Graph of acaricidal efficiency (corrected mortality) and repellency for *T. urticae* of different formulations, active ingredients emulsioned (EM_CUR+CVC), control nanoparticles (NP_CTL) and nanoencapsulated active ingredients (NP_CUR+CVC). The concentration of CUR and CVC was 0.03 mg/mL and 1.250 mg/mL, respectively. The statistic test realized were Two-way Anova with Tukey 's Multiple Comparisons test. The letters a, b and c represent the significant variation between groups as a function of time; a- comparison with time 1 day; b- comparison with time 3 days and c- comparison with time 5 days. The symbols o, #, $ and & represent significant variation between different treatments within the same assessment day; o - comparison with Control in Repellency; # - comparison with EM_CUR+CVC; $ comparison with NP_CTL; & - comparison with NP_CUR+CVC. Significance of $p<0.05$ was considered.

We also evaluated the repellency activity of the formulations (Figure 6 B) and it is possible to see the repellent activity increased as a function of time for all treatments tested. When comparing the repellency efficacy of the emulsion and nanoencapsulated active ingredients, there are only significant differences between them on the third and fifth day after treatment, while on the last day (7 days) there is no significant difference. Unlike what was observed for the acaricidal activity, on the last day of observation, the NP_CUR+CVC showed a significantly higher repellency than the NP_CTL.

Larvae (*Spodoptera sp.*)

The activity of the formulations was tested on caterpillars of the species *Helicoverpa armigera, Spodoptera eridania, Spodoptera frugiperda and Spodoptera cosmioides*. The mortality data and sublethal effect that were obtained for the four species are shown in Table 2 and Figure 6. The concentration of CUR and CVC was 0.03 mg/mL and 1.250 mg/mL, respectively, and the same dilutions were used for the control nanoparticles. For the evaluation of the sublethal effect, ten individuals of each species tested were randomly chosen and their larval and pupal weights were monitored. The mortality assessment was completed on the 7th day and the weight of the caterpillars was assessed on the 5th day after the end of the mortality assessment (12th day after application). The twelfth day was chosen because it is sufficient time for practically all caterpillars, regardless of treatment, to remain in pre-pupal phase.

Table 2: Biological activity of mortality and mass of larvae and pupae of *Spodoptera* sp. Data of corrected mortality and sublethal effects for four species of caterpillar Helicoverpa armigera, *Spodoptera eridania*, *Spodoptera frugiperda* and *Spodoptera cosmioides* against of the treatments, active ingredients emulsioned (EM_CUR+CVC), control nanoparticles (NP_CTL) and nanoencapsulated active ingredients (NP_CUR+CVC).

Species	Treatment	Corrected Mortality (%)	Weight Larvae 12º day after application (g)	Weight Pupa - g (n)	Dead (units)
Helicoverpa armigera	EM_CUR+CVC	58.7 ± 15.3	0.07 ± 0.05	0.22 ± 0.02 (5)	5
	NP_CTL	67.01 ± 19.57	0.18 ± 0.16	0.27 ± 0.05 (4)	6
	NP_CUR+CVC	72.16 ± 19.45	0.19 ± 0.2	0.25 ± 0.10 (3)	7
	Control	3 ± 7.3	0.16 ± 0.12	0.19 ± 0.08 (10)	0
Spodoptera cosmioides	EM_CUR+CVC	5.20 ± 2.17	0.68 ± 0.23	0.0 (0)	10
	NP_CTL	< control	0.73 ± 0.17	0.35 ± 0.04 (5)	5
	NP_CUR+CVC	87.5 ± 7.48	0.43 ± 0.17	0.42 ± 0.0 (1)	9
	Control	4 ± 8.2	0.29 ± 0.04	0.30 ± 0.07 (10)	0
Spodoptera eridania	EM_CUR+CVC	29.59 ± 12.34	0.16 ± 0.12	0.29 ± 0.05 (5)	5
	NP_CTL	16.3 ± 10.2	0.19 ± 0.10	0.28 ± 0.01 (9)	1

	NP_CUR+CVC	64.28 ± 20.99	0.21 ± 0.10	0.25 ± 0.03 (4)	6
	Control	2 ± 6.1	0.31 ± 0.12	0.25 ± 0.06 (10)	0
Spodoptera frugiperda	EM_CUR+CVC	50 ± 18.79	0.27 ± 0.12	0.21 ± 0.05 (9)	1
	NP_CTL	52.08 ± 21.13	0.28 ± 0.10	0.23 ± 0.02 (8)	2
	NP_CUR+CVC	47.91 ± 19.77	0.28 ± 0.10	0.23 ± 0.01 (7)	3
	Control	4 ± 8.2	0.31 ± 0.10	0.23 ± 0.02 (10)	0

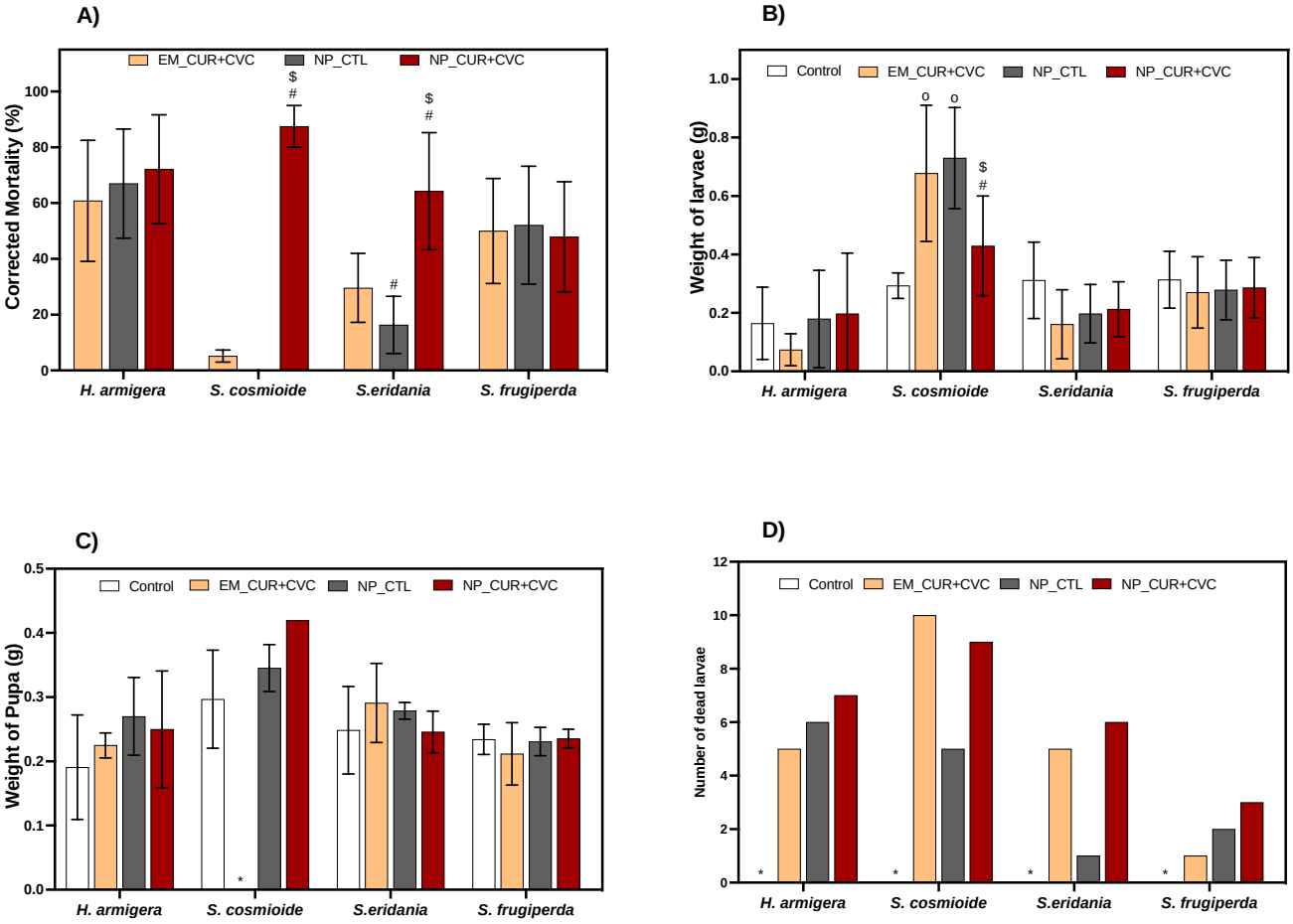

Figure 7: Mortality and sublethal effects of the nanoformulations against larvae (Spodoptera sp.) A) Corrected mortality of the larvae treated with different formulations; **B)** Weight of the larvae after 5 days of treatment with different formulations; **C)** Weight of the pupae treated with different formulations and **D)**. The concentration of CUR and CVC was 0.03 mg/mL and 1.250 mg/mL, respectively. The statistic test realized were Two-way Anova with Tukey 's Multiple Comparisons test. The symbols o, #, $ and & represent significant variation between different treatments within the same assessment day; o - comparison with Control in Repellency; # -

comparison with EM_CUR+CVC; $ comparison with NP_CTL; & - comparison with NP_CUR+CVC. Significance of $p<0.05$ was considered.

For the mortality test, all evaluated treatments show a significantly greater effect than the control (Figure 7 A). Mortality evaluation for *H. armigera* and *S. frugiperda* does not show difference between treatments. As for *S. cosmioide* and *S. eridania*, there is a significant increase in mortality observed for nanoencapsulated assets, 87.5 ± 7.48 % and 64.28 ± 20.99 %, respectively, against emulsified assets, 5.20 ± 2.17 % and 29.59 ± 12.34 %, respectively. The evaluation of the sublethal effect (Figure B-D) for the species *H.armigera*, *S. eridania* and *S. frugiperda*, did not show significant changes in the weight of the caterpillars (Figure 7 C) in relation to the control group, whereas for the species *S. cosmioide* the nanoparticle without active and the emulsified actives caused a significant increase in the weight of the caterpillars. Regarding the mass of the pupa (Figure 7 B), there were no significant changes.

de Oliveira *et al.* (2019) observed a decrease in the weight of caterpillars and pupae of *Chrysodeixis includes* after treatment with empty zein nanoparticles (negative zeta potential) and emulsified and nanoencapsulated botanical compounds (positive zeta potential). The mortality rate for formulations with actives was approximately 80% and for nanoparticles without actives was 47.6 ± 3.1%. Bonser *et al.* (2020) also observed a decrease in weight for *Anticarsia gemmatalis* and *Chrysodeixis includes* (3rd instar) when treated with empty zein nanoparticles with positive zeta potential, but without increased mortality, while for Heliothis virescens there was no significant change in weight and mortality. The weight of *Chrysodeixis includes* pupae were evaluated and showed no significant changes.

The number of dead larvae at the end of the sublethal effect assessment (Figure 7 C) was counted. For the species *S. cosmioide* and *S.eridania*, the highest number of deaths occurred in treatments with emulsified and nanoencapsulated actives. Despite there being no differences in pupae mass, there seems to be a tendency for caterpillars to enter the pre-pupal phase a little earlier and remain in it longer for *S. cosmioide* and for *H. armigera*, many of them died before the pre-pupa stage.

The control nanoparticle also shows a positive effect on mortality (Figure 7 A) of *H. armígera* caterpillars (67.01 ± 19.57 %), *S. frugiperda* (52.08 ± 21.13 %) and to a lesser

extent for *S. eridania* (13.30 ± 21.13 %). The positive effect can be influenced by the zeta potential of the nanoparticles. Monteiro *et al.*, (2021) had a mortality rate of 18 ± 10 % for the *S. frugiperda* species when treated with control zein nanoparticles with negative zeta potential, this value not being statistically different from the control.

Conclusion

CUR and CVC-loaded zein nanoparticles showed a good physicochemical property, high encapsulation efficiency, spherical shape and stability over storage time (90 days). The CUR+CVC-loade nanoparticles decreased the cell viability for both cell lines tested, however keratinocytes cells (HaCaT) were more sensitive when compared to fibroblast (3T3) ones. On the other hand, no phytotoxicity effects were found after the application of both encapsulated and non-encapsulated compounds in aerial part (levaes) of soybean seedlings. The nanoparticles are able to release both compouds in a sustainable way, being CVC released in a greater amount when compared to CUR in the same period of time, due the to higher aqueous solubility of CVC (8-fold) when compared to CUR. Both control NPs and CUR+CVC encapsulated in zein nanoparticles or not showed acaricidal activity against *T. urticae,* however, there is a trend of formulation with active ingredient, especially the non-encapsulated ones, to be more efficient. The same trend was observed when the repplent activity of the formulations was evaluated against the mites. Among the all-caterpillar species tested, the best results were obtained for *Spodoptera cosmioide* and *Spodoptera eridania*, where nanoencapsulated actives showed significantly higher mortality rates (87.5 ± 7.4% and 64.2 ± 21%, respectively) compared to emulsified actives (5.2 ± 2.1% and 29.6 ± 12.3%). These results demonstrated that the zein nanoparticles co-loading CUR and CVC could be a promising drug delivery system aiming pest control, however, further studies are needed to understand the mechanisms of action of these nanoparticles and their possible off-target effects.

Acknowledgments

Authors are grateful to the São Paulo Research Foundation (FAPESP, grants, #2022/00509-0, #2022/03399-0, #2019/04758-1 and #2017/21004-5), Conselho Nacional de Desenvolvimento Científico e Tecnológico (CNPq - 308439/2021-0), and

Coordenação de Aperfeiçoamento de Pessoal de Nível Superior – Capes (88887.695285/2022-00; 88887.351694/2019-00; 88887.817514/2023-00).

References

AHMADI, Z.; SABER, M.; AKBARI, A.; MAHDAVINIA, G. R. Encapsulation of Satureja Hortensis L. (Lamiaceae) in Chitosan/TPP Nanoparticles with Enhanced Acaricide Activity against Tetranychus Urticae Koch (Acari: Tetranychidae). Ecotoxicology and Environmental Safety, v. 161, p. 111–119, out. 2018.

AKTAR, W.; SENGUPTA, D.; CHOWDHURY, A. Impact of Pesticides Use in Agriculture: Their Benefits and Hazards. Interdisciplinary Toxicology, v. 2, n. 1, p. 1–12, 28 fev. 2009.

AUGUSTINE, R.; HASAN, A.; PRIMAVERA, R.; WILSON, R. J.; THAKOR, A. S.; KEVADIYA, B. D. Cellular uptake and retention of nanoparticles: Insights on particle properties and interaction with cellular components. Materials Today Communications, v. 25, n. 101692, dez. 2020. Disponível em: <http://www.scopus.com/inward/record.url?scp=85091501540&partnerID=8YFLogxK>. Acesso em: 6 set. 2023.

AZEVEDO NETO, A. D. de; PEREIRA, P. P. A.; COSTA, D. P.; SANTOS, A. C. C. dos. Fluorescência da clorofila como uma ferramenta possível para seleção de tolerância à salinidade em girassol. Revista Ciência Agronômica, v. 42, p. 893–897, dez. 2011.

BOEDEKER, W.; WATTS, M.; CLAUSING, P.; MARQUEZ, E. The global distribution of acute unintentional pesticide poisoning: estimations based on a systematic review. BMC Public Health, v. 20, n. 1, p. 1875, 7 dez. 2020.

BONSER, C. A. R.; CHEN, X.; ASTETE, C. E.; SABLIOV, C. M.; DAVIS, J. A. Elucidating Efficacy of Ingested Positively Charged Zein Nanoparticles Against Noctuidae. Journal of Economic Entomology, v. 113, n. 6, p. 2739–2744, 1 dez. 2020.

CAMPOS, E. V. R.; PROENÇA, P. L. F.; DA COSTA, T. G.; DE LIMA, R.; FRACETO, L. F.; DE ARAUJO, D. R. Using Chitosan-Coated Polymeric Nanoparticles-Thermosensitive Hydrogels in association with Limonene as Skin Drug Delivery Strategy. BioMed Research International, v. 2022, p. 9165443, 7 abr. 2022.

CAMPOS, E. V. R.; PROENÇA, P. L. F.; OLIVEIRA, J. L.; PEREIRA, A. E. S.; DE MORAIS RIBEIRO, L. N.; FERNANDES, F. O.; GONÇALVES, K. C.; POLANCZYK, R. A.; PASQUOTO-STIGLIANI, T.; LIMA, R.; MELVILLE, C. C.; DELLA VECHIA, J. F.; ANDRADE, D. J.; FRACETO, L. F. Carvacrol and Linalool Co-Loaded in β-Cyclodextrin-Grafted Chitosan Nanoparticles as Sustainable Biopesticide Aiming Pest Control. Scientific Reports, v. 8, n. 1, p. 7623, dez. 2018.

CARVALHO, L. B.; GODOY, I. S.; PREISLER, A. C.; PROENÇA, P. L. de F.; SARAIVA-SANTOS, T.; VERRI, W. A.; OLIVEIRA, H. C.; DALAZEN, G.; FRACETO, L. F. Pre-Emergence Herbicidal Efficiency and Uptake of Atrazine-Loaded Zein Nanoparticles: A Sustainable Alternative to Weed Control. Environmental Science: Nano, v. 10, n. 6, p. 1629–1643, 15 jun. 2023.

CORDEIRO, E. M. G.; PANTOJA-GOMEZ, L. M.; DE PAIVA, J. B.; NASCIMENTO, A. R. B.; OMOTO, C.; MICHEL, A. P.; CORREA, A. S. Hybridization and introgression between Helicoverpa armigera and H. zea: an adaptational bridge. BMC Evolutionary Biology, v. 20, n. 1, p. 61, 25 maio 2020.

DE OLIVEIRA, J. L.; CAMPOS, E. V. R.; BAKSHI, M.; ABHILASH, P. C.; FRACETO, L. F. Application of Nanotechnology for the Encapsulation of Botanical Insecticides for Sustainable Agriculture: Prospects and Promises. Biotechnology Advances, v. 32, n. 8, p. 1550–1561, dez. 2014.

DE OLIVEIRA, J. L.; CAMPOS, E. V. R.; GERMANO-COSTA, T.; LIMA, R.; VECHIA, J. F. D.; SOARES, S. T.; DE ANDRADE, D. J.; GONÇALVES, K. C.; DO NASCIMENTO, J.; POLANCZYK, R. A.; FRACETO, L. F. Association of Zein Nanoparticles with Botanical Compounds for Effective Pest Control Systems. Pest Management Science, v. 75, n. 7, p. 1855–1865, jul. 2019.

DE OLIVEIRA, J. L.; CAMPOS, E. V. R.; PEREIRA, A. E. S.; NUNES, L. E. S.; DA SILVA, C. C. L.; PASQUOTO, T.; LIMA, R.; SMANIOTTO, G.; POLANCZYK, R. A.; FRACETO, L. F. Geraniol Encapsulated in Chitosan/Gum Arabic Nanoparticles: A Promising System for Pest Management in Sustainable Agriculture. Journal of Agricultural and Food Chemistry, v. 66, n. 21, p. 5325–5334, 30 maio 2018.

FAO. FAO - News Article: Climate change fans spread of pests and threatens plants and crops, new FAO study. Disponível em: <https://www.fao.org/news/story/en/item/1402920/icode/>. Acesso em: 14 set. 2022.

FENG, J.; ZHANG, Q.; LIU, Q.; ZHU, Z.; MCCLEMENTS, D. J.; JAFARI, S. M. Chapter 12 - Application of Nanoemulsions in Formulation of Pesticides. *Em*: JAFARI, S. M.; MCCLEMENTS, D. J. Nanoemulsions. [s.l.] Academic Press, 2018. p. 379–413.

GERMANO-COSTA, T.; BILESKY-JOSÉ, N.; GUILGER-CASAGRANDE, M.; PASQUOTO-STIGLIANI, T.; ROGÉRIO, CB.; ABRANTES, DC.; MARUYAMA, CR.; OLIVEIRA, JL.; FRACETO, LF.; LIMA, R. Use of 2D and co-culture cell models to assess the toxicity of zein nanoparticles loading insect repellents icaridin and geraniol. Colloids and Surfaces B: Biointerfaces, v. 216, p. 112564, 1 ago. 2022.

GUO, J.; ZHAO, X.; WANG, X.; JIA, L.; ZHOU, Y.; XIE, M.; LI, Q.; SU, E.; FAN, L. Transcriptome Analysis of Soybean Roots in Response to Boron Deficiency. Biotechnology & Biotechnological Equipment, v. 37, n. 1, p. 2200510, 10 abr. 2023.

HAMPF, A. C.; NENDEL, C.; STREY, S.; STREY, R. Biotic Yield Losses in the Southern Amazon, Brazil: Making Use of Smartphone-Assisted Plant Disease Diagnosis Data. Frontiers in Plant Science, v. 12, 2021. Disponível em: <https://www.frontiersin.org/articles/10.3389/fpls.2021.621168>. Acesso em: 5 set. 2023.

HU, K.; MCCLEMENTS, D. J. Fabrication of Surfactant-Stabilized Zein Nanoparticles: A PH Modulated Antisolvent Precipitation Method. Food Research International, v. 64, p. 329–335, out. 2014.

IBÁÑEZ, M. D.; BLÁZQUEZ, M. A. Curcuma longa L. Rhizome Essential Oil from Extraction to Its Agri-Food Applications. A Review. Plants, v. 10, n. 1, p. 44, 28 dez. 2020.

LUIS, A. I. S.; CAMPOS, E. V. R.; DE OLIVEIRA, J. L.; GUILGER-CASAGRANDE, M.; DE LIMA, R.; CASTANHA, R. F.; DE CASTRO, V. L. S. S.; FRACETO, L. F. Zein Nanoparticles Impregnated with Eugenol and Garlic Essential Oils for Treating Fish Pathogens. ACS Omega, v. 5, n. 25, p. 15557–15566, 30 jun. 2020.

MIRCIOIU, C.; VOICU, V.; ANUTA, V.; TUDOSE, A.; CELIA, C.; PAOLINO, D.; FRESTA, M.; SANDULOVICI, R.; MIRCIOIU, I. Mathematical Modeling of Release Kinetics from Supramolecular Drug Delivery Systems. Pharmaceutics, v. 11, n. 3, p. 140, 21 mar. 2019.

MONTEIRO, R. A.; CAMARA, M. C.; DE OLIVEIRA, J. L.; CAMPOS, E. V. R.; CARVALHO, L. B.; PROENÇA, P. L. de F.; GUILGER-CASAGRANDE, M.; LIMA, R.; DO NASCIMENTO, J.; GONÇALVES, K. C.; POLANCZYK, R. A.; FRACETO, L. F. Zein based-nanoparticles loaded botanical pesticides in pest control: An enzyme stimuli-responsive approach aiming sustainable agriculture. Journal of Hazardous Materials, v. 417, p. 126004, 5 set. 2021.

MORA-HUERTAS, C. E.; FESSI, H.; ELAISSARI, A. Polymer-based nanocapsules for drug delivery. International Journal of Pharmaceutics, v. 385, n. 1, p. 113–142, 29 jan. 2010.

NICOLOPOULOU-STAMATI, P.; MAIPAS, S.; KOTAMPASI, C.; STAMATIS, P.; HENS, L. Chemical Pesticides and Human Health: The Urgent Need for a New Concept in Agriculture. Frontiers in Public Health, v. 4, 2016. Disponível em: <https://www.frontiersin.org/articles/10.3389/fpubh.2016.00148>. Acesso em: 5 set. 2023.

OVERTON, K.; MAINO, J. L.; DAY, R.; UMINA, P. A.; BETT, B.; CARNOVALE, D.; EKESI, S.; MEAGHER, R.; REYNOLDS, O. L. Global crop impacts, yield losses and action thresholds for fall armyworm (Spodoptera frugiperda): A review. Crop Protection, v. 145, p. 105641, 1 jul. 2021.

PANDEY, A. K.; SILVA, A. S.; VARSHNEY, R.; CHÁVEZ-GONZÁLEZ, M. L.; SINGH, P. Curcuma-based botanicals as crop protectors: From knowledge to application in food crops. Current Research in Biotechnology, v. 3, p. 235–248, 1 jan. 2021.

PARRA, J. R. P.; COELHO, A.; CUERVO-RUGNO, J. B.; GARCIA, A. G.; DE ANDRADE MORAL, R.; SPECHT, A.; NETO, D. D. Important Pest Species of the Spodoptera Complex: Biology, Thermal Requirements and Ecological Zoning. Journal of Pest Science, v. 95, n. 1, p. 169–186, 1 jan. 2022.

PASCOLI, M.; DE ALBUQUERQUE, F. P.; CALZAVARA, A. K.; TINOCO-NUNES, B.; OLIVEIRA, W. H. C.; GONÇALVES, K. C.; POLANCZYK, R. A.; VECHIA, J. F. D.; DE MATOS, S. T. S.; DE ANDRADE, D. J.; OLIVEIRA, H. C.; SOUZA-NETO, J. A.; DE LIMA, R.; FRACETO, L. F. The Potential of Nanobiopesticide Based on Zein Nanoparticles and Neem Oil for Enhanced Control of Agricultural Pests. Journal of Pest Science, v. 93, n. 2, p. 793–806, 1 mar. 2020.

PATEL, A.; HU, Y.; TIWARI, J. K.; VELIKOV, K. P. Synthesis and Characterisation of Zein–Curcumin Colloidal Particles. Soft Matter, v. 6, n. 24, p. 6192–6199, 30 nov. 2010.

PATIR, K. Nanoemulsion and Its Application in Pesticide Formulation. *Em*: Handbook of Research on Nanoemulsion Applications in Agriculture, Food, Health, and Biomedical Sciences. [s.l.] IGI Global, 2022. p. 401–424.

PAWLAK, K.; KOŁODZIEJCZAK, M. The Role of Agriculture in Ensuring Food Security in Developing Countries: Considerations in the Context of the Problem of Sustainable Food Production. Sustainability, v. 12, n. 13, p. 5488, jan. 2020.

PEHAREC ŠTEFANIĆ, P.; KOŠPIĆ, K.; LYONS, D. M.; JURKOVIĆ, L.; BALEN, B.; TKALEC, M. Phytotoxicity of Silver Nanoparticles on Tobacco Plants: Evaluation of Coating Effects on Photosynthetic Performance and Chloroplast Ultrastructure. Nanomaterials, v. 11, n. 3, p. 744, 16 mar. 2021.

PERRONE, D.; ARDITO, F.; GIANNATEMPO, G.; DIOGUARDI, M.; TROIANO, G.; LO RUSSO, L.; DE LILLO, A.; LAINO, L.; LO MUZIO, L. Biological and Therapeutic Activities, and Anticancer Properties of Curcumin. Experimental and Therapeutic Medicine, v. 10, n. 5, p. 1615–1623, nov. 2015.

PLATEL, A.; CARPENTIER, R.; BECART, E.; MORDACQ, G.; BETBEDER, D.; NESSLANY, F. Influence of the Surface Charge of PLGA Nanoparticles on Their in Vitro Genotoxicity, Cytotoxicity, ROS Production and Endocytosis. Journal of applied toxicology: JAT, v. 36, n. 3, p. 434–444, mar. 2016.

SANTAMARIA, M. E.; ARNAIZ, A.; ROSA-DIAZ, I.; GONZÁLEZ-MELENDI, P.; ROMERO-HERNANDEZ, G.; OJEDA-MARTINEZ, D. A.; GARCIA, A.; CONTRERAS, E.; MARTINEZ, M.; DIAZ, I. Plant Defenses Against Tetranychus Urticae: Mind the Gaps. Plants, v. 9, n. 4, p. 464, abr. 2020.

SHI, H.; GUO, J.; AN, J.; TANG, Z.; WANG, X.; LI, W.; ZHAO, X.; JIN, L.; XIANG, Y.; LI, Z.; ZHANG, F. Estimation of Chlorophyll Content in Soybean Crop at Different Growth Stages Based on Optimal Spectral Index. Agronomy, v. 13, n. 3, p. 663, 24 fev. 2023.

SHINDE, P.; AGRAVAL, H.; SRIVASTAV, A. K.; YADAV, U. C. S.; KUMAR, U. Physico-chemical characterization of carvacrol loaded zein nanoparticles for enhanced anticancer activity and investigation of molecular interactions between them by molecular docking. International Journal of Pharmaceutics, v. 588, p. 119795, 15 out. 2020.

SINGH, A.; TIWARI, S.; PANDEY, J.; LATA, C.; SINGH, I. K. Role of Nanoparticles in Crop Improvement and Abiotic Stress Management. Journal of Biotechnology, v. 337, p. 57–70, ago. 2021.

SOSA-GÓMEZ, D. R.; SPECHT, A.; PAULA-MORAES, S. V.; LOPES-LIMA, A.; YANO, S. A. C.; MICHELI, A.; MORAIS, E. G. F.; GALLO, P.; PEREIRA, P. R. V. S.; SALVADORI, J. R.; BOTTON, M.; ZENKER, M. M.; AZEVEDO-FILHO, W. S. Timeline and Geographical Distribution of *Helicoverpa Armigera* (Hübner) (Lepidoptera, Noctuidae: Heliothinae) in Brazil. Revista Brasileira de Entomologia, v. 60, p. 101–104, mar. 2016.

STACKE, R. F.; ARNEMANN, J. A.; ROGERS, J.; STACKE, R. S.; STRAHL, T. T.; PERINI, C. R.; DOSSIN, M. F.; POZEBON, H.; DE ARRUDA CAVALLIN, L.; GUEDES, J. V. C. Damage assessment of Helicoverpa armigera (Lepidoptera: Noctuidae) in soybean reproductive stages. Crop Protection, v. 112, p. 10–17, 1 out. 2018.

TONG, F.; GROSS, A. D.; DOLAN, M. C.; COATS, J. R. The Phenolic Monoterpenoid Carvacrol Inhibits the Binding of Nicotine to the Housefly Nicotinic Acetylcholine Receptor. Pest Management Science, v. 69, n. 7, p. 775–780, 2013.

ZHANG, H.; OS, W. L. van; TIAN, X.; ZU, G.; RIBOVSKI, L.; BRON, R.; BUSSMANN, J.; KROS, A.; LIU, Y.; S. ZUHORN, I. Development of Curcumin-Loaded Zein Nanoparticles for Transport across the Blood–Brain Barrier and Inhibition of Glioblastoma Cell Growth. Biomaterials Science, v. 9, n. 21, p. 7092–7103, 2021.

ZOU, L.; ZHENG, B.; ZHANG, R.; ZHANG, Z.; LIU, W.; LIU, C.; XIAO, H.; MCCLEMENTS, D. J. Enhancing the bioaccessibility of hydrophobic bioactive agents using mixed colloidal dispersions: Curcumin-loaded zein nanoparticles plus digestible lipid nanoparticles. Food Research International, v. 81, p. 74–82, 1 mar. 2016.

SUPPLEMENTARY MATERIAL

Table S1: Mathematical model parameters, such as release constant (k), correlation coefficient (r) and release exponent (n) after application of Zero order, first order, Higuchi and Korsmeyer-Peppas models to the release curve of CUR and CVC from different formulations.

Parameter	Zero Order	First Order	Higuchi	Korsmeyer-Peppas
EM_CUR				
Release Constant (k)	3.8×10^{-2} min^{-1}	7.9×10^{-5} min^{-1}	2.4×10^{-1} $min^{-1/2}$	**5.39 min^{-1}**
Correlation Coefficient (r)	0.1354	0.1279	0.2949	**0.8868**
Release exponent (n)	-	-	-	**2.3**
NP_CUR				
Release Constant (k)	6.7×10^{-3} min^{-1}	1.5×10^{-4} min^{-1}	3.8×10^{-1} $min^{-1/2}$	**4.5 min^{-1}**
Correlation Coefficient (r)	0.2419	0.2101	0.4130	**0.8040**
Release exponent (n)	-	-	-	**1.8**
EM_CVC				
Release Constant (k)	3.8×10^{-1} min^{-1}	4.9×10^{-3} min^{-1}	5.9 $min^{-1/2}$	**1.5 min^{-1}**
Correlation Coefficient (r)	0.9600	0.8460	0.9755	**0.9932**
Release exponent (n)	-	-	-	**0.96**
NP_CVC				
Release Constant (k)	2.4×10^{-2} min^{-1}	3.2×10^{-4} min^{-1}	1.2 $min^{-1/2}$	**1.5 min^{-1}**
Correlation Coefficient (r)	0.4273	0.3060	0.6463	**0.9855**
Release exponent (n)	-	-	-	**0.53**

Capítulo III

Insights On Mechanisms of Uptake and Translocation of FITC-Labelled Zein Nanoparticles Co-Loading Curcumin and Carvacrol in Soybean Plants

Abstract

The use of nanotechnology in agriculture has potential for revolutionizing the industry, offering promising avenues for increased crop yields, reduced resource consumption, and enhanced pest control. However, despite these promising benefits, the full extent of their mechanism of action remains a subject of ongoing research. The intricacies of how nanomaterials interact with plants, soils, and ecosystems are not yet fully understood, necessitating further investigation to ensure the safe and sustainable integration of nanotechnology into agricultural practices. In this way, labelling polymeric nanoparticles with fluorescent probe is pivotal for their visualization and quantification on the biological compartments. FITC-labeled zein nanoparticles co-loading curcumin and carvacrol had a mean diameter around 100 $\pm$ 1 nm, polydispersion index above 0.2 and positive zeta potential 23 $\pm$ 2 mV. Zein nanocarriers containing curcumin and carvacrol displayed the ability to been uptake on leaf structures, effectively penetrating the mesophyll and exhibiting mobility throughout the leaf tissue. Notably, they displayed a strong attraction to the apex of the leaflet. Additionally, these nanocarriers demonstrated a preference for trichomes post-absorption, becoming detectable even in trichomes situated at considerable distances from the point of application. Importantly, after penetrating the leaf tissues, a leaf-to-root translocation phenomenon was observed, suggesting a possible route through the phloem for their movement. These initial findings have indicated that zein nanoparticles exhibit the capability to migrate to various plant tissues following foliar application. Nevertheless, more comprehensive investigations are imperative to gain a deeper comprehension of the uptake and translocation mechanisms of these nanoparticles. Further research is needed to provide a more comprehensive understanding of the processes involved in nanoparticle movement within the plant.

Keywords: zein nanoparticles, curcumin, carvacrol, uptake, translocation, FITC

Introduction

According to the latest report from the United Nations in 2022, the global population is expected to grow further to 9.7 billion people by 2030 (UNITED NATIONS, 2019). This population surge has led to a reduction in cropland area per capita in most regions, highlighting the need for more efficient farming practices (FAO, 2017). As agricultural lands become limited in the face of increasing regional populations, nanotechnology emerges as a potential solution to meet the demand for higher productivity without expanding agricultural areas (BARTOLUCCI et al., 2022).

Nanotechnology offers various agricultural benefits, including the controlled release of active compounds, targeted pest control, protection of active ingredients from premature degradation, plant nutrition, as well as soil remediation (KUMAR et al., 2019). However, despite the promise of nano-enabled agriculture, concerns about the environmental impact of nanomaterials persist. Questions about their fate in soil, potential bioaccumulation in plants and harm to consumers, impact on soil microbe communities, and contamination of local watersheds remain largely unanswered. As research on engineered nanomaterials continues, it is essential to approach their application in open environments with caution, considering their non-biodegradable nature and potential long-term consequences (UPADHYAY et al., 2022).

Biodegradable polymers offer a potential alternative, and recent efforts have focused on investigating biological polymers like polysaccharides, proteins, and nucleic acids for creating nanoparticles in agriculture (CAMPOS et al., 2022b). These biopolymeric nanoparticles have shown promise in improving plant fertilizer uptake, encapsulating pesticides and herbicides, controlling fertilizer release, enhancing water retention in soil, and serving as post-harvest food packaging materials (CAMPOS et al., 2018c; CARVALHO et al., 2023; MARUYAMA et al., 2016; OLIVEIRA et al., 2015; PEREIRA; OLIVEIRA; FRACETO, 2019). With their biocompatibility, biodegradability, abundance, and cost-effectiveness, biodegradable polymers present a potential avenue for sustainable and responsible agricultural practices in the future.

In general, the concerns surrounding the destiny and effects of polymeric nanoparticles differ from those associated with inorganic metallic and metal oxide nanoparticles, often viewed as potentially toxic (RASTOGI et al., 2017). Consequently, studies investigating the impact of engineered nanoparticles on plant growth,

germination, and root elongation have predominantly focused on inorganic variants. Understanding the environmental fate of inorganic nanoparticles has been vital in determining particle accumulation in soil and plants, thereby influencing their potential application in agriculture. However, the uptake mechanisms of both inorganic and polymeric nanoparticles remain inadequately understood, despite evidence suggesting plant uptake through roots and leaves. The hypothesis posits that engineered nanoparticles may traverse the root epidermis and endodermis to access the xylem vessels, facilitating further translocation to the plant's aerial parts. Additionally, engineered nanoparticles can enter leaves through stomata, allowing them to reach the vascular system and subsequently move to other plant tissues via the phloem.

Tracking polymeric nanoparticles in the environment poses significant challenges due to their small size, complex interactions with diverse environmental components, and potential alterations during transport (DEVASENA et al., 2022). The nanoparticles can disperse widely and be subject to various transformations that hinder their accurate monitoring and fate assessment (LEAD et al., 2018). However, labelling nanoparticles with fluorescent probes offers a powerful and effective solution to overcome these difficulties. Fluorescently tagging polymeric nanoparticles enables real-time and non-invasive tracking, allowing researchers to precisely follow their movement and distribution in environmental systems. This approach offers valuable insights into their behavior, interactions with biota and abiotic factors, and potential accumulation in specific locations (PROENÇA et al., 2022). Additionally, fluorescent labelling facilitates the identification of various nanoparticle types in complex matrices, distinguishing them from naturally occurring particles, and enabling their quantification. By harnessing the advantages of fluorescent probes, researchers can advance their understanding of polymeric nanoparticle dynamics in the environment, supporting the development of safer and more sustainable nanotechnologies for various applications (SVECHKAREV; MOHS, 2019).

Accurate visualization and quantification of polymeric nanoparticles within biological compartments hold crucial significance in assessing their fate, intracellular trafficking, and cellular levels in plants and the environment. Furthermore, precise dose quantification is vital for establishing the correlation between dosage and toxicological outcomes. To achieve this, fluorescently labelling polymeric nanoparticles becomes

essential, as it allows for their visualization and quantification in biological compartments. Organic dyes serve as the preferred choice for fluorescent biological imaging due to their versatility, widespread availability, and cost-effectiveness (FÄRKKILÄ et al., 2021). These fluorescent probes can be incorporated into the nanoparticle core during synthesis or covalently attached to the polymer backbone before nanoparticle formation, enabling the production of fluorescently labelled nanoparticles with enhanced tracking and analytical capabilities (PROENÇA et al., 2022).

Fluorescein isothiocyanate (FITC) serves as an excellent fluorescent probe for tracking nanoparticles in plant systems due to its high sensitivity and stability (LE GUERN et al., 2020). Researchers have utilized FITC-labelled nanoparticles to investigate their behavior and distribution within plant tissues (WANG et al., 2023). Zein nanoparticles labeled with fluorescein isothiocyanate were studied in hydroponic soybean and sugarcane cultures. The nanoparticles had a mean diameter of 135 ± 3 nm, a polydispersity index of 0.202 ± 0.034, and a positive zeta potential of 81 ± 4 mV. In soybean plants, uptake and accumulation of nanoparticles in the roots were concentration and time-dependent, with low and high doses resulting in 0.37 mg NP/mg dry weight roots and 0.58 mg NP/mg dry weight roots, respectively. Fluorescence in leaves was lower than in roots and fluctuated over time. The authors could not determine if the fluorescence in leaves resulted from the translocation of whole nanoparticles or unidentified fluorescent particles (RISTROPH et al., 2017). In sugarcane, confocal images showed nanoparticles along the epidermal layer of roots and translocation to the cortex and endodermis at the highest concentration (1.75 mg/L). The amount of nanoparticles translocated to sugar cane leaves depended on the dosage used, with low and high doses resulting in 4.8 µg NP/mg dry weight and 12.9 µg NP/mg dry weight, respectively (PRASAD; BHATTACHARYYA; NGUYEN, 2017).

In this study, we aim to investigate the uptake and translocation of FITC-labelled zein nanoparticles when applied directly on leaves in a pot experiment. Unlike previously published works that focused on hydroponic evaluations, our research approach involves a pot experiment, providing a more realistic and relevant assessment of nanoparticle behavior within a plant system. By applying the nanoparticles directly on leaves, we can better mimic real-world scenarios and gain valuable insights into their uptake and movement within the plant, ultimately contributing to a deeper

understanding of nanoparticle-plant interactions and their potential applications in agriculture and environmental settings.

Materials and methods

Materials

Fluorescein 5(6)- isothiocyanate (FTIC ≥ 90%); zein powder, curcumin (≥ 65%), carvacrol (98%) Kolliphor P188 were purchased from Sigma-Aldrich and were used without further purification. Ethanol (ETOH), Acetonitrile (ACN) was obtained from J.T. Baker. Other reagents (analytical grade or not) were obtained from local suppliers.

Methods

FITC-labelled zein

In order to facilitate the tracking of polymeric nanoparticles, a covalent conjugation of zein and a fluorophore was undertaken. The functionalization of FITC with zein was carried out following the methodology outlined in the work of Prasad et al. (2018) with minor modifications as cited. The experimental procedure commenced by dissolving 3 mg of zein in 100 mL of dimethylformamide under gentle stirring. Subsequently, 0.1 mL of triethylamine and 80 mg of FTIC were slowly added to the solution. After 24 hours of continuous and gentle stirring, the volume of the solution was reduced to 25 mL under high vacuum conditions. The ensuing suspension was precipitated in 400 mL of dichloromethane. A thorough washing of the precipitate through filtration was performed to eliminate any residual free FTIC. The precipitate was then subjected to a drying process in a desiccator for 24 hours and subsequently stored at 4°C. It is noteworthy that during all stages of the procedure, stringent light shielding measures were employed to safeguard both the solution and the final product. The FITC-labeled zein, synthesized by our group, have been characterized and published previously, detailing their physicochemical properties (CARVALHO et al., 2023).

Zein-labeled nanoparticles

The nanoparticles were prepared by precipitation with anti-solvent methodology described by (HU; MCCLEMENTS, 2014), with some modifications. A 2% (w/v) solution of zein and FITC-labeled zein (80:20) was prepared with an 85% (v/v) ethyl

alcohol solution, which was kept under stirring (overnight). After this time of stirring, the zein solution was heated to 75°C in a water bath for 15 min and, as soon as it reached room temperature, it was centrifuged for 25 minutes at 869g and the supernatant was filtered through a 0.45 µm Millipore® membrane to removing insoluble particles. The active ingredients were weighed (75 mg of CVC, 2 mg CUR) and 10 mL of zein solution was added to them and kept under stirring for approximately 20 minutes. The zein solution with the actives was poured into 30 mL of Pluronic F-68® solution (pH4.0) under magnetic stirring, remaining under stirring for at least 20 minutes. The formulation was evaporated at 40°C to evaporate the ethanol solvent added together with the zein solution (10 mL), resulting in a final solution of 30 mL. In this study containing curcumin and carvacrol (NPZ_CUR+CVC) was prepared. The final concentration of curcumin and carvacrol in each formulation is 0.066 mg/mL and 2.5 mg/mL, respectively.

Physicochemical characterization of zein-labeled nanoparticles

Nanoparticle characterization was performed using various techniques. The average diameter and polydispersity index were determined through dynamic light scattering with a Malvern-Zetasizer Nano ZS90 meter at 25ºC and a detection angle of 90º. After appropriate dilution in Milli-Q water, the average diameter was calculated based on three determinations for each sample. Zeta potential measurements were conducted using electrophoretic mobility with the same equipment, and the values were represented as the average of three determinations after dilution in Milli-Q water. For assessing the average diameter and concentration of nanoparticles/mL, nanoparticle tracking technique (NTA) was employed. The samples were diluted and measured using a NanoSight LM10 and data collected using a sCMOS camera controlled by NanoSight v.3.2 software (Malvern). Results were reported as the mean of three determinations. To determine encapsulation efficiency, the ultrafiltration/centrifugation methodology was utilized, and the concentrate of CUR and CVC was analyzed by High-Performance Liquid Chromatography (HPLC) (CAMPOS et al., 2022a).

Plant growth conditions

Soybean (*Glycina max* (L) Merr.) was selected as the model plant due to its profound significance in the global economy. Renowned for its high nutritional value, it plays a pivotal role in both human and animal nutrition. To conduct leaf absorption and mobility tests, confocal spectral microscopy images were acquired using soybean plants cultivated within a controlled greenhouse environment situated at the Biological Sciences Center of the State University of Londrina, Paraná, Brazil. Specifically, seeds of the Glycine max cultivar BRS 257 were sown in 1 L plastic pots measuring 14 cm in upper diameter, 9.5 cm in lower diameter, and 10.5 cm in height. These pots were filled with a substrate comprising 780 g of Oxisol blended with sand in a 1:1 ratio. Importantly, the seeds underwent no prior treatment. Throughout the experimental period, the plants were maintained under ambient conditions of light and temperature. The FITC-labeled formulations (1 mL) were applied in the aerial part of each soybean plant.

Translocation studies involving the quantification of FITC were conducted in Sorocaba, São Paulo, Brazil. Soybean seeds of the BRS 257 cultivar, generously provided by the Laboratory of Plant Ecophysiology at the State University of Londrina, Paraná, Brazil, were sown in plastic pots with a capacity of 3 liters (measuring 20 cm in upper diameter, 15 cm in lower diameter, and 15 cm in height). The substrate utilized for planting comprised 450 g of Carolina Soil. Seeds were sown at a depth of 2 cm and were placed within a greenhouse covered with a 150 µm transparent canvas. Throughout the experimental period, the plants were exposed to natural light and ambient temperature conditions, with watering administered every other day during the initial week, transitioning to a schedule of once every two days in the second week, and as needed in the subsequent weeks.

Analysis of foliar absorption of zein nanoparticles loaded with curcumin and carvacrol

In order to assess the absorption and intrafoliar distribution of nanoparticles, a precise volume of 30 µL of nanoparticles (NP_CUR+CVC_FTIC) was carefully applied to the central leaflet of the third trefoil, specifically within the middle third of the adaxial surface. Following the application, the plants were retained within a controlled

greenhouse environment, exposed to natural lighting conditions, until the designated collection times of 1- and 24-hours post-treatment. The collection procedure entailed sampling from four distinct regions of the leaflet, each encompassing an area of 1 cm^2. These regions consisted of the application site (middle third, adaxial face), apex (upper third, adaxial face), base (lower third, adaxial face), and the region opposite to the application site (middle third, abaxial face). Subsequently, the collected samples were meticulously prepared and mounted on slides at the Plant Ecophysiology Laboratory (State University of Londrina). A Fluormount mounting medium (Southern Biotech) was employed during the mounting process. For the subsequent analysis, a Leica TCS SP8 confocal microscope (Leica Microsystems, Wetzla, Germany) located at the Materials and Molecule Analysis Laboratory (State University of Londrina) was utilized. The analysis involved the application of Z analysis to define the regions of interest, with a deliberate exclusion of the cut edge to prevent any potential fluorescence carryover. The quantification of fluorescence intensities was conducted using Leica LAS X LS software.

Evaluation of FITC-labeled nanoparticles translocation in soybean plants

Nanoparticles, synthesized from FITC-functionalized zein, were employed to investigate their translocation within the plant. In this assessment, all leaves of soybean seedlings at the 2 to 3 trefoil stage were uniformly sprayed with a 5 mL solution of the NP_CUR+CVC formulation, which had been diluted by a factor of 2. Precautions were taken to shield the stems and soil to prevent inadvertent nanoparticle contamination. Following application periods of 1 and 24 hours, the plants were harvested and dissected into three distinct components: leaves, stems, and roots. These segregated samples were promptly frozen in a biofreezer at -80°C. Subsequently, the samples underwent lyophilization and were subsequently reduced to a fine powder through maceration before being stored in a freezer at -20°C, awaiting further processing for FITC extraction.

The experiment was conducted in quintuplicate, each involving 10 seedlings. For FITC extraction, a modified version of the protocol described by (PRASAD et al., 2018) was adhered to (Figure 1). Specifically, for every 3 mg of sample, 1 mL of 1M NaOH was

introduced. The sample-containing tubes were then subjected to incubation in a water bath at 70°C for 60 minutes, with periodic vortexing at 10-minute intervals. Post-incubation, the samples were centrifuged for 15 minutes at 1700 g, after which the separated supernatant was diluted by a factor of 10, and the FITC fluorescence was immediately quantified using a fluorimeter (Cary Eclipse Fluorescence Spectrophotometer G9800A) under consistent measurement conditions. A 1 M NaOH solution served as a blank and diluent for the samples, and these samples were disposed of following measurement. To construct the calibration curve, different concentrations of FITC (0.01875; 0.0375; 0.075, 0.15 and 0.3 µg/mL), were diluted in NaOH, were assessed within a fluorimeter employing an excitation wavelength of 495 nm and an emission wavelength of 515 nm. The resultant calibration curve exhibited an R^2 value of 0.9989 and followed the linear equation y = 2066*x + 3.558. To present the findings, the mean fluorescence values of the treated groups (1 and 24 hours) were adjusted by subtracting the mean fluorescence of the control group, representing a baseline reference (CARVALHO et al., 2023).

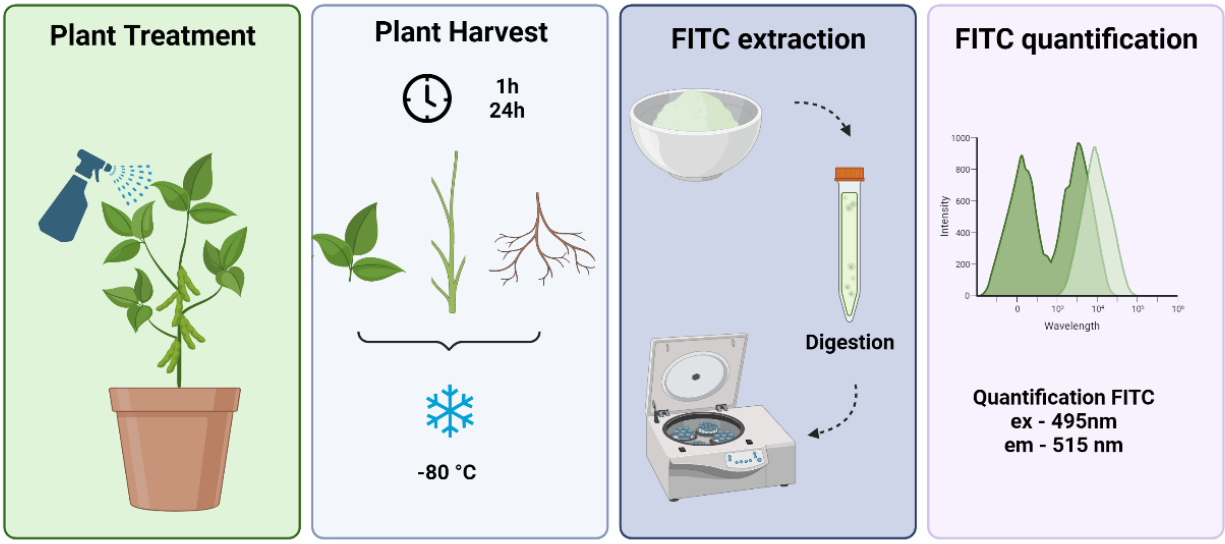

Figure 1: Schematic representation extraction and quantification of FITC from soybean plants treated with formulations. Nanoparticles were applied via spray on plants, and after 1 and 24 hours, the plants were categorized into leaf, stem, and root groups. Samples were subsequently frozen, freeze-dried, and transformed into a fine powder through maceration. FITC was extracted from the plant tissues using a NaOH solution

and temperature-based digestion, followed by quantification of FITC in various plant parts using a fluorimeter.

Statistical analysis

All data collected in this study were analyzed using two-way ANOVA, followed by Tukey's multiple comparisons test using Graphpad Prism 8 software.

Results and discussion

Physicochemical characterization of FITC-labeled zein nanoparticles

The nanoparticles' physicochemical properties, such as size and zeta potential are important parameters that can influence the absorption and translocation of particles by plants. In this way, we characterized the physicochemical properties of FITC-labeled zein nanoparticles to check if the addition of this fluorescent probe would change drastically these properties. To study the nanoparticle-plant interaction, zein nanoparticles containing curcumin and carvacrol needed to be labeled with a fluorescent probe, in this case the probe used was FITC. This probe was functionalized to zein protein (Zein-FITC) and its characterization was described in the article published (CARVALHO et al., 2023). The physicochemical characterizations are summarized in Figure 2.

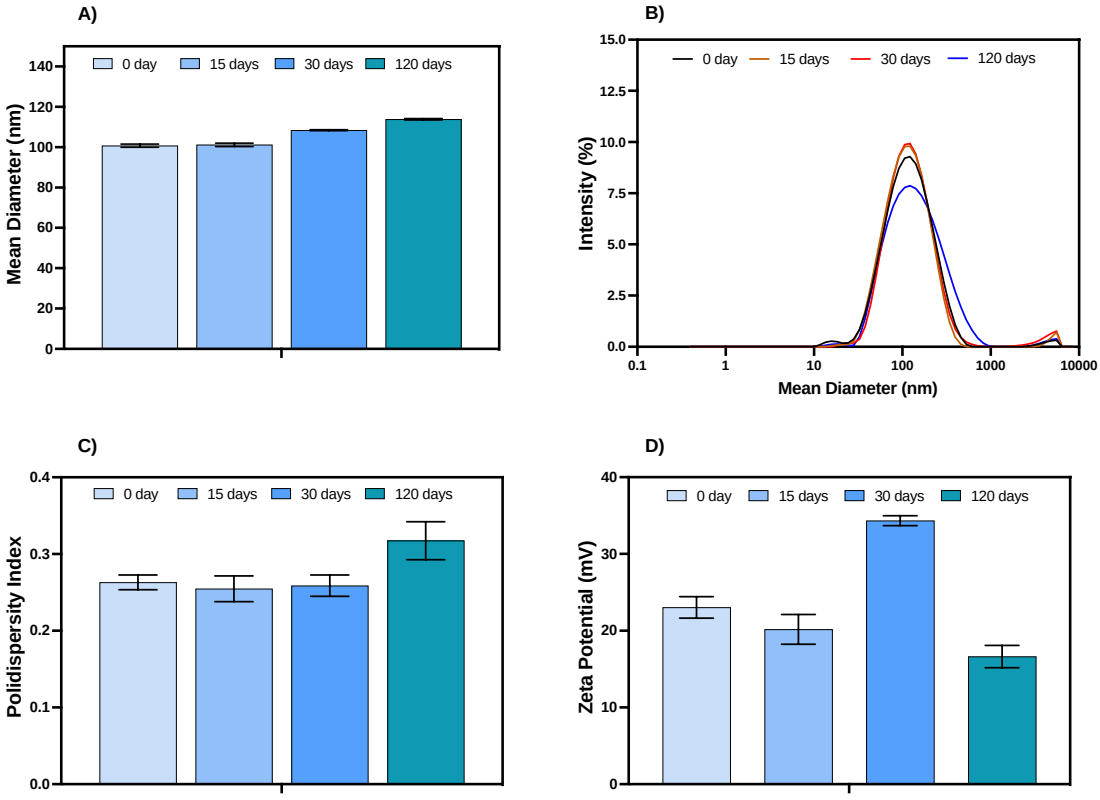

Figure 2: Physicochemical characterization of FITC-labeled zein nanoparticles loading CUR and CVC. A) Mean diameter determined (nm); B) size distribution (nm); C) polydispersity index (PDI) and D) Zeta potential (mV). The values represent the means of three determinations.

The nanoparticles were prepared using an 80:20 (w/w) ratio of zein to zein-FITC. For traceability in plants, it is noteworthy that most of the time fluorescent markers do not lead to changes in the structural integrity of nanoparticles (MEDER et al., 2016). As shown in Figure 1A, the initial mean diameter of the nanoparticles was 100 ± 1 nm and no significant changes were observed in the mean diameter as a function of storage time (120 days). Regarding the size distribution (Figure 1B), the presence of a second population of particles can be observed, since the first day of analysis, which was not observed for the unlabeled nanoparticles. The presence of this second population was also evidenced by the increase in the polydispersion index, which were greater than 0.2 since the initial time and remained without significant changes as a function of storage time, in contrast, unlabeled nanoparticles had a polydispersion index lower than 0.2.

The zeta potential of FITC-labelled nanoparticles was positive around 23 mV and after 120 days there is a decreased in the value of this parameter. It is essential to highlight the incorporation of Pluronic F-68 as a surfactant in the formulations

developed in this study. This non-ionic surfactant plays a pivotal role in enhancing stability to the nanoformulation by augmenting steric repulsion, thus mitigating particle coalescence. This addresses a significant limitation associated with zein nanoparticles, primarily attributed to their pronounced surface hydrophobicity, as previously discussed by Davidov-Pardo et al. (DAVIDOV-PARDO; JOYE; MCCLEMENTS, 2015), which tends to promote aggregation in aqueous solution. Finally, we evaluated the encapsulation efficiency (EE) of CUR and CVC in zein nanoparticles. The EE of CUR was around 90 $\pm$ 0.1%, with are similar to the obtained for the unlabeled NPs, however, for CVC there is a decrease around 20% of the amount of compound encapsulated. However, it is worth to mention, that there are no significative changes in the encapsulation efficiency over the storage time (120 days). The results of physicochemical characterization of the FITC-labeled zein nanoparticles are in accordance to those obtained by Carvalho et al., (2023), who use this fluorescent labeled nanoparticle to delivery atrazine to plants.

Analysis of absorption and mobility of nanoparticles in soybean leaf

To investigate the absorption and translocation of polymeric nanoparticles applied via the leaves in plants, they need to be traceable, therefore, the nanoparticles were prepared using the zein functionalized with the FITC probe in the ratio of 80:20 (w/w) of zein to zein-FITC. Confocal microscopy images were performed to verify the absorption and possible mobility of nanoparticles in the leaf tissue. To be able to verify this displacement, the treatment was applied by deposition. A volume of 30 uL of nanoparticles, containing actives, prepared with zein-FITC, diluted 1/2 in distilled water was deposited on the soybean leaf. The application site chosen was the middle third of the leaf, on one side of the midrib. The concentration of actives in the test was 0.066 mg/mL for curcumin and 2.5 mg/mL for carvacrol. The samples for making the images were collected 1 and 24 hours after exposure. Four different sites were chosen for observation. The deposition site itself, the base region, the apex region and the side opposite the application (abaxial surface).

The application site is the region with the highest fluorescence intensity (IF) as can be seen in Figure 3, both for 1h and 24h, even after the decrease (Table 1/Figure 2). After 1h of application the FI was 76.2 ± 12.8 falling to 16.9 ± 7 after 24h. ($p \leq 0.0001$). 4.5 times drop. The mean control FI for this site was 6.0 ± 0.1.

Table 1: Intensity of fluorescence captured by images taken by spectral microscopy "Fluorescence intensity quantification in distinct leaf regions at 1- and 24-hours post-deposition of nanoparticles containing the fluorescent marker. The reduction in fluorescence intensity at the application site, accompanied by an increase in other regions, signifies their mobility within the leaf tissue. Statistically distinct values within the same line are denoted by different letters, as determined by ANOVA followed by Tukey's test ($p<0.05$)."

	Control	**1h**	**24h**
Application site	6.05 ± 0.13a	76.23 ± 14.78	16.90 ± 8.04a
Apex	4.13 ± 0.83	6.68 ± 1.32	10.90 ± 1.50
Base	10.26 ± 0.45	9.30 ± 1.67	10.47 ± 2.11
Opposite side	5.64 ± 0.45	7.53 ± 2.40	8.10 ± 1.81

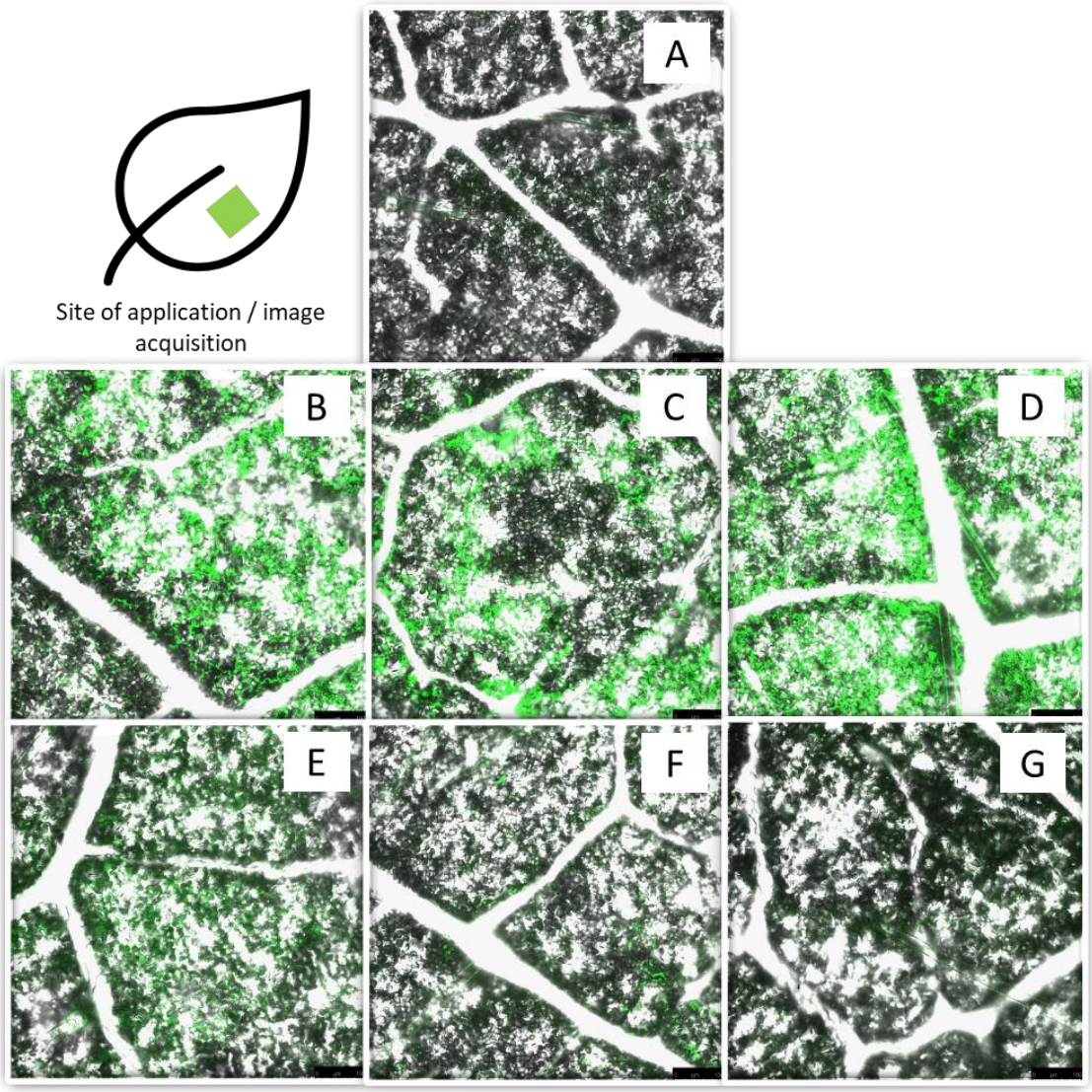

Figure 3: Representative confocal spectral microscopy images of zein nanoparticles, containing the actives curcumin and carvacrol, from the application site of the nanoparticles marked with the FITC probe, at 1 and 24 hours after deposition on soybean leaves. A, represents the control treatment; B – D represents the group treated 1h after application and E – G - represents the group treated 24h after application. The size bar corresponds to 100 µm.

Possibly, the decrease in IF values for this location, not only reduced by exposure to light, but also by the absorption and distribution of nanoparticles in the leaf tissue. 3D images taken from these sections show the internalization of nanoparticles in the leaf tissue (Figure 4). 3D images, performed along the z axis, were obtained from the beginning to the end of fluorescence capture.

The nanoparticles identified in the 3D images are probably in the mesophyll region, most likely in the palisade parenchyma, due to the apparently elongated structure and also due to the thickness presented from the beginning to the end of the fluorescence capture. Fluorescence uptake on the z axis of the control leaf had an average depth of 50 µm and 55 µm for both treatment times. The adaxial epidermis has an average thickness of 14 µm and the palisade parenchyma 78 µm, with the leaf having an average total thickness of 145 µm (LOURENÇO et al., 2011)

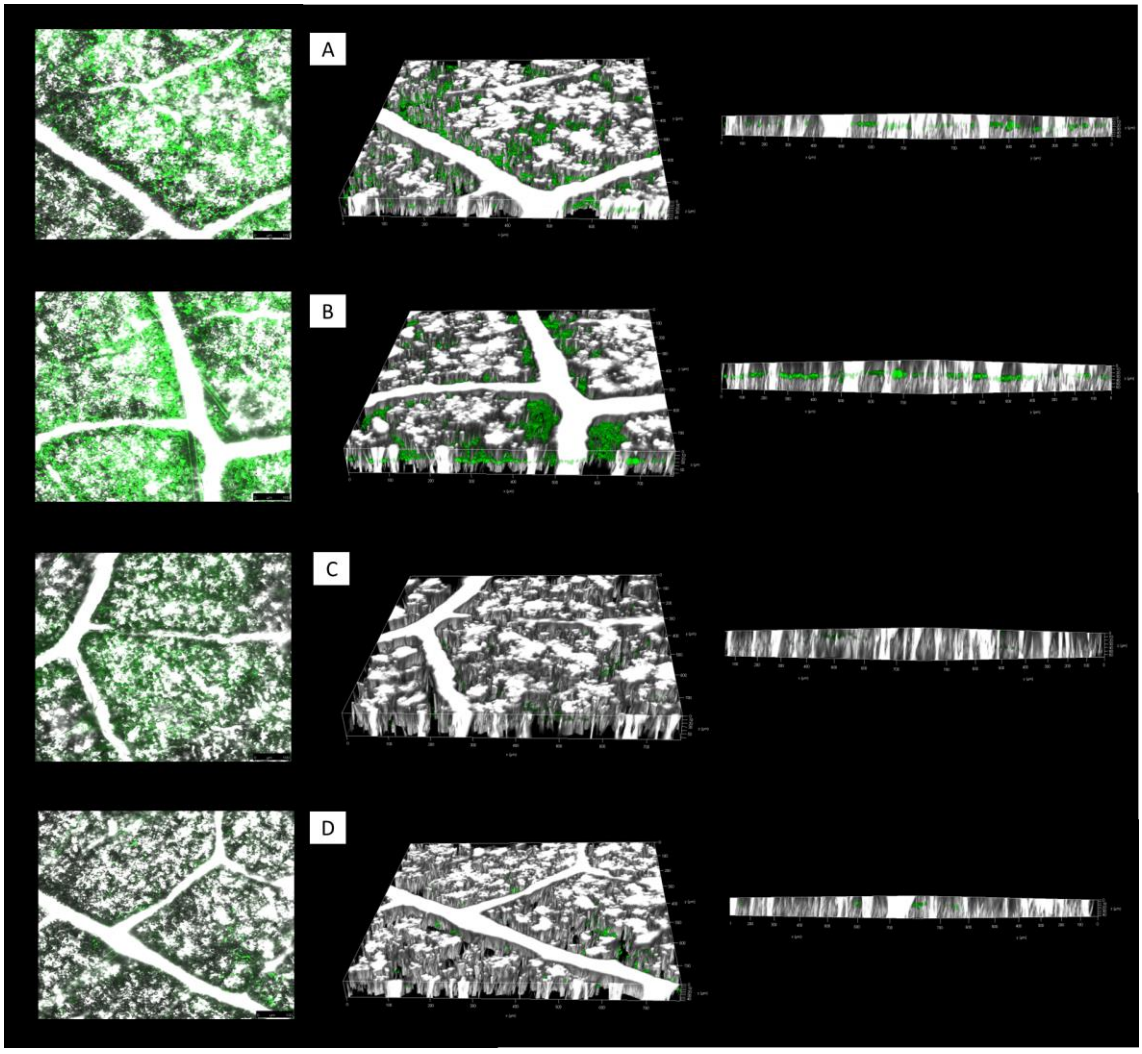

Figure 4: Representative confocal spectral microscopy images (2D and 3D) of FITC-labeled nanoparticles loading CUR and CVC, from the central region, site of application at 1 and 24 hours after deposition on soybean leaves. A and B represent the group treated with 1 hour of exposure and C and D represent the group treated 24 hours after application. The size bar corresponds to 100 µm.

The distribution pattern of nanoparticles within the leaf tissue is discernible through the observed increase in fluorescence intensity (FI) in various analyzed regions.

Statistically, the FI at the 1-hour application site stands as the sole significantly distinct value in comparison to the other sampled sites. However, there exists a notable tendency toward elevated FI levels in the apex region (as illustrated in Figure 4 - A - control, D - 1h, and G - 24h post-exposure). In the case of the control group, the FI for the apex region was measured at 4.1 ± 0.8. Following a 1-hour application, this value increased to 6.7 ± 1.3, further escalating to 10.9 ± 1.5 after 24 hours. This signifies a 1.6-fold augmentation relative to the 1-hour measurement and a 2.6-fold augmentation when contrasted with the control FI.

Similarly, the central region opposite to the application site (abaxial side) displays a discernible trend toward augmented FI levels (as depicted in Figure 4 - B - control, E - 1h, and H - 24h post-exposure). The control FI registered at 5.6 ± 0.5, rising to 7.5 ± 2.4 at the 1-hour mark and subsequently reaching 8.1 ± 1.8 after 24 hours. This reflects an increase of 1.08-fold over the 1-hour measurement and a 1.4-fold increase over the control FI. Conversely, in the region corresponding to the base of the leaflet, there is no observable trend indicating a consistent rise or fall in FI levels following treatment at the specified time intervals (as presented in Figure 5 - C - control, F - 1h, and I - 24h post-exposure).

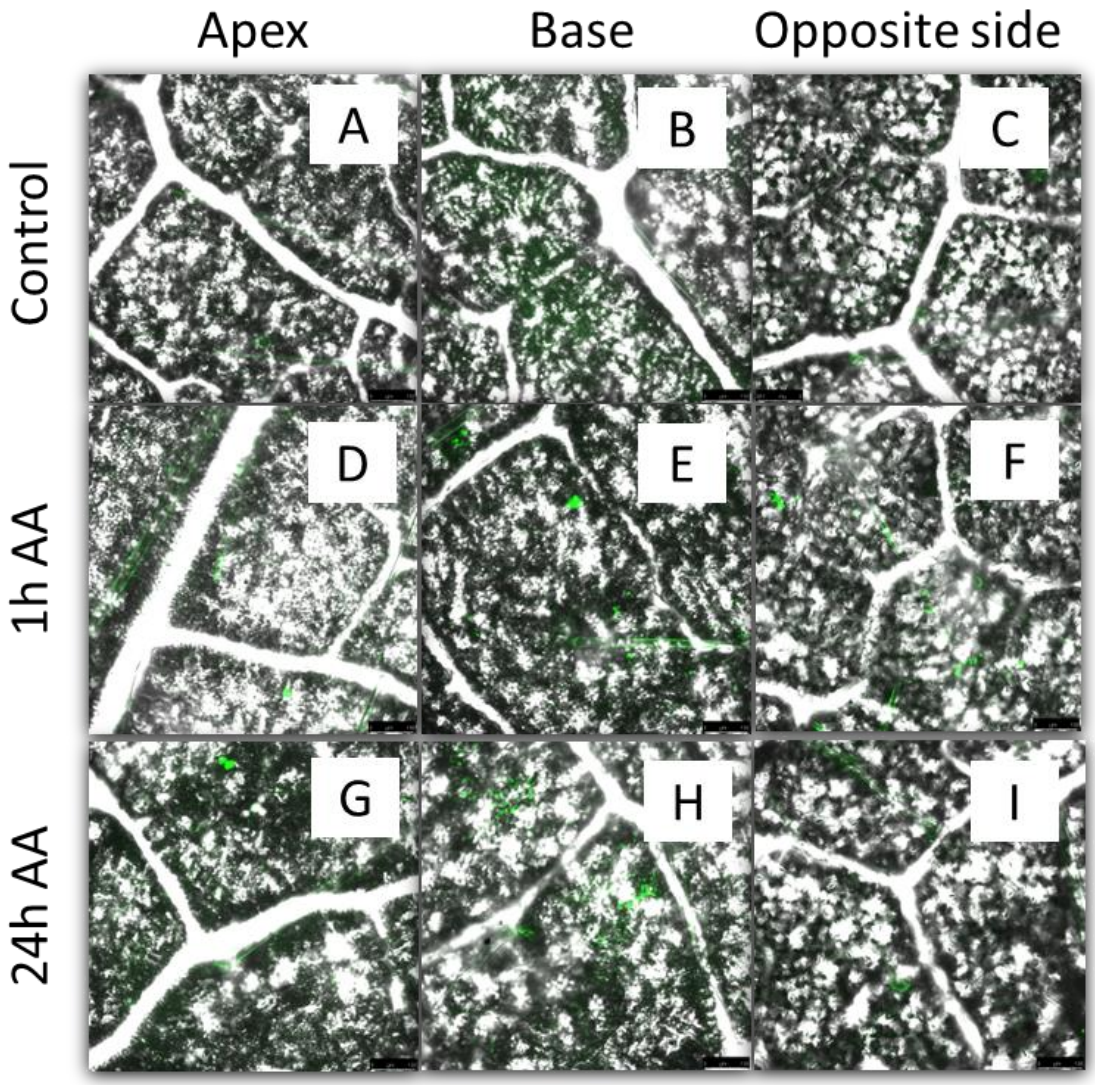

Figure 5: Representative confocal spectral microscopy images (2D and 3D) of zein nanoparticles labeled with the FITC probe, containing the actives curcumin and carvacrol, from the region of the apex, base and center opposite the application site (abaxial side), at times of 1 and 24h after deposition on soybean leaves. In the first line of the panel are presented the micrographs of the control plants, being A the image of the Apex, B the image of the base and C the image of the center opposite the application site. The second line presents images of the group treated with 1h of exposure, being D the image of the Apex, E the image of the base and F the image of the center opposite the application site and the third line the group treated with 24h of exposure, being G the Apex image, H the base image and I the image of the center opposite the application site. The size bar corresponds to 100 µm.

A more detailed observation of the images obtained by confocal microscopy of the treated group (1 and 24h after exposure) reveal that the trichomes (Figure 6) exhibit greater agglomeration of nanoparticles.

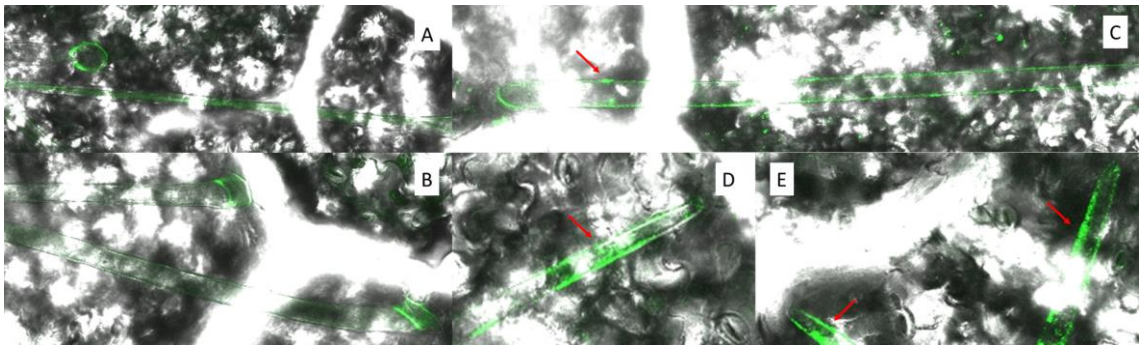

Figure 6: Representative confocal spectral microscopy images (2D and 3D) of zein nanoparticles marked with the FITC probe, containing the actives curcumin and carvacrol, 1h after deposition on soybean leaves, showing the trichomes. A and B represent images from the control group. C, represents the region at the base of the leaf and D and E, represent the central region on the side opposite to the application (abaxial side). Arrows indicate clusters of nanoparticles. Images have unscaled enlargements.

Figure 5 provides enlarged depictions of previously presented images, with a specific focus on the trichomes. Images A and B capture the typical fluorescence pattern of trichomes in a control plant, showcasing uniform coloring along the epicuticular hairs, with a higher degree of fluorescence intensity at their base. Trichomes are known to secrete exudates, which exhibit fluorescence properties akin to FITC fluorescence (as documented in (WAGNER; WANG; SHEPHERD, 2004).

Image C, on the other hand, illustrates a trichome from the basal region of a leaf treated for 1 hour. In this instance, while fluorescence is more pronounced, it does not significantly deviate from the control fluorescence, indicating the presence of small nanoparticle aggregates.

In contrast, images D and E, depicting the middle section of the leaf on the side opposite to the application site, reveal a heightened fluorescence intensity along the trichomes, accompanied by numerous nanoparticle aggregates. This observation reinforces the accumulating evidence that nanoparticles have been absorbed and translocated within the leaflet, with trichomes potentially serving as sites of preference for either nanoparticle accumulation or exudation.

The exudation of nanoparticles possessing pesticidal properties by trichomes offers advantages, particularly when contact toxicity is the desired outcome. Compounds exuded by trichomes are often found in higher concentrations at insect joints, facilitating their ingress into the interior of insects (LIN; WAGNER, 1994).

Our current findings align with observations made in previous investigations involving translocation studies of polymer-coated gold nanoparticles. These studies demonstrated the detectability of such nanoparticles at the leaf apex and the base of trichomes in wheat leaves (AVELLAN et al., 2019). This convergence of results substantiates our own observations, specifically the heightened fluorescence intensity observed at the leaflet apex and the aggregation of nanoparticles within trichomes.

An additional investigation into the translocation of metallic nanoparticles reveals a pattern in which metals accumulate at the trichome base subsequent to root exposure to these nanoparticles, potentially as a defensive mechanism involving metal exudation as reported in Servin et al., (2012). Regarding foliar application of Au-NPs, their distribution is concentrated along the midrib and lateral veins, with a notable prevalence of Au-NPs association with trichomes, particularly those situated in proximity to the petiole and along the midrib. In this scenario, the presence of hydrophobic epicuticular waxes and trichomes acts as a barrier, effectively retaining a significant portion of Au-NPs on the cell surface. This phenomenon delays the infiltration of nanoparticles into the leaf tissue (BALLIKAYA et al., 2023)

Figure 7 provides magnified views (without scale) of micrographs capturing the central region, the site of application. Within these images, it is challenging to definitively identify the specific structures or precise nanoparticle locations. To achieve such clarity, higher magnification levels and cross-sectional imagery of soybean leaves would be necessary. Nevertheless, certain observations can be made, in the control image (A), there is a faint trace of fluorescence, likely originating from chloroplasts. Conversely, in the treated leaf at 1-hour post-application (B), the fluorescence emanating from the nanoparticles appears to be in close proximity to the cells, likely situated in the vicinity of or surrounding the cell wall. After 24 hours of exposure, this fluorescence diminishes, indicative of nanoparticle translocation.

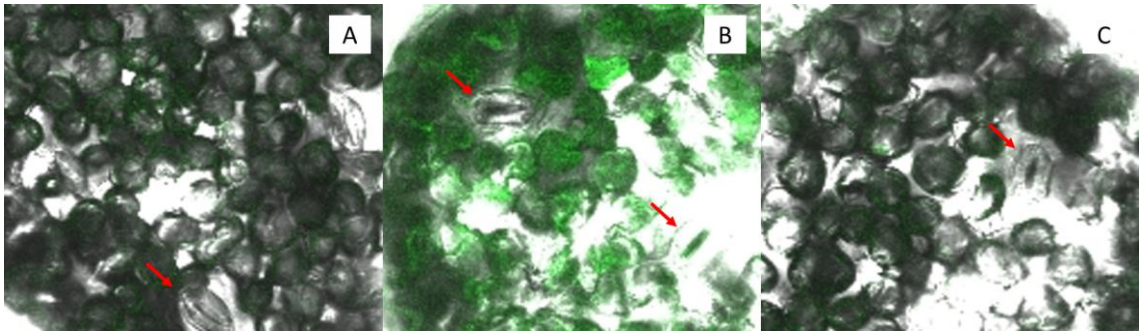

Figure 7: Representative confocal spectral microscopy images of zein nanoparticles labeled with the FITC probe, containing the actives curcumin and carvacrol, from the region of the application site, at 1 and 24 hours after deposition on soybean leaves. A represents the control, B represents the group treated 1h after application and **C** represents the group treated 24h after application. Images have unscaled enlargements. Arrows point to the stomata.

Chloroplasts have emerged as potential destinations for nanoparticles upon their penetration into leaf tissues. Notably, chloroplasts possess a net negative charge, a characteristic that would seemingly render them an inherent attraction for positively charged nanoparticles. Nonetheless, Wong et al. (2016) research findings have demonstrated that metallic nanoparticles, regardless of their charge polarity, exhibit penetrating capabilities within chloroplasts, provided their potential exceeds 30 mV. In this investigation, carbon nanotubes coated with polymers characterized by a substantial zeta potential—whether negative or positive—were effectively transported into intact chloroplasts. This phenomenon was notably absent when polymers formed coatings with a more neutral charge. It is pertinent to note that chloroplasts are equipped with porins in their outer membrane, featuring a pore diameter of 2.5-3 nm, facilitating the passage of small molecules. Despite this, the nanoparticles in question in Fulano's study possessed diameters ranging from 3 to 30 nm, yet they were observed within the chloroplasts (WONG et al., 2016). Furthermore, PCL nanoparticles, characterized by dimensions of 256 ± 2 nm and a polymeric zeta potential of -32 mV, were also identified within protoplasts and chloroplasts (BOMBO et al., 2019). While the possibility of nanoparticles, as produced in our research, being present within chloroplasts or associating with them warrants further investigation, it is noteworthy that any such presence does not appear to disrupt the photosynthetic processes of the plant, as demonstrated in Chapter 2.

Translocation analysis of nanoparticles in the plant through FITC probe quantification

To explore the translocation patterns of nanoparticles following foliar application within soybean plants, the leaves of these plants were uniformly subjected to a 2x dilution of the zein-FITC formulation. By examining the emitted fluorescence originating from the FITC probe, insights into the nanoparticle distribution were gained (Figure 8). As illustrated in Figure 9, our observations allow us to deduce that foliarly applied nanoparticles exhibit movement from the leaves to the stem, with limited penetration into the root region. It is plausible that the observed limitation in nanoparticle presence within the roots may be attributed to the relatively short duration of our analysis, conducted at intervals of 1 and 24 hours.

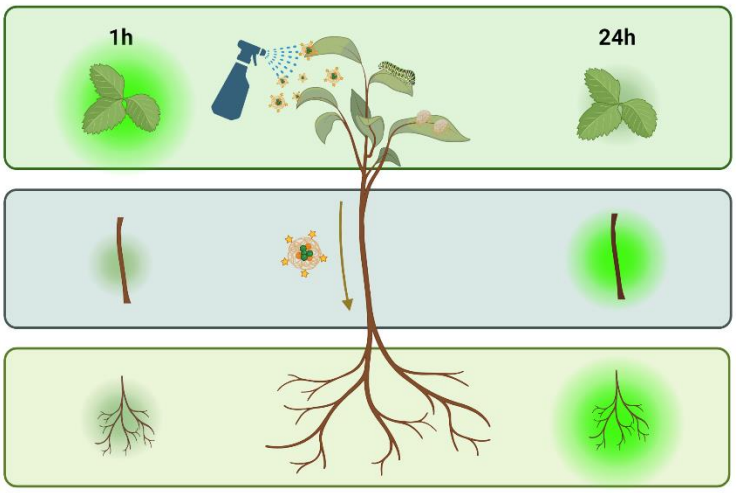

Figure 8: Schematic representation of nanoparticles translocation after foliar application. Fluorescence intensity quantification in distinct leaf regions at 1- and 24-hours post-deposition of nanoparticles containing the fluorescent probe. The reduction in fluorescence intensity at the application site, accompanied by an increase in other regions, signifies their mobility within the leaf tissue. Statistically distinct values within the same line are denoted by different letters, as determined by ANOVA followed by Tukey's test ($p<0.05$).

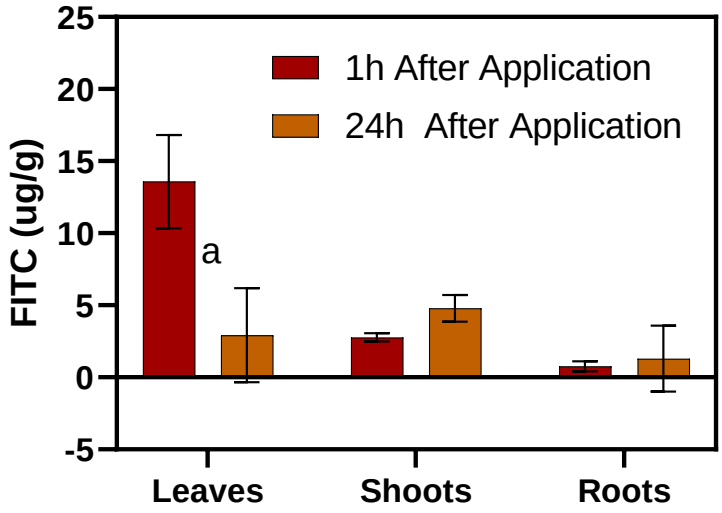

Figure 9: Quantification of the FITC probe associated with zein nanoparticles, which encapsulate the bioactive compounds curcumin and carvacrol, was conducted across three distinct segments of the soybean plant, specifically the leaf, stem, and root. The reported average values were derived by subtracting the corresponding average values obtained from the control group. Notably, the lowercase letter (a) is employed to indicate a statistically significant difference concerning the 1-hour post-application time point.

The reduction in fluorescence intensity within the leaf tissue, observed between the 1-hour and 24-hour post-application time points, signifies a substantial 4.65-fold decrease. This trend aligns with the findings of our previous experiment, which indicated a comparable 4.5-fold reduction in fluorescence intensity at the site of nanoparticle deposition over the same time frame. These consistent observations suggest the likelihood of nanoparticle translocation within the leaf tissue. The translocation of these nanoparticles is further underscored by a notable increase in fluorescence intensity within the stem, in contrast to the control group. While no statistically significant difference is discerned between the 1-hour and 24-hour measurements, the quantification of FITC within the stem registers a 1.72-fold increase after 24 hours, signifying augmented translocation with the passage of time. The elevated FITC quantification after 24 hours in the stem corroborates the absence of stem contamination at the moment of nanoparticle leaf application. Concerning the quantification of FITC within the root structures, no statistically significant differences

are detected among the experimental groups. However, an observable trend indicates an inclination toward increased FITC levels in the roots at the 24-hour mark following leaf exposure to nanoparticles. It is conceivable that an experiment with an extended post-exposure duration might reveal a more pronounced increase in root-associated FITC concentrations.

Based on the findings presented in Figure 7, it is reasonable to infer that zein nanoparticles incorporating curcumin and carvacrol have been absorbed by the leaves and subsequently translocated to the root structures. Various anatomical features, such as stomata, hydathodes, trichomes, and necrotic regions, have been identified as potential polar pathways through which nanoparticles may penetrate plant tissues. In regions characterized by trichomes and necrotic areas, the cuticle—a waxy and lipophilic layer with a thickness ranging from 100 to 250 nm—may either be absent or exhibit reduced thickness. Conversely, in stomata and hydathodes, the cuticle is inherently absent, further facilitating the interaction and potential penetration of nanoparticles within the plant. Additionally, the possibility of non-polar penetration route, involving the cuticle and its pores, cannot be dismissed (BALLIKAYA et al., 2023). At present, the specific mechanisms governing how nanoparticles traverse leaf tissues and subsequently reach the vascular system remain elusive and necessitate further comprehensive investigation.

The entry of nanoparticles through stomata is widely acknowledged as the prevailing route of penetration. Evidence supporting this contention has been demonstrated in mustard leaves, where polymeric PCL nanoparticles (with dimensions of 350 nm and bearing a negative zeta potential) were identified within stomata. This identification was facilitated by the utilization of a fluorescent probe, namely rhodamine B, in conjunction with confocal micrography. Within the initial 24-hour period following application, these nanoparticles were found to adhere to the leaf surface. Subsequently, beyond this time frame, their presence extended into subcellular compartments. After a duration of 96 hours, the nanoparticles were observable within the stomata, primarily concentrated in the hydathode region (BOMBO et al., 2019). It is pertinent to note that the hydathode region is notably characterized by modified stomata that are intricately connected to the vascular system.

The current body of knowledge regarding the foliar absorption of nanoparticles predominantly stems from research involving metallic nanoparticles. Nevertheless, our understanding of the intricate mechanisms governing their penetration and transport within plants remains limited.

Multiple parameters can exert influence over the adhesion, absorption, and translocation of nanoparticles within plant systems. These parameters encompass factors such as plant species, nanoparticle dimensions, zeta potential, surface coating, and more. For instance, So and colleagues investigated employing foliar-applied Au-NPs with diverse coatings, each yielding distinct zeta potentials (null, negative, and positive), across two distinct tree species. Their results, recorded after a 20-day period post-application, indicated that the highest Au-NP concentrations were localized within the leaves, followed by lower concentrations in the stems and roots. Importantly, there were discernible disparities in the outcomes between the two tree species, suggesting divergent rates of internalization. These variances could potentially be associated with disparities in stomatal density. Additionally, Au-NPs with varying zeta potentials were observed to reach the roots, with the authors speculating that the lower concentration of Au-NPs in the roots might be linked to root-soil exudation (BALLIKAYA et al., 2023).

Furthermore, interactions between nanoparticle coatings and leaf surfaces play a pivotal role in shaping the interplay between adhesion and absorption. This phenomenon is exemplified by PLA nanoparticles, measuring 450 nm, which exhibit divergent adhesion capacities to leaf surfaces contingent upon their functionalization and corresponding zeta potentials. Specifically, PLA nanoparticles functionalized with H2N groups and bearing a positive zeta potential demonstrated heightened adhesion to leaf surfaces, facilitated by mechanisms involving hydrogen bonds, covalent bonds, and electrostatic interactions (YU et al., 2017).

Conclusions

Nanopesticides exhibit substantial potential for application in agriculture. Hence, comprehending the underlying mechanisms is of paramount significance, serving both safety considerations and the enhancement of system efficiency. In this context, zein nanocarriers encapsulating curcumin and carvacrol were found to be absorbed by the leaf, subsequently penetrating the mesophyll and demonstrating mobility within the

leaf tissue, with a notable affinity for the leaflet apex. Furthermore, these nanocarriers exhibited a proclivity for trichomes after their initial absorption, becoming evident within trichomes located at considerable distances from the application site. Importantly, following nanoparticle penetration into leaf tissues, a phenomenon of leaf-to-root translocation was observed, potentially occurring via the phloem. Nevertheless, to elucidate the precise mechanisms governing nanoparticle leaf penetration and their eventual translocation within the vascular system, further in-depth investigations are warranted.

Acknowledgments

Authors are grateful to the São Paulo Research Foundation (FAPESP, grants, #2022/00509-0, #2022/03399-0, #2019/04758-1 and #2017/21004-5), Conselho Nacional de Desenvolvimento Científico e Tecnológico (CNPq - 308439/2021-0), and Coordenação de Aperfeiçoamento de Pessoal de Nível Superior – Capes (88887.695285/2022-00; 88887.351694/2019-00; 88887.817514/2023-00).

References

AVELLAN, A. et al. Nanoparticle Size and Coating Chemistry Control Foliar Uptake Pathways, Translocation, and Leaf-to-Rhizosphere Transport in Wheat. **ACS Nano**, v. 13, n. 5, p. 5291–5305, 28 maio 2019.

BALLIKAYA, P. et al. First evidence of nanoparticle uptake through leaves and roots in beech (Fagus sylvatica L.) and pine (Pinus sylvestris L.). **Tree Physiology**, v. 43, n. 2, p. 262–276, 1 fev. 2023.

BARTOLUCCI, C. et al. What makes nanotechnologies applied to agriculture green? **Nano Today**, v. 43, p. 101389, abr. 2022.

BOMBO, A. B. et al. A Mechanistic View of Interactions of a Nanoherbicide with Target Organism. **Journal of Agricultural and Food Chemistry**, v. 67, n. 16, p. 4453–4462, 24 abr. 2019.

CAMPOS, E. V. R. et al. Carvacrol and linalool co-loaded in β-cyclodextrin-grafted chitosan nanoparticles as sustainable biopesticide aiming pest control. **Scientific Reports**, v. 8, n. 1, p. 7623, dez. 2018.

CAMPOS, E. V. R. et al. Using Chitosan-Coated Polymeric Nanoparticles-Thermosensitive Hydrogels in association with Limonene as Skin Drug Delivery Strategy. **BioMed Research International**, v. 2022, p. 9165443, 7 abr. 2022a.

CAMPOS, E. V. R. et al. Nature-Based Nanocarrier System: An Eco-friendly Alternative for Improving Crop Resilience to Climate Changes. **Anthropocene Science**, 28 jul. 2022b.

CARVALHO, L. B. et al. Pre-emergence herbicidal efficiency and uptake of atrazine-loaded zein nanoparticles: a sustainable alternative to weed control. **Environmental Science: Nano**, v. 10, n. 6, p. 1629–1643, 15 jun. 2023.

DAVIDOV-PARDO, G.; JOYE, I. J.; MCCLEMENTS, D. J. Encapsulation of resveratrol in biopolymer particles produced using liquid antisolvent precipitation. Part 1: Preparation and characterization. **Food Hydrocolloids**, v. 45, p. 309–316, 1 mar. 2015.

DEVASENA, T. et al. Insights on the Dynamics and Toxicity of Nanoparticles in Environmental Matrices. **Bioinorganic Chemistry and Applications**, v. 2022, p. e4348149, 31 jul. 2022.

FAO (ED.). **The future of food and agriculture: trends and challenges**. Rome: Food and Agriculture Organization of the United Nations, 2017.

FÄRKKILÄ, S. M. A. et al. Fluorescent nanoparticles as tools in ecology and physiology. **Biological Reviews**, v. 96, n. 5, p. 2392–2424, out. 2021.

HU, K.; MCCLEMENTS, D. J. Fabrication of surfactant-stabilized zein nanoparticles: A pH modulated antisolvent precipitation method. **Food Research International**, v. 64, p. 329–335, out. 2014.

KUMAR, S. et al. Nano-based smart pesticide formulations: Emerging opportunities for agriculture. **Journal of Controlled Release**, v. 294, p. 131–153, 28 jan. 2019.

LE GUERN, F. et al. Fluorescein Derivatives as Fluorescent Probes for pH Monitoring along Recent Biological Applications. **International Journal of Molecular Sciences**, v. 21, n. 23, p. 9217, 3 dez. 2020.

LEAD, J. R. et al. Nanomaterials in the environment: Behavior, fate, bioavailability, and effects-An updated review: Nanomaterials in the environment. **Environmental Toxicology and Chemistry**, v. 37, n. 8, p. 2029–2063, ago. 2018.

LIN, Y.; WAGNER, G. J. Rapid and Simple Method for Estimation of Sugar Esters. **Journal of Agricultural and Food Chemistry**, v. 42, n. 8, p. 1709–1712, 1 ago. 1994.

LOURENÇO, H. et al. ANATOMIA FOLIAR DE DIFERENTES CULTIVARES DE SOJA E SUA RELAÇÃO COM INCIDÊNCIA E SEVERIDADE DE DOENÇAS. v. 4, 13 dez. 2011.

MARUYAMA, C. R. et al. Nanoparticles Based on Chitosan as Carriers for the Combined Herbicides Imazapic and Imazapyr. **Scientific Reports**, v. 6, n. 1, p. 19768, 27 jan. 2016.

OLIVEIRA, H. C. et al. Nanoencapsulation Enhances the Post-Emergence Herbicidal Activity of Atrazine against Mustard Plants. **PLOS ONE**, v. 10, n. 7, p. e0132971, 17 jul. 2015.

PEREIRA, A. DO E. S.; OLIVEIRA, H. C.; FRACETO, L. F. Polymeric nanoparticles as an alternative for application of gibberellic acid in sustainable agriculture: a field study. **Scientific Reports**, v. 9, n. 1, p. 7135, dez. 2019.

PRASAD, A. et al. Zein Nanoparticles Uptake and Translocation in Hydroponically Grown Sugar Cane Plants. **Journal of Agricultural and Food Chemistry**, v. 66, n. 26, p. 6544–6551, 5 jul. 2018.

PRASAD, R.; BHATTACHARYYA, A.; NGUYEN, Q. D. Nanotechnology in Sustainable Agriculture: Recent Developments, Challenges, and Perspectives. **Frontiers in Microbiology**, v. 8, p. 1014, 20 jun. 2017.

PROENÇA, P. L. F. et al. Fluorescent labeling as a strategy to evaluate uptake and transport of polymeric nanoparticles in plants. **Advances in Colloid and Interface Science**, v. 305, p. 102695, 1 jul. 2022.

RASTOGI, A. et al. Impact of Metal and Metal Oxide Nanoparticles on Plant: A Critical Review. **Frontiers in Chemistry**, v. 5, 2017.

RISTROPH, K. D. et al. Zein Nanoparticles Uptake by Hydroponically Grown Soybean Plants. **Environmental Science & Technology**, v. 51, n. 24, p. 14065–14071, 19 dez. 2017.

SERVIN, A. D. et al. Synchrotron Micro-XRF and Micro-XANES Confirmation of the Uptake and Translocation of TiO2 Nanoparticles in Cucumber (Cucumis sativus) Plants. **Environmental Science & Technology**, v. 46, n. 14, p. 7637–7643, 17 jul. 2012.

SVECHKAREV, D.; MOHS, A. M. Organic Fluorescent Dye-based Nanomaterials: Advances in the Rational Design for Imaging and Sensing Applications. **Current Medicinal Chemistry**, v. 26, n. 21, p. 4042–4064, 19 set. 2019.

UNITED NATIONS. **World Population Prospects 2019: Highlights**. , 2019. Disponível em: <https://reliefweb.int/sites/reliefweb.int/files/resources/WPP2019_Highlights.pdf>

UPADHYAY, S. K. et al. Risks and Concerns of Use of Nanoparticles in Agriculture. Em: RAJPUT, V. D. et al. (Eds.). **The Role of Nanoparticles in Plant Nutrition under Soil Pollution: Nanoscience in Nutrient Use Efficiency**. Sustainable Plant Nutrition in a Changing World. Cham: Springer International Publishing, 2022. p. 371–394.

WAGNER, G. J.; WANG, E.; SHEPHERD, R. W. New Approaches for Studying and Exploiting an Old Protuberance, the Plant Trichome. **Annals of Botany**, v. 93, n. 1, p. 3–11, jan. 2004.

WANG, X. et al. Nanoparticles in Plants: Uptake, Transport and Physiological Activity in Leaf and Root. **Materials**, v. 16, n. 8, p. 3097, 14 abr. 2023.

WONG, M. H. et al. Lipid Exchange Envelope Penetration (LEEP) of Nanoparticles for Plant Engineering: A Universal Localization Mechanism. **Nano Letters**, v. 16, n. 2, p. 1161–1172, 10 fev. 2016.

YU, M. et al. Development of functionalized abamectin poly(lactic acid) nanoparticles with regulatable adhesion to enhance foliar retention. **RSC Advances**, v. 7, n. 19, p. 11271–11280, 2017.

Conclusão geral

Com o substancial aumento da população global, a crescente demanda por um aumento na oferta de alimentos, considerando as preocupações relacionadas à contaminação ambiental e à resistência resultante do uso extensivo de produtos químicos na agricultura, tem estimulado vigorosamente o desenvolvimento de alternativas destinadas ao controle de pragas e à ampliação da produção agrícola. Um exemplo ilustrativo dessa tendência é a fusão de substâncias de origem natural com a implementação da nanotecnologia. A despeito do notório aumento nas pesquisas científicas dedicadas a essa área, a comercialização de produtos que empregam essa abordagem permanece notavelmente restrita. Ademais, a ausência de regulamentações específicas para tais produtos constitui um desafio considerável. Outro obstáculo a ser superado reside na concentração predominante dos estudos nas fases iniciais da produção de nanoformulações, abarcando sua concepção e caracterização, enquanto a avaliação de sua eficácia, toxicidade e consequências ambientais frequentemente é relegada a um plano secundário. Diante do exposto, destaca-se a relevância do presente trabalho, onde além de serem desenvolvidos formulações com atividade acaricida e repelente, também foi avaliado a captação de translocação destas nanopartículas em plântulas de soja.

Ao longo da tese foi demonstrado que as nanopartículas de zeína são excelentes sistemas carreadores para os biopesticidas curcumina e carvacrol. Ressalta-se que não existem estudos anteriores que avaliem a liberação conjunta desses compostos e nem que demonstrem a translocação dessas partículas para as raízes das plantas após a aplicação foliar. As nanopartículas foram eficazes de controlar a população de ácaros e diferentes lagartas (*Spodoptera sp)* em testes *in vitro.* Ademais, não foram observados efeitos fitotóxicos em plantas de soja expostas a estas formulações.

Os resultados obtidos indicam que as nanopartículas de zeína que co-encapsulam curcumina e carvacrol podem representar um sistema promissor para a administração de biopesticidas, com potencial aplicação no controle de pragas. Contudo, é imperativo conduzir pesquisas adicionais com o intuito de aprofundar o entendimento dos mecanismos de ação dessas nanopartículas e investigar eventuais.